POSSIBILITY OF USING CAPILLARY BARRIERS FOR LANDSLIDE RISK REDUCTION

Erasanayagam Havisanth

198021L

Degree of Master of Science

Department of Civil Engineering

University of Moratuwa

Sri Lanka

April 2021

POSSIBILITY OF USING CAPILLARY BARRIERS FOR LANDSLIDE RISK REDUCTION

Erasanayagam Havisanth

198021L

Thesis submitted in partial fulfilment of the requirements for the degree
Master of Science in Civil Engineering

Department of Civil Engineering

University of Moratuwa
Sri Lanka

April 2021

DECLARATION

I declare that this is my own work, and this thesis does not incorporate without acknowledgement of any material previously submitted for a Degree or Diploma in any other University or institute of higher learning and to the best of my knowledge and belief it does not contain any material previously published or written by another person except where the acknowledgement is made in the text.

Also, I hereby grant to University of Moratuwa the non-exclusive right to reproduce and distribute my thesis, in whole or in part in print, electronic or other medium. I retain the right to use this content in whole or part in future works (such as articles or books).

…… ……..

E. Havisanth Date

The above candidate has carried out research for the Master's thesis under my supervision.

…….. ……..

Prof. S.A.S. Kulathilaka Date

ACKNOWLEDGMENT

I would like to take this opportunity to express my heartfelt gratitude to my research supervisor Prof. S.A.S. Kulathilaka, Senior Professor, Department of Civil Engineering, University of Moratuwa, for his exemplary guidance, valuable feedback, and constant encouragement throughout the duration of the research project.

My sincere appreciation is extended to Dr. (Mrs) J.C.P.H. Gamage, Research Coordinator, Department of Civil Engineering, University of Moratuwa, for her supportive guidance and for providing necessary guidelines regarding the progress evaluations. I would like to thank Dr Nadeej Priyankara, Department of Civil and Environmental Engineering, University of Ruhuna, and all panel members for providing valuable comments during the progress evaluations.

Further, I would like to express my gratitude to the Soil mechanics laboratory and its staff and Workshop and chief mechanic, University of Moratuwa for the immense help provided for the experimental works.

Finally, I would like to thank the Department of Civil Engineering, University of Moratuwa for funding this research project.

ABSTRACT

Possibility of Using Capillary Barriers for Landslide Risk Reduction.

Rainfall induced slope failures are a very critical issue in Sri Lanka. The risk of rainfall induced slope failures has increased over the past few years in Sri Lanka due to the introduction of new cut slopes as a part of development, as well as due to an increase in the number of intense rainfall events with climate change effect. Natural or cut slopes which remain stable during the dry season due to prevalence of high matric suction undergo failure because of loss of matric suction and pore water pressure buildup during prolong intense rainfalls. Presently cut off drains, berm drains and cascade drains together with vegetation cover and impermeable material on surface are used to reduce infiltration into cut slopes. But these techniques are not effective enough o cut off the infiltration into the slope during prolong intense rainfall events.

Capillary barrier cover system is a cost-effective system with natural soils that could minimize infiltration of rainwater. Capillary barriers are unsaturated cover system that functions in response to change in negative pore water pressure. This research on applicability of capillary barrier cover system on local Sri Lankan cut slopes was done through rainfall experiments on laboratory physical model and 2-D & 3-D numerical simulation using GeoStudio, 2012 SEEP/W software, and Midas GTS-NX software.

The research study concludes that 20cm thick river sand placed over 10cm thick M-sand(coarse) develops a capillary barrier effect which can significantly cut off the rainfall infiltration into the cut slopes even during 20mm/hr rainfall for 5 continuous days. Performance of this cover increase with slope angle and when the layer materials are sufficiently dry.

Keywords: landslides, matric suction, capillary barrier, infiltration

TABLE OF CONTENTS

LIST OF FIGURES

LIST OF TABLES

1 INTRODUCTION

1.1 General

Sri Lanka experiences catastrophic rainfall-induced slope failures from time to time in both existing natural slopes and cut slopes during intense rainfall events. The risk of rainfall-induced slope failures has increased over the past few years in Sri Lanka due to the introduction of new cut slopes as a part of development, as well as due to an increase in the number of intense rainfall events with climate change effect.

1.1.1 Climate of Sri Lanka

Sri Lanka receives a tremendous amount of rainfall because of its tropical features through major monsoons, where the maximum annual precipitation in wet zones can reach up to 3000mm/annum(Yoshinori, 2015). Sri Lanka experiences intense rainfall events from inter-monsoon other than major northeast and southwest monsoon(Suppiah & Yoshino, 1984). Rainfall of intensities exceeding 100/day has triggered cut slopes and natural slopes failures in the country(Somaratne, 2015). Based on past experiences and studies National Building Organization of Sri Lanka has established the following rainfall thresholds; alert level rainfall – 75mm/day, warning level rainfall – 100mm/day, evacuation level rainfall – 75mm/hr or 150mm/day.

1.1.2 Rainfall induced slope failures

Rainfall-triggered slope failures are one of the frequently faced natural hazards by Sri Lankans throughout history. The country's landmass covered with almost 20% with mountainous terrain leads to the existence of various shallow to steep natural slopes as well as formed cut slopes during development projects. Most of these cut slopes are found along roadsides, which are more vulnerable to failures during rainy days. Generally, both natural and cut slopes remain stable during the dry season of the year due to presence of high matric suction in slopes which increases stability due to high interparticle forces. The factor of safety of slope is basically defined as follows by Eq. (1),

$$F = \frac{\tau_f}{\tau_m} \tag{1}$$

Where, F is factor of safety of slope, τ_f is shear strength and τ_m is mobilized shear strength for equilibrium.

Shear strength in unsaturated soil is given by Eq. (2)(Fredlund & Rahardjo, 1993),

$$\tau_f = c' + (\sigma_n - u_a)\tan\emptyset' + (\sigma_a - u_w)\tan\emptyset^b \quad (2)$$

Where, τ_f is shear strength, σ_n is total normal stress, $\emptyset'$ is effective angle of shearing resistance, u_a is pore air pressure, u_w is pore water pressure and $\emptyset^b$ is angle indicating the rate of increase in shear strength relative to matric suction.

During the period of dry weather, the water table is deep and soil at the upper level is in an unsaturated state with both air and water occupying the voids. Pore water pressure u_w is less than atmospheric pore air pressure u_a due to air/water interface. This results in matric suction $(u_a - u_w)$ in upper levels of the slope. Therefore, negative pore pressure exists above the water table level in slope. Figure 1.1 represents the presence of unsaturated zone in dry weather, where the solid line (a) indicates the hydrostatic variation of pore pressure and line (b) shows the possible pore pressure variation that could exist in an unsaturated slope considering the possible maximum limit of matric suction. This presence of an unsaturated zone leads to an increase in shear strength in the soil(Eqn. (2))leading to increased stability during dry weather.

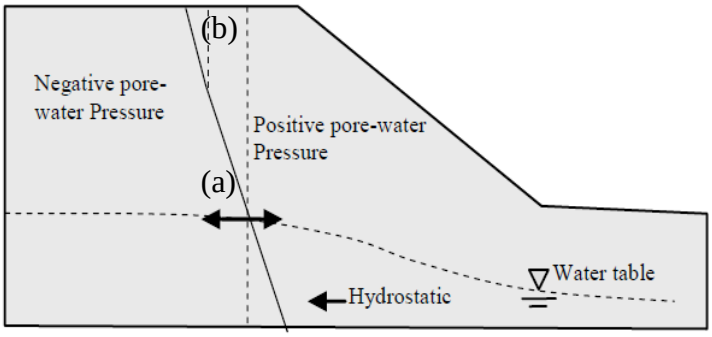

Figure 1.1: Pore water distribution in an unsaturated slope(Sujeevan & Kulathilaka, 2011)

But prolonged and intense precipitations result in significant rainfall infiltration into the slopes, causing a loss in matric suction and even leading to the development of positive pressure along the slopes. This loss of matric suction results in instability of these slopes because of a reduction in shear strength of soil which makes them

vulnerable to catastrophic failures. More than 35 major slope failures have been recorded in the period 1974 – 2006, where the majority of them are rainfall-induced failures(Disaster management centre, 2009).

There were massive landslides in natural slopes due to extensive rainfall, Meeriyabedda landslide in Koslanda estate on 29/10/2014 is a catastrophic rainfall induced landslide that occurred in the recent past costing 12 deaths and 23 people missing(Somaratne, 2015). Intense prolonged rainfall for three consecutive days exceeding 100mm/day was identified to be the triggering factor of this failure.

Other than rainfall induced natural slope failures there are many recorded cut slope failures along roadsides. Slope failures along Kegalle bypass (refer to figure 1.2), Southern expressway at CH 42+340 – 42+400, Kahagolla landslide, Welipenna, landslide along Kandy - Mahiyanganaya road, Ginigathhena (Avissawella-Hatton-Nuwara Eliya Road (A007)) Landslide are few examples of cut slope failures experienced in recent times in Sri Lanka. All these slope failures occurred during prolonged intense rainfall events.

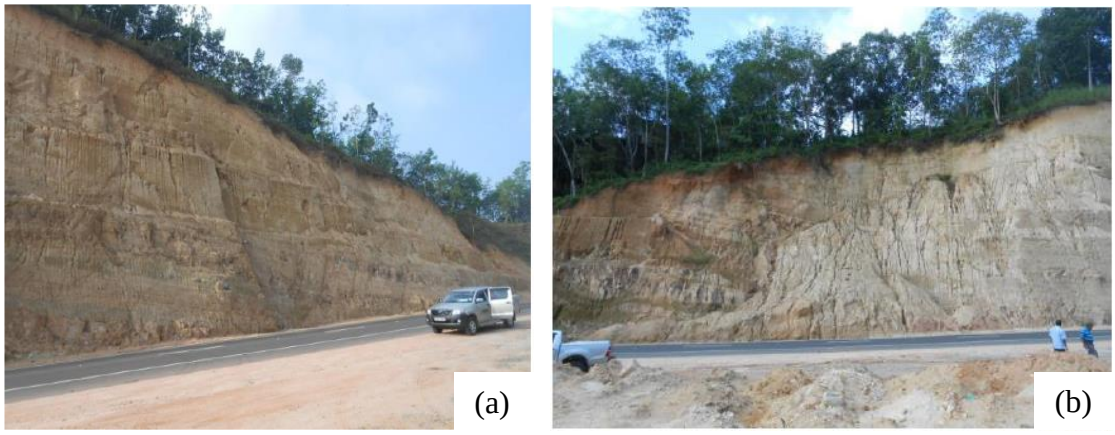

Figure 1.2: (a) Kegalle bypass - Steep cut slope remain stable during dry weather due to presence of high matric suction, (b) Kegalle bypass -Slope failure immediately after one rainy season

1.1.3 Measures for mitigation of slope failures

Presently surface drainage, subsurface drainage, vegetation covers, soil nailing and earth retaining walls, are adopted as rectification measures for stabilizing these cut slopes. Generally, these mitigation measures are costly and even causes damage to the aesthetic view of the landscape.

- **Surface drainage**

Infiltration into the slope from surface runoff is the main reason for rainfall triggered slope failures. To reduce infiltration from surface runoff, adequate and efficient surface drainages systems should be introduced on cut slopes to collect surface water from both the catchment area and slope. Sealed berm drains shall be used to collect the surface runoff while cascade drains at adequate spacing shall be introduced to bring the water collected in berm drains down the slope without any overflow. In addition to these berms and cascade drains, vegetation covers can be adopted on the slope surface to reduce the permeability of topsoil which will reduce the infiltration and facilitate the runoff. Regular maintenance should be carried out on these drainage systems to avoid blocks and leakage from the drains into the slope which may result in loss of matric suction in slope. Main reason behind failure of cut slope along the section on the southern expressway was leaking water from a cascade drain(Dharmasena, Bandara, & Karunawardena, 2015).

- **Subsurface drainage**

Subsurface drains are installed in slopes to ensure their stability by maintaining a low water table even during intense rainfall events in addition to surface drains. Generally, subsurface drains are installed at different orientations inside the slope to ensure that there is no development of perched water tables. Horizontal perforated drainpipes with sufficient strength and flexibility are widely used as subsurface drains along most of the cut slopes. Subsurface drains are more effective if series of drains at closer spacings are installed carefully intercepting possible failure plane. Water that enters the pipes is removed out of the slope through these drain pipes. There prevails long lag time in response to lower the water table by these subsurface drains in clayey soils. It will take nearly 5 years for the full lowering of the ground water table with almost 50 percent change taking place in the first year after the installation of drains,(Highland & Bobrowsky, 2008). But in slope with sandy soils, the water table will change in a few months after the installation. The fluctuation of the water table during seasonal variation is very low in slope with clayey soil with the fairly stable water level, while water level fluctuates with rainfall in sandy soil. The rise of groundwater table during

intense rainfall was the reason behind the slope failure in upcountry railway line at Watawala since the 1950s, which was later mitigated through providing sufficient subsurface drainage along with pumping wells year 1990.

- **Structural mitigation measures**

Cut slopes with steep gradients often need structural strengthening in the forms of soil nails, anchors and earth retaining structures to keep them stable in addition to surface and subsurface drainages. Designs specific to the site are done after thorough site and subsoil investigation based on engineering principles considering possible adverse rainfall events. Generally, the costs of these mitigation measures are high when compared to other rectification techniques.

Soil nailing is widely used over various steep slopes to stabilize them by reinforcing the slope with steel bars. Nails are introduced into the slope at adequate spacing and the slope face is stabilized by shotcreeting the surface, this forms a zone of reinforced surface which will act as a single unit of resisting unit to support the soil mass behind it. Reinforced earth walls, gabion walls, retaining walls and lattice frame protection works are other forms of structural strengthening used to stabilize the cut slope in the country.

Failure at Welipenna in the southern expressway was rectified by adopting soil nailing along with gabion retaining walls along toe of the slope(Dharmasena et al., 2015). Rectification of cut slopes that failed during the widening of Kandy – Mahiyangana road involves gabion retaining walls at the toe of the slope in addition to berm drains, cascade drains, subsurface drains, and vegetation cover to reduce rainfall infiltration into the slope.

1.1.4 Introduction to Capillary Barriers

A capillary barrier is a cover technique which controls the flow of water due to contrast in hydraulic conductivity of layer materials. The capillary barrier cover system consists of a layer of finer soil over a layer of coarser soil with proper contrast on their hydraulic conductivity. Figure 1.3 depicts the diagram of a two-layer capillary barrier cover system. This unsaturated cover system functions in response to a change in negative pore pressure in soil cover materials. Capillary barrier phenomenon is formed because

of contrast in the variation of hydraulic conductivity of finer soil and coarser soil with matric suction. At relatively high matric suction values, the coarse-grained soil has extremely low permeability than that of fine-grained soil.

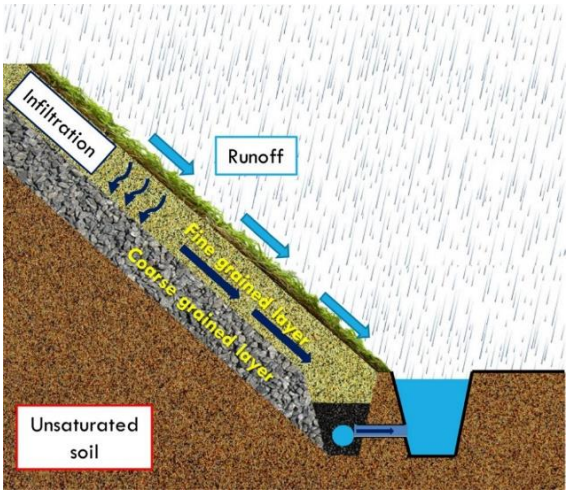

Figure 1.3: Capillary Barrier soil cover(Harianto Rahardjo, Kim, & Satyanaga, 2019)

Figure 1.4(a) illustrates the variation of permeability of fine and coarse soil with matric suction. Although the saturated permeability of coarse soil is higher than fine soil with the increase in matric suction permeability of both fine and coarse soil reduces. But the rate of reduction in conductivity of fine-grained soil is higher than coarse-grained soil, this causes the development of hydraulic impedance along the boundary of fine-coarse layers. Hence, the fine-coarse soil layer interface performs as a barrier preventing moisture movement from infiltrating through the cover system and resisting any moisture movement into coarse layer. Infiltration is held in a fine layer by its capillary forces. This phenomenon is known as the capillary barrier effect in soil mechanics. Figure 1.4(b) illustrates the formation of the capillary barrier effect in soil.

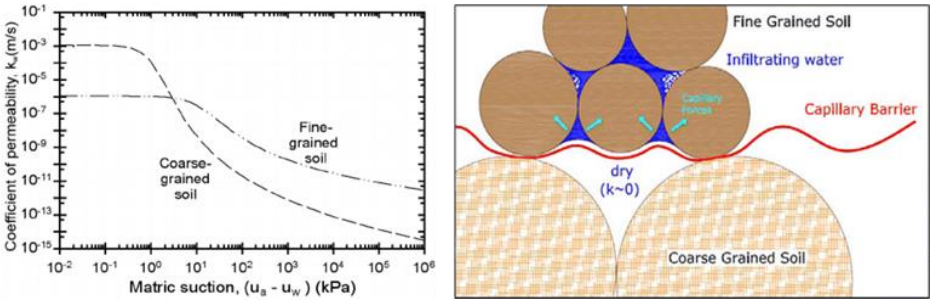

Figure 1.4: (a) SWCC of fine/coarse soil layer(Tami, Rahardjo, Leong, & Fredlund, 2004b), (b) Development of a capillary barrier effect(Mancarella & Simeone, 2012).

- **Breakthrough in capillary barrier**

In the capillary barrier cover, infiltration is initially held in fine layer of soil. But with time water gets accumulated in the fine layer and it reaches the fine-coarse interface, which results in loss of matric suction at interface leading to reduction of matric suction in coarse layer at interface. When matric suction of the coarse soil layer get to its water entry value, its hydraulic conductivity increases rapidly and once the conductivity exceeds the conductivity of the fine soil breakthrough occurs in capillary barrier cover. The capillary barrier effect is no more available after the occurrence of breakthrough in the cover system until the fine and coarse layer dry out sufficiently to develop adequate negative pore pressure.

Therefore, to keep capillary barrier cover efficiently the infiltration that enters the fine layer should be removed from the cover without allowing it to get accumulated at the soil layer interface. Infiltration can be removed by the combined effect of evaporation, transpiration, drainage, and lateral diversion along fine-coarse interface. Lateral diversion is the most effective way of keeping the cover dry throughout the operational period. A sloped capillary barrier (cover formed by maintaining the fine-coarse interface at a particular dip angle) can be adopted to divert the infiltration laterally along the interface. During, lateral diversion of moisture along the interface, the water content in the down-ward direction increases, while upper portion remains sufficiently dry. When the matric suction reaches water entry value of coarse layer along down-dip direction of interface breakthrough occurs in the capillary barrier. The capillary barrier is not effective after this point at the interface. Length along the interface until the breakthrough occurs in the barrier is defined as diversion length of capillary barrier cover.

1.2 Problem statement

Rainfall induced landslides are identified to be the most catastrophic natural hazard in tropical countries like Sri Lanka. In the dry season, tropical slopes are in an unsaturated condition with a relatively deep-water table, but the rainfall infiltration significantly affects the development of porewater pressure which will result in increased porewater pressure and reduction in shear strength of soils. Improvement of surface drainage is the most primary method of maintaining stability by minimizing infiltration of rainwater into the slope. However, infiltration could not be completely cut off. An effective capillary barrier cover system can achieve a more significant cutoff of infiltration under conditions of intense rainfall. With this, it would be possible to minimize the need for structural measures such as soil nailing or the retaining structures at the toe. Capillary barriers can be utilized properly to maintain the high matric suction of tropical soils even during rainfall to prevent rainfall induced landslide in Sri Lanka. Although there are records of research done in some other tropical countries, there were no studies conducted in Sri Lanka accounting for specific conditions that prevail. This research attempts to study the development of capillary barrier with local Sri Lankan soils and to establish the critical parameters such as layer thicknesses, effective combination of constitute materials for capillary barrier configurations, the inclination of layers to the horizontal, and characteristics of the soil layers (such as SWCC) to optimize the performance.

1.3 Objective of the study

Investigating the possibility of using capillary barriers for landslide risk reduction in cut slope in Sri Lanka by using laboratory rainfall experiment and numerical modelling method. This can be further subdivided as;

- Obtain SWCC and basic soil parameters of soils used in the study: river sand and manufactured sand.
- Determine the effectiveness of these materials and deriving appropriate layer thicknesses and slope.
- Study the performance of sloped capillary barrier under various rainfall patterns and different interface angle through rainfall experiment and verify the results using numerical modelling.

- Study the field applicability of the capillary barrier for multi-level cut slopes through numerical modelling.

1.4 Methodology

A literature study was done to identify the key findings of the capillary barrier cover system and aspects of physical rainfall experiments and numerical modellings involving the capillary barrier effect. Then the research was carried out in three main phases as follows,

- Material selection, determination of layer thickness and development of physical laboratory rainfall model
- Rainfall experiments and numerical verification of results
- Field applicability of capillary barrier for multi-level cut slopes with numerical modelling under 3D conditions.

1.5 Outline of thesis

There are six chapters in this thesis.

The second chapter presents the literature review on the capillary barrier effect and identifies the research gap.

Third chapter presents material properties that were determined through laboratory experiments and SWCC parameters of materials that were obtained through undergraduate research. Also, this chapter discusses the laboratory physical experiments.

Fourth chapter presents the preliminary study of the effectiveness of capillary barrier in minimizing infiltration of rainfall into local cut slopes. Determination of dimensions and layer thickness of the laboratory physical model through 2-D numerical studies is discussed in this chapter. Further, this chapter discusses the numerical studies on the development of capillary barrier effect when using river sand and M-sand as fine and coarse layer materials, respectively. Later this chapter discusses the numerical verification of rainfall experimental results using 2-D numerical simulation with SEEP/W program of GeoStudio software.

Simulations of the multi-level cut slope infield with 3-D numerical study with Midas GTS-NX was discussed in chapter 5. Problems experienced in the 2-D numerical study and need to extend to a 3-D study are discussed in this chapter.

Finally, the sixth chapter presents conclusions derived through this research study and recommendations for future research.

2 LITERATURE REVIEW

2.1 Effect of rainfall on cut slopes and mitigation of slope failures

In tropical countries, most of the slope failures occur during the rainy season due to infiltration of water into slope which leads to loss in matric suction. Soil, air, contractile skin, and water are the four main phases of unsaturated soil which has negative pore water pressure when compared to pore air pressure(Fredlund & Rahardjo, 1993). The negative pore water pressure in the unsaturated slope enhances the shear strength of soil material.

Traditionally rainfall induced slope stability analyses are done integrating the impacts by altering groundwater flow and rising water table. This analysis is not appropriate because different pore water regimes like perched water table underlined by unsaturated region near the surface may prevail in the slope based on the slope's infiltration characteristics(Collins & Znidarcic, 2004). Matric suction values in soil vary linearly along the depth having a maximum value at ground surface due to exposure to longer evaporation and transpiration(Tran, Trinh, Lee, Oh, & Nguyen, 2015). Antecedent rainfall before any prolong rainfall causes the reduction in matric suction of soil resulting in increase of permeability which makes the slope more vulnerable to failure(Tran et al., 2015). The effect of negative pore water pressure on shear strength is accounted into the calculation based on modified Mohr-Coulomb failure criteria for determining the factor of safety (FOS) of slope(Cho & Lee, 2001).

During rainfall events, slopes with finer soils take a longer period compare with coarser soil to fail due to rainfall infiltration, because their initial matric suctions are higher than coarser soil resulting in higher initial FOS. The time difference for slope failure on a slope with finer soil for increasing rainfall intensity is low. The rate of reduction in shear strength of different soils varies depending on their soil-water characteristic parameters: air entry value, residual water content, saturated water content, which can be utilized for landslide early warning. Higher intensity rainfall for a short duration and prolonged low intensity rainfall can cause cut slope failures due to loss of matric suction(Ahmad-adli, Huvaj, & Kartal Toker, 2014).

Cut slopes that remain stable during the dry season fail during intense prolonged rainfall due to the development of positive pore water pressure, this even leads to the reduction of FOS of slope less than unity(Sujeevan & Kulathilaka, 2011). Incorporating surface drainage berm drains and vegetation cover the reduction in safety margin in slope during intense rainfall event can be mitigated effectively(Kulathilaka & Kumara, 2011). In slopes where use of vegetation cover is not possible, shotcreeting the surface shall be adopted to reduce the surface permeability of the cut slope to reduce rainfall infiltration. The use of vegetation covers with berm drains on slopes reduces infiltration and also their deep roots perform as nails on slopes increasing their stability(Dharmasena & Kulathilaka, 1998).

Horizontal drains are used as subsurface drainage measures to reduce the fluctuation in the water table in slope during rainfall events. Drain type, number of pipes, length, spacing and location of instalment inside the slope affect the functioning of horizontal drainage system(Lau & Kenney, 1984). The horizontal drainage system can be used only to keep the water table low during infiltration, and they do not function to develop matric suction beneath the slope surface(Rahardjo, Hritzuk, Leong, & Rezaur, 2003).

2.2 Design of capillary barrier cover

Design of the capillary barrier date back to early 1959 with researchers first identifying the capillary barrier effect phenomenon in layered soil in geotechnical engineering and the theory behind it. Capillary forces in the capillary layer (fine-grained soil layer) delay the infiltration into the capillary block (coarse-grained soil layer) under high matric suction values. Medium sand and fine gravel are common fine and coarse layer material combination for the capillary barrier. Under natural climatic conditions, capillary barriers are effective in reducing the infiltration into large waste deposits(Kampf & Montenegro, 1997). The final capping layer with the capillary barrier is used often as an effective alternative mitigation measure to reduce rainfall infiltration on municipal waste yards because of their low cost of construction and stability in the long terms(Stormont & Anderson, 1999a)

Through a clear study of soil water characteristic curves: hydraulic conductivity curve and volumetric water content curve, one can understand the capillary barrier effect in

unsaturated soil layers. Significant contrast in hydraulic conductivity in the fine and coarse layer is required to form the capillary barrier effect. SWCC of soil can be established through techniques of axis translation, experiments using tensiometers, chilled mirror hygrometers and experiments with capacitance sensors. The difference in calculated and experimental results on capillary barrier involving expansive clay as fine layer is due to its state-dependent SWCC parameters(Stormont & Anderson, 1999b).

In a capillary barrier cover during the start of infiltration of rainfall is absorbed by the soil, then water get start to ponding near the surface. Following that due to the combined effect of gravity and capillary force in the fine layer at unsaturated state water flows down into the pores of the soil. With the infiltration of moisture, the soil becomes near saturation and flow occurs only under gravity(Wang, Li, & Wu, 2018).

2.2.1 Theoretical modelling of capillary barrier

A breakthrough occurs in the capillary barrier when matric suction at interface reduces to the value where coarse layer material permeability becomes higher than the fie layer(Stormont & Morris, 1997).

Breakthrough head: head at which breakthrough occurs in capillary barrier can be obtained from the permeability function of soil and SWCC and theoretical estimation based on air-water-solid interface mechanical equilibrium. Eq. (3) represents the theoretical estimation of the breakthrough head(Stormont & Anderson, 1999a).

$$h_c \geq \frac{1}{\rho_w g \alpha_{fine}} - \frac{2}{\rho_w g \alpha_{coarse}} \quad (3)$$

Where, h_c is breakthrough head and α is the parameter used in modelling SWCC of soil.

The water holding capacity of fine-grained soil depends on layer thickness, initial degree of compaction, the intensity of rainfall and other factors. Based on the averaging concept moisture content throughout the fine layer can be estimated, from this water holding capacity of the fine layer is determined by Eqn. (4)(Wang et al., 2018). Materials for fine soil layer can be selected based on the estimation of water holding capacity.

$$C = (\theta_f - \theta_0)AH \tag{4}$$

Where, C is water holding capacity of the fine layer, θ_0 is initial volumetric water content, θ_f is average volumetric water content of fine layer at the time of breakthrough, A is the cover area, and H is fine layer thickness.

Time taken for a breakthrough in capillary barrier depends on hydraulic conductivity of fine and coarse layer materials, the initial volumetric water content of the soil, layer thickness, dry density and saturated volumetric water content of fine layer and intensity of rainfall. Eqn. (5) gives the simplified estimation of breakthrough time(Wang et al., 2018).

$$T = \frac{C}{Ak_i} \tag{5}$$

Where, T is the breakthrough time, C is water holding capacity of fine layer, A is the cover area and k_i is rate of infiltration of water into soil cover(m/s).

$$k_i = \begin{cases} q, q < k_s \\ \lambda k_s, q > k_s \end{cases} \tag{6}$$

Rate of infiltration k_i to estimate breakthrough time is given in Eqn. (6). Where, q is the rainfall intensity and k_s is the saturated hydraulic conductivity.

To avoid the accumulation of water that enters the capillary cover during infiltration the evaporation capacity of the dry season should be sufficiently high. Eqn. (7) is used to determine the efficiency of the capillary barrier cover system(Wang et al., 2018).

$$C = (\theta_f - \theta_0)AH \ \leq \ Q_E \frac{(T_a - T_{rs})}{T_a} \tag{7}$$

Where, Q_E is evaporation during the dry season, T_a is total time in year, and T_{rs} is duration of the rainy season.

For an effective capillary barrier cover effect, fine layer thickness should be sufficiently thick to satisfy the condition water holding capacity greater than rainfall infiltration. Eq. (8) is used to estimate the fine-grained layer thickness(Wang et al., 2018). But considering the cost of construction and convenience, the fine layer thickness should be between 150mm – 500mm.

$$H \geq \frac{\min(q_r, \lambda K_s) T_r}{\theta_f - \theta_0} \quad (8)$$

Where, H is fine layer thickness, and q_r is average rainfall density during the rainy season. Based on the above equation if the estimated fine layer thickness is too large, the required thickness can be reduced by decreasing the saturated permeability of the fine soil layer adopting techniques of compaction, the addition of cement, bentonite and clay content in the fine soil layer(Wang et al., 2018).

Average rainfall density during the rainy season can be estimated using Eq. (9)(Wang et al., 2018).

$$q_r = \frac{\eta Q_r - \frac{Q_E}{T_a}(T_{rs} - T_r)}{T_a} \quad (9)$$

Where, Q_r is the total annual rainfall, Q_E is evaporation during dry season, η is accounted percentage of rainfall during the rainy season in annual rainfall estimation, T_{rs} is duration of rainy season, and T_r is the number of rainy days.

Based on the above set of equations following design criteria are obvious,

- With the increase of fine layer thickness, the storage capacity and time taken for the breakthrough in the capillary barrier increases.
- Infiltration reduces with an increase in fine-grained soil layer thickness.
- Capillary barrier is effective with high water holding capacity and slower infiltration when the initial moisture content of the fine soil layer is low.
- Evaporation during dry days of the year should be higher than infiltration during rainy days.

2.2.2 Materials of Capillary barrier cover

The contrast in hydraulic conductivity of fine and coarse layer material under high matric suction controls the infiltration of water into the soil. Therefore, capillary barrier cover materials should be selected based on their soil water characteristics parameters such that there prevails the contrast on their hydraulic conductivity.

Materials for the capillary barrier cover layers can be selected based on the analytical model proposed by Ross in 1990 to estimate steady state diversion capacity of capillary

barrier cover. Eq. (10) is the Ross model to estimate steady state diversion capacity of cover(Ross, 1990).

$$Q_{max} = k_{sat} * \tan \emptyset \int_{\varphi_{c\_coarse}}^{\varphi_{c\_fine}} cd\psi \quad (10)$$

Where, Q_{max} is diversion capacity of capillary barrier cover, k_{sat} is saturated permeability, k_{sat} is relative hydraulic conductivity function, $\emptyset$ is capillary barrier cover interface angle, φ_{c_fine} is maximum suction value found in fine layer for particular infiltration rate under unit gradient, φ_{c_coarse} is maximum suction value found in coarse layer for given infiltration rate.

Based on the Ross model diversion length of capillary barrier cover can be estimated using Eqn. (11).

$$L = \frac{Q_{max}}{q} \quad (11)$$

Where, L is the diversion length of capillary barrier cover and q is the given particular infiltration rate in to cover.

Eqn. (11) shows that the diversion capacity of the cover system depends on the hydraulic conductivity of layer materials and their maximum suction value limits for a given infiltration rate. Hence, constituting materials for fine and coarse layer should satisfy the above-mentioned requirements(Parent & Cabral, 2005).

Figure 2.1 shows the method to select the best capillary barrier cover fine layer and coarse layer. Where numbers 1,2,3,4 indicated in the graph shows the selection criteria of materials.

- 1 -maximum suction existing in the coarse layer should be low enough for a given infiltration rate
- 2 -maximum suction existing in the fine layer should be high enough for a given infiltration rate
- 3&4 -permeabilities of fine soil layer corresponding to maximum suction values in the fine and coarse layer should be high enough.

Therefore, the fine layer should possess the high capillary barrier forces to retain the moisture that enters the cover system while the coarse layer should have weak capillary barrier forces for a given infiltration rate, in addition, the permeability of the fine layer must be high enough within the φ_{c_fine} & φ_{c_coarse} suction range(Parent & Cabral, 2005).

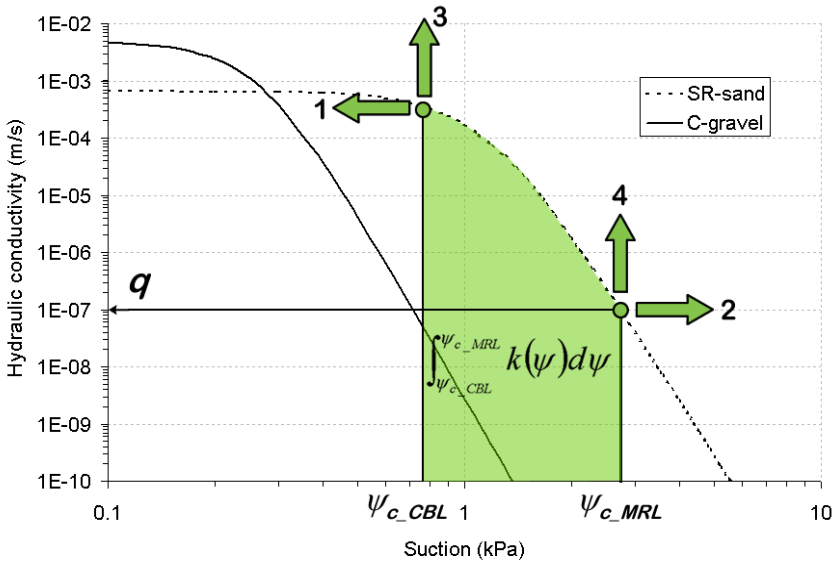

Figure 2.1: Hydraulic conductivity function to select the best capillary barrier cover materials(Parent & Cabral, 2005)

From the parametric studies based on laboratory physical experiment, it was found that the following three parameters control the selection of capillary barrier cover layer materials(Tami et al., 2004b),

- Water entry value of coarse layer material
- Water entry value ratio of the fine and coarse layer material
- Fine layer material's saturated hydraulic conductivity

The minimum ratio of water entry value of fine layer and coarse layer material must be 10 to create the capillary barrier phenomena in the layered cover system, while water entry value of coarse layer material should be low enough to keep the capillary barrier effect for a longer duration(Tami et al., 2004b).

Material for fine soil layer should be selected such that it has low fine content because low fine content will result in steep soil water characteristics curve and increase of

draining ability of the layer(Tami, Rahardjo, & Leong, 2007). Low fine content also helps in the prevention of crack in the fine soil layer during prolong dry seasons(Tami et al., 2007).

2.2.3 Diversion length and diversion capacity

Infiltration that enters the capillary barrier cover system accumulates in the fine-grained soil layer due to the prevalence of capillary barrier effect is efficiently removed through combined effect of lateral diversion, evaporation and transpiration(Rahardjo, Hua, Leong, & Santoso, 2011). Lateral diversion occurs only in capillary barrier cover systems with the sloped fine-coarse interface.

In a capillary barrier cover system built on a flat region where lateral diversion is not available the technique of store and release can be adopted. Here the infiltration into the system can be retained in the fine soil layer due to its sufficiently large storage capacity, and retained moisture can be removed through evapotranspiration(Aubertin et al., 2006). But fine layer thickness should be sufficiently large enough to have high water storage capacity, which causes a disadvantage in constructing a cover system without slope angle.

- **Lateral diversion capacity**

At a relatively dry state, the moisture that enters the capillary barrier cover system retains in the fine soil layer due to capillary forces. Moisture that accumulates in the fine layer is prevented from entering the coarser soil layer because of the low hydraulic conductivity of the coarse layer than the fine layer at high matric suction(Aubertin et al., 2006). Therefore the accumulation of infiltration takes place in the fine layer until the negative pore water pressure at the fine-coarse interface reaches the water entry value of coarse layer material(Aubertin et al., 2006). Once negative pressure at the interface reaches the water entry value the moisture that retained in the fine layer infiltrates into the coarse layer making the capillary barrier ineffective.

During lateral diversion of water along fine-coarse interface in a capillary barrier cover system at down dip direction of slope the interface becomes wetter due to the collection of infiltration from the cover. At a certain point in the interface, the moisture collected become sufficient to develop the pressure equivalent to the water entry value of coarse

layer material. At this downdip limit point, water enters the coarse layer material making the capillary barrier ineffective(Ross, 1990). The diversion capacity of the sloped capillary barrier cover system is defined as the amount of infiltrated water that accumulated and diverted along the fine-coarse interface until a downdip limit point(Ross, 1990). Eqn. (10) given in chapter 2.2.2 is used to estimate the steady state diversion capacity of the capillary barrier(Ross, 1990).

- **Lateral diversion length**

The lateral diversion length of a sloping capillary barrier cover system is defined as the distance along the interface of the fine layer and coarse layer along which the infiltration is diverted until the breakthrough occurs in the capillary barrier cover(Stormont, 1996a). That is, the length from the upper dip limit point to the downdip limit point is the diversion length. Figure 2.2 illustrates the lateral diversion mechanism and lateral diversion length in a capillary barrier cover system.

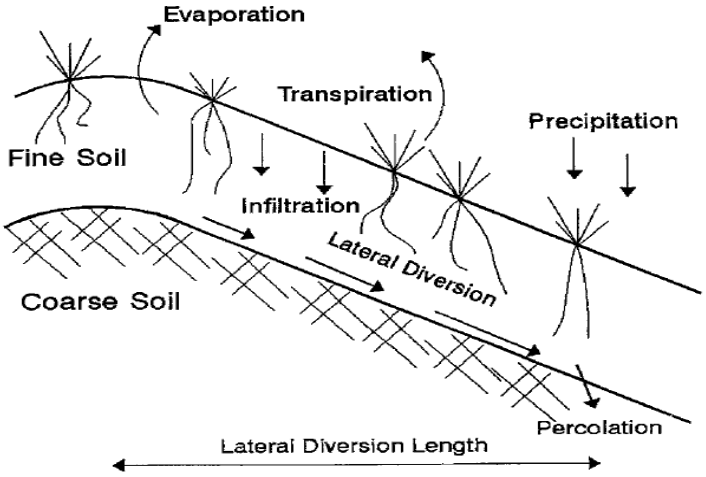

Figure 2.2: Lateral diversion length & removal of infiltration from cover(Stormont, 1996a)

For the effective diversion length of the capillary barrier cover to be large enough the hydraulic conductivity of the fine soil layer should be relatively high when compared to the infiltration rate during intense rainfall events. Generally, silts and loams soil which are mostly preferred as a good medium for rooting and water storage have low hydraulic conductivity(Nyhan, Hakonson, & Drennon, 1990).

Rainfall intensity, slope angle, the thickness of fine soil layer and properties of cover materials are identified to be the factors affecting the lateral diversion capacity and length of the capillary barrier cover system(Aubertin et al., 2006).

Diversion length can be increased by adopting the following techniques(Stormont, 1996a),

- Construction of cover with the fine layer having high hydraulic conductivity
- Construction of anisotropic fine layer such that permeability in the direction parallel to the fine and coarse layer interface is increased
- Unsaturated transport layer can be used within the fine soil layer along the fine-coarse interface

Although using a fine layer with greater hydraulic conductivity seems to be the most obvious technique to increase diversion length, it has several limitations in site construction of cover(Goode, 1986),

- Increase in cost of construction due to shortage of material at the site
- Selected fine soil material may not provide sufficient rooting medium for vegetation
- Storage capacity of the material may be comparatively low
- Adequate contrast in soil water characteristics properties maybe not presented in a selected material to develop an efficient capillary barrier effect

2.2.4 Fine soil & Coarse soil layer thickness

A two-layer capillary barrier cover is constructed by placing a fine soil layer with contrast in unsaturated hydraulic conductivity over a coarse soil layer. In these two-layer cover systems with slope fine-coarse interface, the fine soil layer serves the purpose of moisture retention and moisture diversion(Stormont & Anderson, 1999b).

Infiltration into the underlying coarse layer can be reduced to a small amount if the storage capacity of the fine soil layer is adequate with sufficient lateral diversion in the cover system(Ward & Gee, 1997). Fine soil layer thickness and its unsaturated hydraulic property can be altered to obtain a cover system with adequate water storage capacity(Khire, Benson, & Bosscher, 2000). In the design of the capillary barrier

cover, fine and coarse layer thickness should be selected such that the percolation into the slope will be less than the maximum permitted amount(Khire et al., 2000).

Fine soil layer thickness is selected such that its storage capacity will be greater than the required capacity at any possible intense rainfall event during the operational period of the cover. The maximum possible storage capacity of the fine soil layer can be estimated incorporating fine soil layer thickness using the following Eq. (12) (Gee, Ward, Meyer, Stormont, & Morris, 1999).

$$S_{fc} = \int_0^t \theta(z + \varphi_B)dz \quad (12)$$

Where, S_{fc} is the storage capacity of the fine soil layer, θ is the volumetric water content of fine soil layer, t is the fine layer thickness, z is the distance above fine-coarse interface, φ_B is the water entry head of the coarse soil layer. Estimated fine layer thickness has to be modified considering the effect of erosion from water, wind erosion, cracks from desiccation and possible excess infiltration into the cover(Khire et al., 2000).

Therefore, the increasing thickness of the fine soil layer will result in effective capillary barrier cover but considering field constructability and cost, fine layer thickness should be properly designed. Deep-rooted vegetation cover should be used on top of the cover to ensure the moisture that infiltrates into the surface layer is removed. the coarser layer thickness is not usually considered in the construction of cover as it does not affect the design like fine layer thickness. But unsaturated hydraulic conductivity of the coarse layer must be accounted for in selecting the material(Khire et al., 2000). Also considering the field constructability, the minimum thickness of the coarse layer should be selected as 100mm(Tami, Rahardjo, Leong, & Fredlund, 2004a).

2.3 Experimental studies on capillary barrier effect

A capillary barrier constructed with 7m length and 1.2m thick on a slope with 10% gradient was tested for its effectiveness in laterally diverting the infiltration. Applicability of layered fine layer (local soil was placed in between fine sand and gravelly) over homogeneous fine layer was also studied in the research. It was found

that capillary barrier made with layered fine layer has sustained during exposure to ambient climate, where the cover with homogenous fine layer has failed over its entire length because the sand layer that was sandwiched between fine and coarse layer in layered cover has acted as a drainage layer while maintaining its suction enough to form the capillary barrier effect with gravel. Therefore, a thin transport layer made with relatively fine soil having higher permeability under low suction values to laterally diverting the percolation should be provided in a capillary barrier cover to increase its effectiveness(Stormont, 1996b).

Although the homogenous capillary barrier fails during intense rainfall events, they are still capable of holding water than a simple soil cover(Stormont, 1996b). Experimental results are presented in figure 2.3.

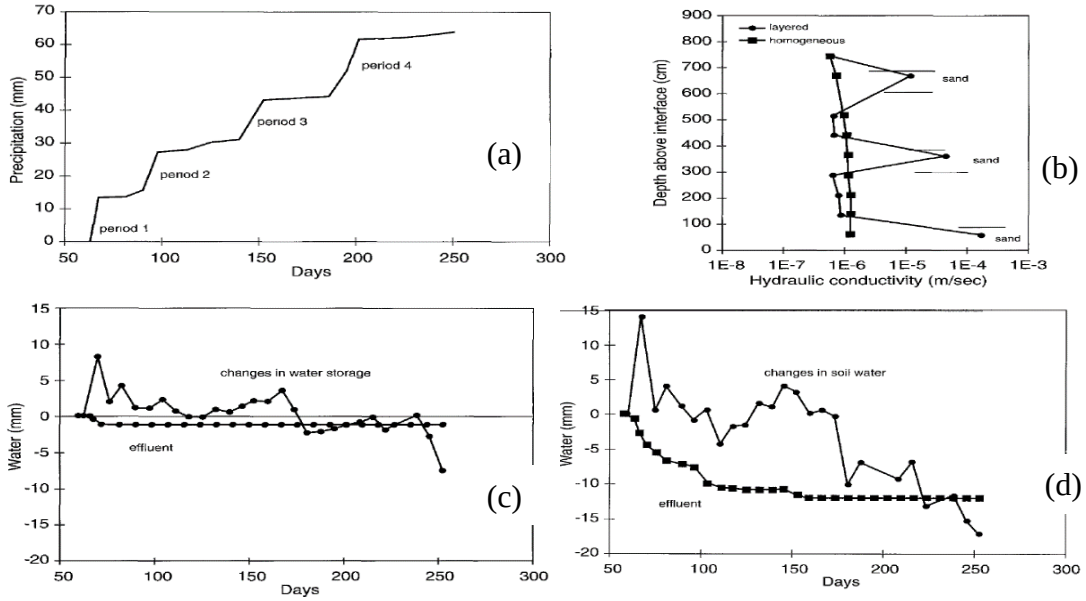

Figure 2.3: Experimental data and results, (a) rainfall during the experiment, (b)variation of calculated permeability with depth, (c)variation of soil water storage and lateral diversion – layered cover, (d)variation of soil water storage and lateral diversion – homogeneous cover(Stormont, 1996b)

John et al (1999). performed soil column tests with silty sand and concrete as a fine layer while varying the coarse layer with concrete sand and pea gravel to study the effect of different coarse soil layers in the development of capillary barrier effect. Study results concluded that the breakthrough head of the coarser soil layer affects the performance of the capillary barrier. That is, the soil that does not absorb a considerable amount of moisture until its head is reduced near zero will have the lower

breakthrough head. Further failed capillary barrier will restore after the infiltration that enters the system drain out sufficiently and its pressure head reduces(Stormont & Anderson, 1999b). Figure 2.4 shows the experimental setup used in the study and the results of the study.

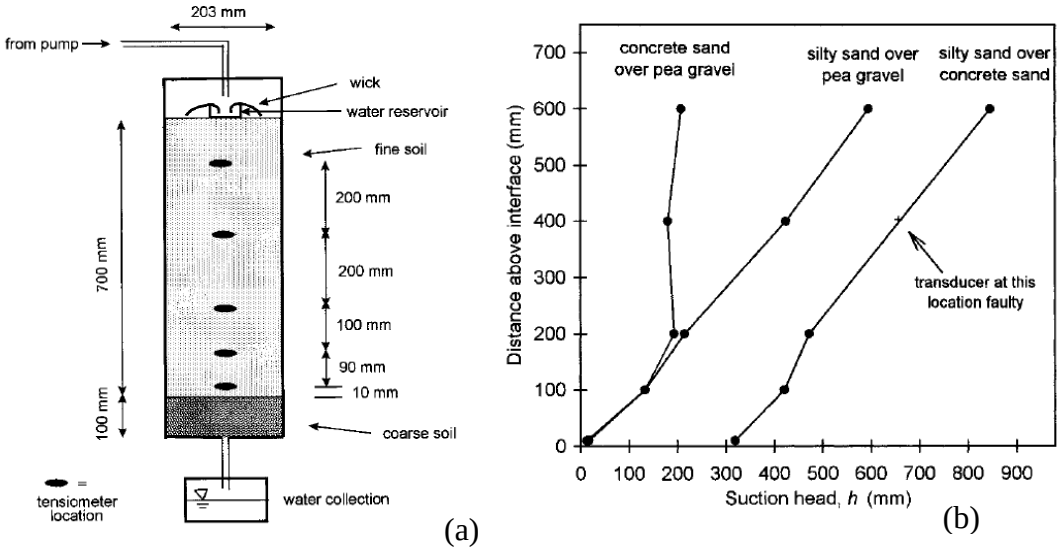

Figure 2.4: (a) Soil column test apparatus setup, (b) matric suction variation for different soil combinations during breakthrough(Stormont & Anderson, 1999b)

The application of capillary barrier cover for slope stabilization was investigated based on a laboratory level experiment by Harianto et al (2004). Study results suggest that under intense rainfall rates the soil column test and physical sloping capillary barrier models can be utilized to experiment the formation and performance of capillary barrier mechanism. Through the experimental study, it was found that increase in the thickness of the fine layer, increase in contrast in hydraulic properties of fine-coarse materials, decrease in water entry head of coarse soil layer, increase in interface slope angle and reduction in the rate of rainfall and its duration will increase the breakthrough capacity of capillary barrier cover. Since properly designed capillary barrier covers are effective in reducing infiltration into slopes, they can be utilized in slope mitigation measures(Harianto Rahardjo & Tami, 2004).

Factors affecting the performance of the capillary barrier cover system was studied by Qian et al (2010). Laboratory infiltration experiments were done in three compartmental testing box utilizing fine quartz and coarse quartz soils as fine and

coarse layers, respectively. The capillary barrier becomes more effective diverting more water laterally with increasing thickness of fine-grained soil layer while even a 1mm thick coarse layer is enough to form an effective capillary barrier cover. While the increase in fine-coarse interface slope angle will result in enhanced lateral diversion through the cover. Investigation showed that the capillary barrier effect had weakened with an increase in springling intensity on experimental model, therefore sufficient fine layer thickness should be provided accounting for extreme intense rainfall events(Qian, Huo, & Zhao, 2010). Experimental results are shown in figure 2.5.

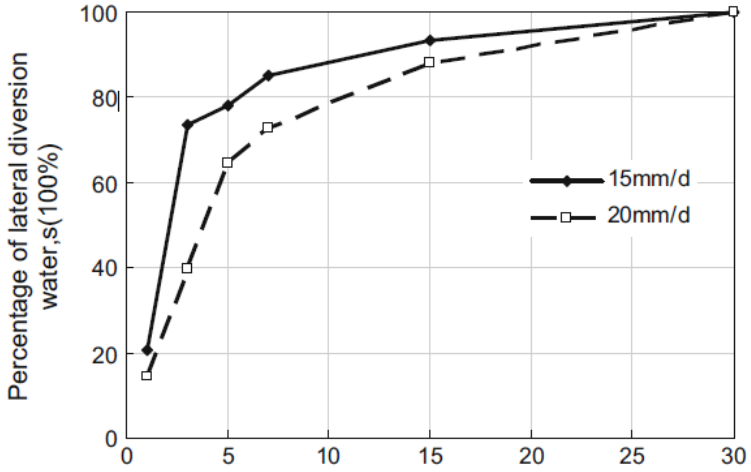

Figure 2.5: Performance of capillary barrier cover with the fine layer thickness(Qian et al., 2010)

Field applicability of capillary barrier cover on a slope that has experienced a shallow slip surface failure was studied by Rahardjo et al (2010). The performance of cover with fine sand and granite chip was studied under intense rainfall conditions. The slope that was mitigated with capillary barrier cover and adjacent slope without cover were monitored using tensiometers and piezometers. Geotextile and geocells were utilized as separation medium between layers and to fill the layer materials, respectively.

Measured pore water pressure results using tensiometers showed that positive pore water pressure has not developed in the slope that was covered with capillary barrier even during extremely intense rainfall. This has helped in maintaining higher shear strength of slope making the slope less vulnerable to failure. However, the effect of

fluctuating groundwater table was not analyzed in this study(Rahardjo et al., 2010). Figure 2.6 shows the measured pore water pressure and groundwater table variation.

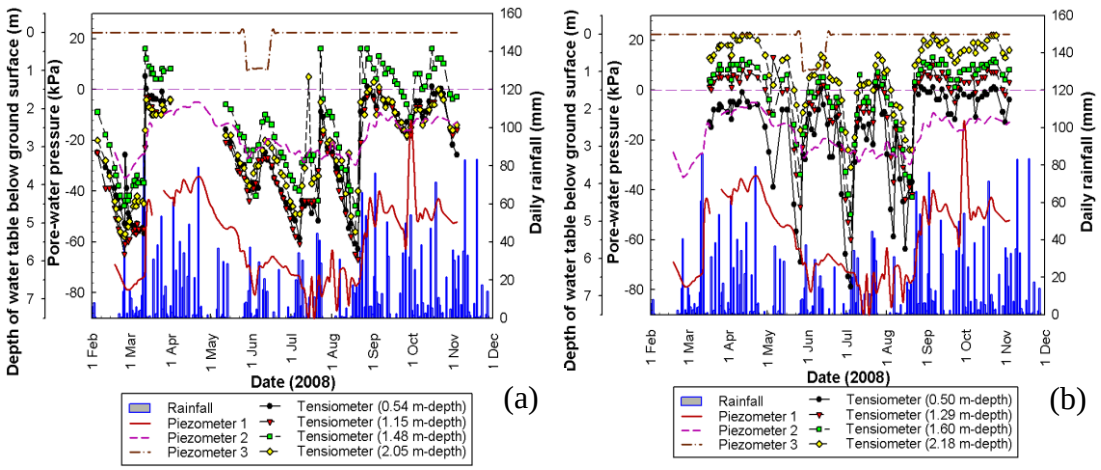

Figure 2.6: Measured pore water pressure and groundwater table variation, (a) slope with capillary barrier cover, (b) slope without capillary barrier cover(Rahardjo, Hua, Leong, & Santoso, 2010)

Performance of three-layer capillary cover as an extension of two-layer cover in humid climate under intense rainfall was investigated by Ng et al (2015). The fume model system (length-3m, width-1m & height-1.5m) was used in the physical experiment. Table 2.1 shows the properties of silty sand, gravelly sand and clay used as the fine layer, coarse layer, and the layer underneath the coarse layer respectively in the experiment. Since the hysteresis behaviour in the wetting and drying path of soil is negligible after three cycles, the test model was subjected to wetting and drying three cycles prior to the investigation. Results show that change in pore water pressure and volumetric water content measured in clay layer even after the failure if capillary barrier effect was negligible because gravelly sand layer had performed as a lateral diversion layer without letting any infiltration into the underlying clay layer. To minimize infiltration to clay layer, saturated hydraulic conductivity of clay should be maintained below $1*10^{-8}$m/s. Investigations on the effect of rainfall intensity & duration, interface slope angle, the thickness of clayey soil layer, field constructability and performance of three-layer cover in the long term run are identified to be the gaps in this study(Ng, Liu, Chen, & Xu, 2015).

Table 2.1 Properties of materials(Ng et al., 2015)

Soil type	Gravelly sand	Silt	Clay
Unified soil classification system	SP	ML	CH
Liquid limit, *LL* (%)	/	22	67
Plastic limit, *PL* (%)	/	16	32
Grain size distribution			
D_{60} (mm)	1.2	0.027	0.006
D_{30} (mm)	0.17	0.007	0.001
D_{10} (mm)	0.09	0.002	/
Coefficient of uniformity, C_u	13.3	/	/
Coefficient of curvature, C_c	0.27	/	/
Fine content (<0.075 mm; %)	0	25	77
Dry density, ρ_d (Mg/m^3)	1.56	1.41	1.25
Void ratio, *e*	0.41	0.75	1.04
Saturated coefficient of permeability, k_s (m/s)	3×10^{-2}–5×10^{-2}	2×10^{-5}–5×10^{-5}	1.0×10^{-9}–6×10^{-9}

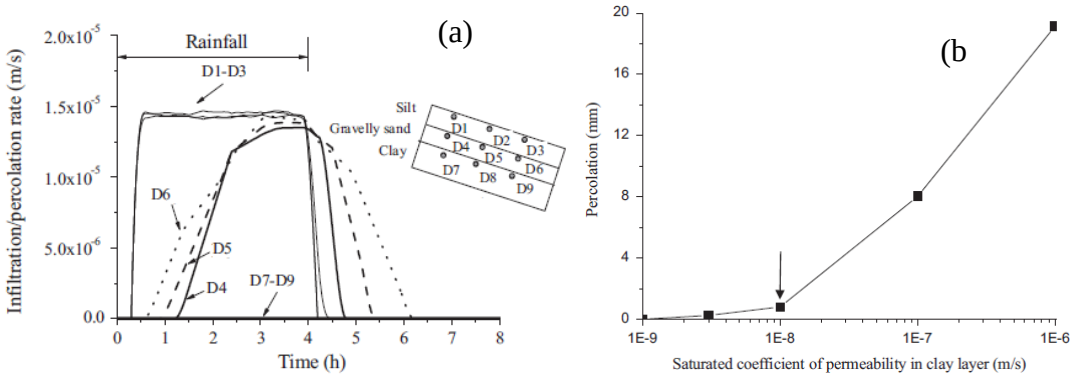

Figure 2.7: Experimental & numerical results, (a) measured infiltration rate into capillary barrier cover with time, (b) effect of saturated hydraulic conductivity of clay on infiltration(Ng et al., 2015)

Wang et al (2018). studied the water holding capacity of capillary barrier cover through soil column test and developed equations that are presented in chapter 2.2.1. Completely decomposed granite and granite soils were utilized as fine and coarse soil layers respectively in the study. Effect of varying thickness and volumetric water content of completely decomposed granite layer had experimented under constant rainfall density. Investigation results showed that infiltration into coarse soil layer reduces, the time taken for the breakthrough in the capillary cover increases and storage capacity of cover increases with an increase in fine soil layer thickness. Infiltration into the system reduces and storage capacity increases with lowering volumetric water content in the fine layer(Wang et al., 2018).

2.4 Numerical studies on capillary barrier effect

Numerical analyses to select the optimum dimension for a laboratory physical model and effective fine-coarse material were studied by Tami et al (2004). using SEEP/W program. In the investigation to select optimum model dimension considering

laboratory accommodability and boundary effects, the length of the model was varied from 1.5m – 3m while the width was varied from 30cm-60cm. studies were done to select fine-coarse layer thickness considering 30^0 slope angle. Numerical simulations show that the influence of the boundary effect on the model was lower than 20cm from the ends of the model. Permeability of the capillary barrier cover materials, rainfall intensity, layer thickness and fine-coarse interface slope angle were identified as the factors affecting the distance at which the boundary conditions affect the pore water pressure distribution in the model. Length- 2.6m, width- 0.4m and slope angle – 30^0 were selected as model dimension through numerical study. Numerical analysis results that used drying path estimated the lateral diversion in the model pretty well while analysis incorporating wetting path predicted the infiltration into the capillary barrier cover reasonably accurately. Figure 2.8 presents the numerical verification of experimental results for both analyses with wetting path and drying path(Tami et al., 2004a).

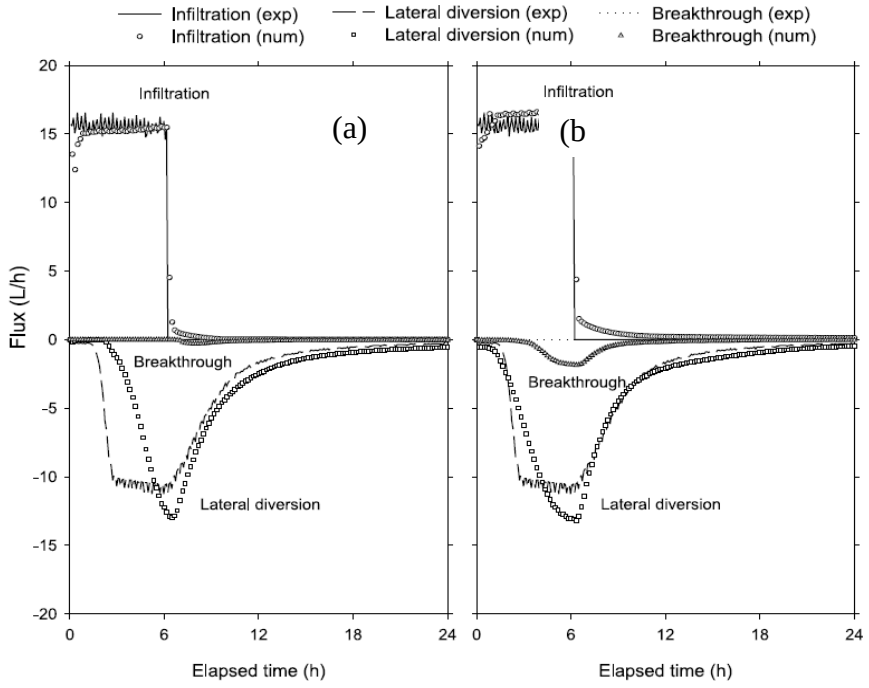

Figure 2.8: Numerical verification of experimental results, (a) analysis with wetting path, (b) analysis with drying path(Tami et al., 2004a)

Numerical investigations were done on a steep inclined capillary barrier cover to explore its performance in both dry and humid climatic condition by Aubertin et al

(2009). Effect of factors like thickness of cover layers, properties of cover materials and precipitation rate on diversion length of the capillary cover was examined. Investigations suggest that 2D transient state analysis are more precise than steady-state analysis to model the capillary barrier effect. The behaviour of these covers varies with time depending on the geometry of the capillary cover, properties of materials and climatic conditions. The analysis shows that capillary barrier covers are more effective in relatively dry climatic conditions(Aubertin et al., 2009). Numerical analysis results indicating the effect of material property and layer thickness on the diversion length of the cover are presented in figure 2.9.

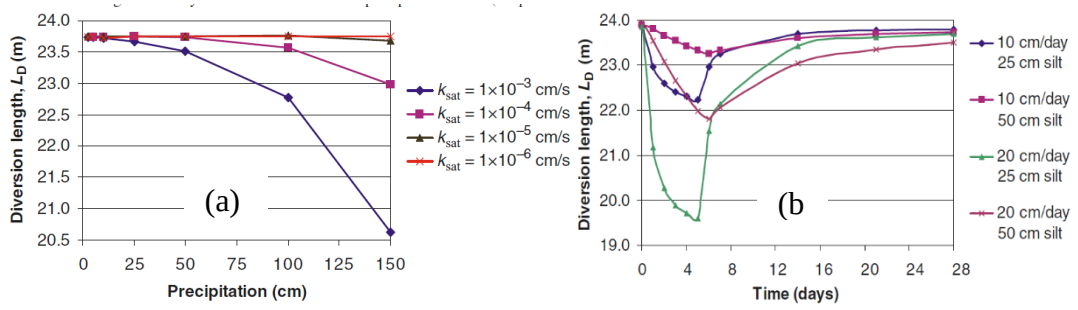

Figure 2.9: Numerical simulation results, (a)variation of diversion length with saturated hydraulic conductivity of fine soil, (b)variation of diversion length with thickness of fine layer(Aubertin et al., 2009)

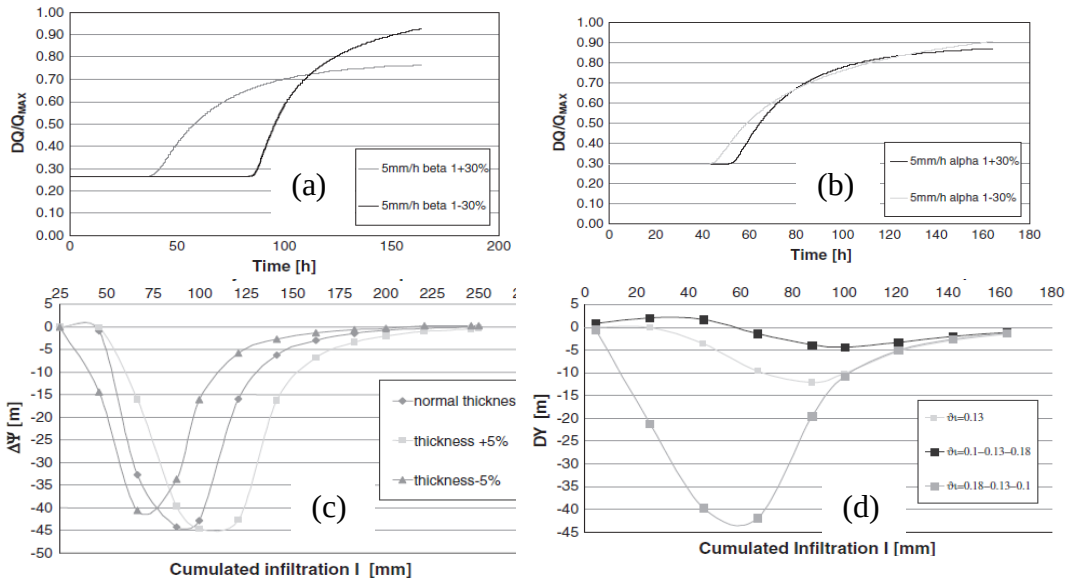

Figure 2.10: Numerical results, (a) variation of normalized water content change with van Ghenucten parameter β, (b)variation of normalized water content with van Ghenucten parameter α, (c)matric suction profile with different layer thickness, (d)moisture content variation along depth(Mancarella, Doglioni, & Simeone, 2012)

Figure 2.10 presents the results of performance analysis of capillary barrier on layered soil deposits on a steep highly conductivity slope by Mancarella et al (2012). Depending on past slope failure experience in May 1998 in Campania, Southern Italy, studies were done on a model with a slope angle of 50^0 by varying the layer thickness, the initial condition of cover and soil water characteristics parameters. From the study, it was concluded that capillary barrier covers are susceptible to more failure rate in prolonging low intensity rainfall events due to higher water storage. Initial moisture condition of cover layers affects the infiltration and performance of cover(Mancarella et al., 2012).

Li et al (2013). investigated the performance of the capillary barrier covers through numerical studies with the SEEP/W program. The effect of three different fine-coarse soil combination such as CL-SC, CL-SM and SC-SM were studied under long-term light rainfall and short-term intense rainfall conditions. Numerical investigations identified CL-SM soil combination perform effectively in both short term and long-term conditions and initial moisture content of capillary barrier cover affects the performance of cover under short-term intense rainfall events, that is cover is more effective when it is sufficiently dry. When adequate drainage measures are provided at the toe of the capillary cover, breakthrough time increases with increasing fine-coarse interface slope angle(Li et al., 2013). Figure 2.11shows the numerical results.

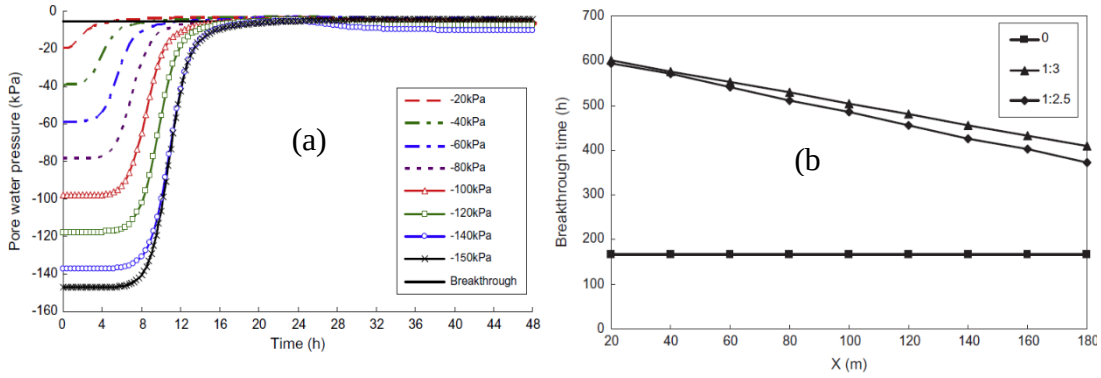

Figure 2.11: Numerical results (a) pore water pressure variation at toe endpoint along the fine-coarse interface with different initial moisture content, (b) breakthrough time variation with different slope angle(Li et al., 2013)

Effects of capillary barrier cover built on steep slope embankments were studied experimentally and numerically by Sato et al (2018). The finite element method was

used to study the inflation into the cover and the circular slip failure mechanism was adopted for slope stability analysis. Analysis results show that even during intense rainfall conditions infiltration into the slope can be reduced to about 65%, diversion length reduces with an increase in saturated permeability ratio($K_{s(fine/coarse)}$) of the fine and coarse layer while deep percolation to inflow ratio increases and stability of steep embankment slope can be increased by effective capillary barrier cover(Sato & Matsumaru, 2018). Figure 2.12 shows the numerical result from the analysis.

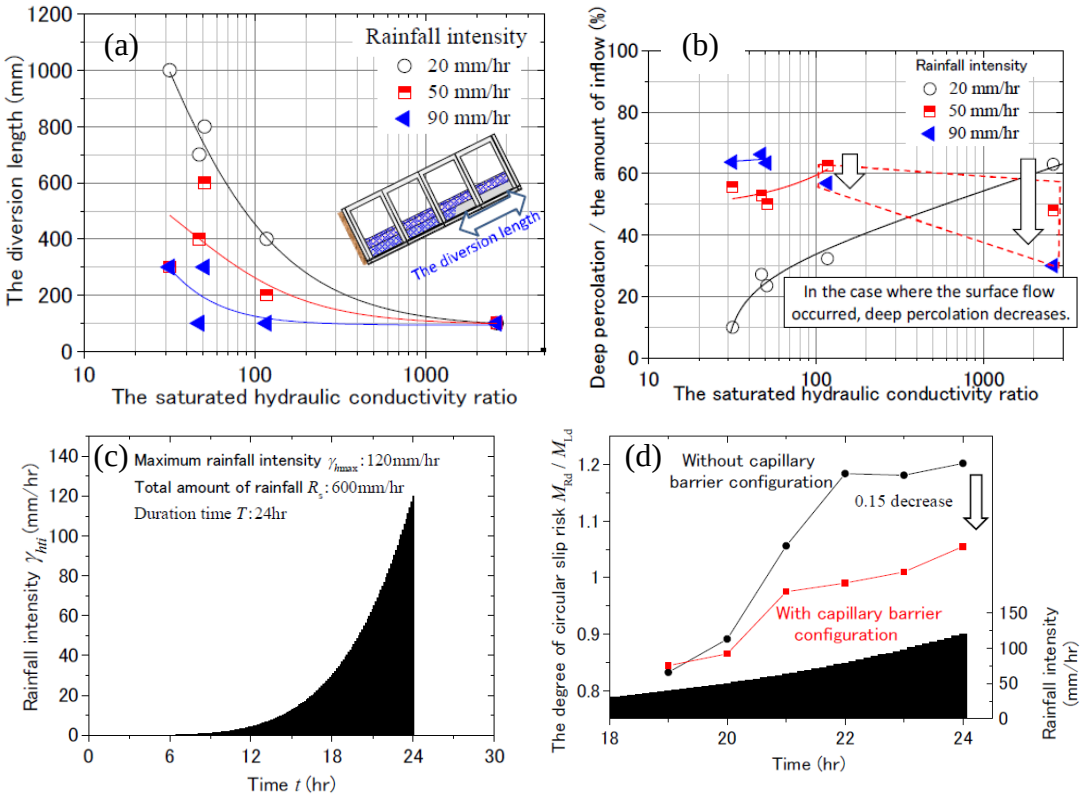

Figure 2.12: Numerical results, (a)variation of diversion length with $K_{s(fine/coarse)}$, (b)variation of deep percolation to inflow ration with $K_{s(fine/coarse)}$, (c)rainfall history used in the study, (d)variation in degree of circular slip risk(Sato & Matsumaru, 2018)

Table 2.1 presents a summary of several other experimental and numerical studies on the capillary barrier effect.

Table 2.2: Summary of Experimental & Numerical studies on capillary barrier cover

Source	Findings
Experimental Study of 1-D Capillary Barrier Model using Geosynthetic material as the Coarse-Grained Layer(Krisdani, Rahardjo, & Leong, 2006)	Capillary barrier effect form in covers with both gravelly sand and geosynthetic material as coarse-grained soil layer, but the latter was more efficient in reducing rainfall infiltration since the permeability of fine layer above the geosynthetic layer was low due to the presence of low-pressure head at the fine-geosynthetic interface.
Water flow through cover soils using modelling and experimental methods(Michel Aubertin, Bussière, Yanful, & De-Souza, 2001)	In cover systems where evaporation is prominent, the use of coupled liquid flow and vapour transport models is preferable than using the pure liquid flow model.
Modelling and field measurements of water percolation through an experimental soil cover on mine tailings(Woyshner & Yanful, 1995)	Properly designed soil cover can be effective in reducing percolation into the soil.
Field data from a capillary barrier and model predictions with UNSAT-H(Khire, Benson, & Bosscher, 1999)	Extreme hydrological events should be considered when designing a capillary barrier cover system. UNSAT-H program predicts the infiltration into the capillary barrier cover more accurately.
On the performance of capillary barriers as landfill cover(Kampf & Montenegro, 1997)b	Under natural climatic conditions, capillary barriers are effective in reducing rainfall infiltration. Lateral diversion, pore pressure distribution in cover and infiltration into the system can be modelled precisely with the numerical model.
A study of infiltration on three sand capillary barriers(Yang,	The capillary barrier effect becomes more effective when using coarse soil with a lower water entry head. When the soil column height is greater than twice the matric suction head of

Rahardjo, Leong, & Fredlund, 2004)	the fine layer the ultimate pore pressure profile is not hydrostatic.
An investigation of factors that influence the water diversion capacity of inclined covers with capillary barrier effects(Aubertin et al., 2006)	Down dip limit point in an inclined capillary barrier cover varied with rainfall intensity. When the precipitation rate increases higher than the critical value the diversity capacity reduces while the DDL point moves toward the upper dip direction along the interface. The effective length of the capillary barrier cover increases with a reduction in saturated hydraulic conductivity of layer materials.
Increasing the diversion length of capillary barriers(Pease & Stormont, 1995)	The transport layer at the bottom of the fine soil layer will increase the diversion capacity of the capillary barrier cover. Capillary covers are more effective in a semi-arid environment than in a humid because of high evapotranspiration and low precipitation.
Infiltration control using capillary barriers for conservation of historical tumulus mounds(Sawada, Mimura, & Yoshimura, 2017)	Studies the possibility of using capillary barriers to protects Tumuli in Japan from rainfall infiltration. Among matric suction, total head, and hydraulic conductivity the latter was identified as the feasible controlling mechanism that affects the water storage capacity of the cover. Material's hydraulic conductivity can be adjusted to control the storage capacity of covers.
Parametric study of unsaturated drainage layers in a capillary barrier(Morris & Stormont, 1999)	Native fine soils which are good rooting medium can be utilized as a fine layer when an unsaturated drainage layer is provided within the capillary barrier while increasing the possibility of using capillary covers in wet climatic conditions too. The diversion length of the cover is directly proportional to the fine-coarse interface angle.

Visualization experiment to investigate capillary barrier performance in the context of a Yucca mountain emplacement drift(Tidwell, Glass, Chocas, Barker, & Orear, 2003)	Fractures and drainage conditions affect the early performance of the capillary barrier and their influence diminishes at the later part of its performance.
Drainage layer fouling as a consideration in capillary barrier design(Ogunro, Podgorney, Inyang, Piet, & Ayoola, 2005)	Static loading reduces the void ratio of cover layer materials which results in a reduction in flow through the fine layer and fouling layer. The coarse soil layer only intrudes in to above lying fine layer due to layer placement and compaction of layers.
Characterizing of a capillary barrier evapotranspirative cover under high precipitation conditions(Zhang, Sun, & Qiu, 2016)	Chances of cover failure are high during consecutive intense rainfall events. Breakthrough in capillary covers occurs when the fine & coarse layer's volumetric water content reaches the critical value. The use of the VODOSE/W program gives more precise results than the HELP program.
Experimental study on dual capillary barrier using recycled asphalt pavement materials(Harnas, Rahardjo, Leong, & Wang, 2014)	Water storage capacity of a dual capillary cover is higher than a traditional single capillary cover. Higher volumetric water content and slower drainage were observed in fine layers of dual capillary cover because of additional layering.

2.5 Research gap

Although capillary barrier covers are effective in reducing rainfall infiltration in to cut slopes, presently in Sri Lanka these types of covers are not used, instead, conventional vegetation covers are being used due to a lack of studies on the applicability of capillary barrier covers with locally available soils and their performance during prolonged intense rainfall events.

3 LABORATORY PHYSICAL MODEL TO STUDY THE EFFECT OF CAPILLARY BARRIER COVER

Before extending the analysis to a cut slope of actual scale with multiple levels of berms it would be prudent to conduct a study with a laboratory scale physical model. For the experimental study, a physical model resembling field condition was constructed. The model dimension, layer thickness and slope inclinations were decided based on the numerical study which will be discussed in chapter 4 of this thesis.

3.1 Design of physical model

From the numerical studies (discussed in chapter 4) and literature study, the influence distance (distance from the walls of the experimental model where the infiltration is affected by boundary effect) was found to be less than 200mm. Based on these studies and the dimension of acrylic sheets (1.8m×1.2m boards, thickness 10mm) available in the market the length of the model was decided to be 1200mm and the width was taken as 600mm. Although there was an initial idea to construct a model with 45^0 slope, due to the above-mentioned limitations model angles of only 30^0 and 15^0 could be used. For the physical laboratory model, effective layer thickness should be determined considering constructability at the laboratory level. Through parametric studies with 2-D numerical simulations (discussed in chapter 4) fine and coarse layer thickness were selected as 20cm and 10cm, respectively. A schematic diagram of the physical model is presented in figure 3.1.

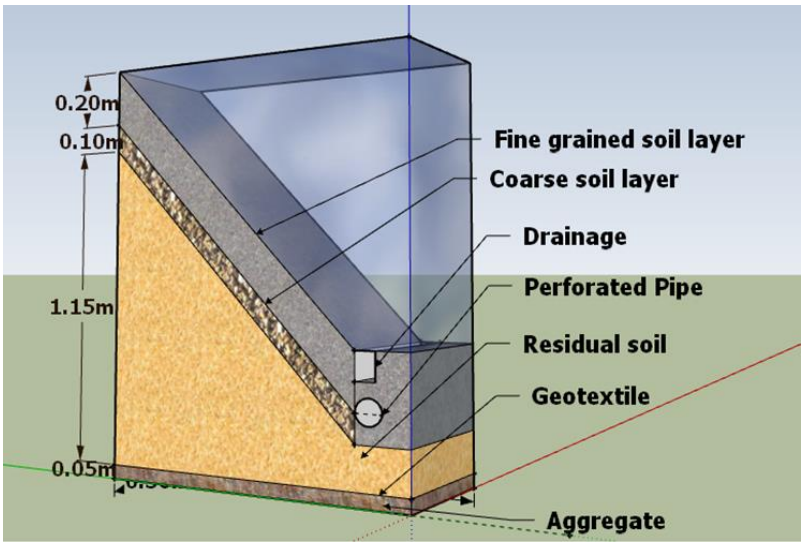

Figure 3.1: Schematic diagram of the proposed laboratory experimental model

The fabrication process involved in the development of the physical laboratory model is shown in figure 3.2.

Figure 3.2: Construction of box for laboratory model with steel frame and acrylic sheet walls on all four sides

3.2 Soil materials used in the physical model

Capillary barrier covers are formed when a fine material having proper contrast in hydraulic conductivity to the coarse layer is placed above a coarse layer. Therefore, CB fine & coarse materials should be carefully selected to construct an effective barrier. The intention was to use locally available river sand and manufactured sand (crushed aggregates) as the fine and coarse layer, respectively. Initially, the properties of these materials were analyzed to assess their suitability in forming an effective capillary barrier cover.

3.2.1 River sand

Fine sand that is obtained from the river basin of Sri Lanka is mainly used as fine aggregate in civil engineering construction works. Since river sand is readily available in bulk, a sample was selected, and its material properties were examined. Through initial experiments following basic soil properties were determined; specific gravity – 2.7, maximum dry density – 1673.8kg/m^3 and optimum moisture content – 7%.

Figure 3.3: River sand

- **Particle size distribution**

The particle size distribution of the selected river sand was determined using dry sieve analysis based on ASTM D422. A 500g of oven-dried sample was sieved through a series of sieves ranging from 5mm – 0.075mm. Figure 3.4 represent the particle size distribution curve obtained.

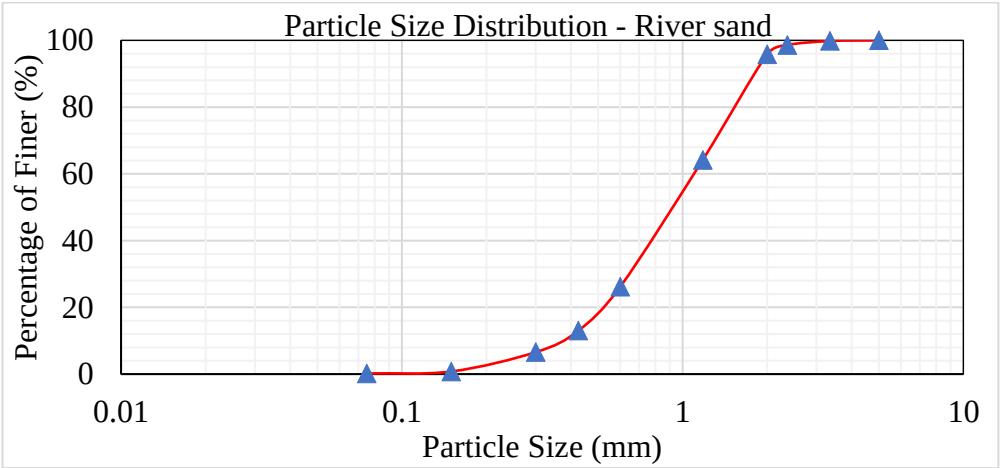

Figure 3.4: Particle size distribution curve – River sand

Unified soil classification

River sand was then classified based on unified soil classification system.

- D60 – 1.12mm (size of 60% finer particles)
- D30 – 0.64mm (size of 30% finer particles)
- D10 – 0.46mm (size of 10% finer particles)
- Coefficient of uniformity, Cu = D60/D10

  = 1.12/0.46

  = 2.44
- Coefficient of curvature, Cc = $D30^2$/(D60*D10)

  = 0.78

Following the unified soil classification system analyzed river sand can be classified as SP (poorly graded sand).

- **Saturated hydraulic conductivity**

Since the saturated hydraulic conductivity of fine soil affects the performance of capillary barrier, K_s of river sand having a dry density of 1580kg/m^3 was determined using a constant head permeability test. The dry density of the sample in the constant head apparatus was controlled by calculating the mass of the sample required to fill the mould, then the sample was filled and compacted with a steel rod. The estimated saturated hydraulic conductivity of river sand is $2.1*10^{-4}$m/s.

- **Soil water characteristic curve**

Soil water characteristic curve (SWCC) represents the relationship between matric suction vs volumetric water content of the soil. SWCC of the materials that are used in the design of the capillary barrier cover should be studied thoroughly prior to the selection of constitutive materials for the cover. Therefore, the SWCC of selected river sand was established experimentally through the method of pressure plate apparatus, method of continuous measurements and obtained through grading curve using empirical methods (Arya & Zapata method, Fredlund Xing method, Zapata method). Figure 3.5 presents the curves obtained through different techniques.

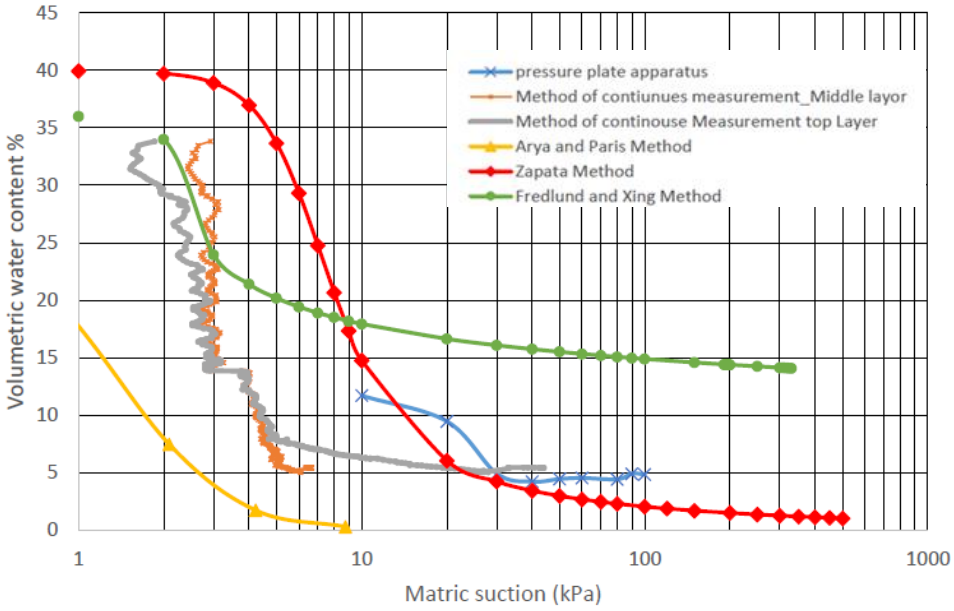

Figure 3.5: Established SWCC through various methods(Muthuhetige & Kulathilaka, 2020)

The best fit curve to be used in the modelling through Geoslope SEEP/W was obtained using Fredlund & Xing method(Fredlund & Anqing Xing, 1994). The curve filling parameters are presented in Table 3.1. Fredlund & Xing best fit parameters were used in numerical simulations to reduce the numerical errors (errors in convergence) in the analysis

Table 3.1: Fredlund Xing best-fit parameters – River sand

Material	$\boldsymbol{\theta_s}$	**Best fit parameters**		
		a(kPa)	m	n
River Sand	0.35	25	0.21	17.23

3.2.2 Manufactured sand

Manufactured sand obtained from the crushing of aggregates is presently used as fine and coarse material in various civil engineering applications due to its wide range of particle size distribution and availability in bulk. Manufactured sand used in this research was purchased from Tokyo super plant. At the beginning of the study, basic properties and SWCC of the manufactured sand were determined through laboratory experiments to check its applicability as a coarse drained soil layer in the capillary barrier cover.

- **Particle size distribution**

The particle size distribution of selected manufactured sand was determined through dry sieve analysis following ASTM D422. Manufactured sand sample of weight 500g of oven-dried sample was sieved through a series of sieves ranging from 10mm – 0.075mm. Figure 3.6 represent the particle size distribution curve obtained through dry sieve analysis. From the graph, it can be seen that the manufactured sand sample has more fine particle which may affect the saturated hydraulic conductivity (factor affecting the formation of capillary barrier effect) of the M-sand.

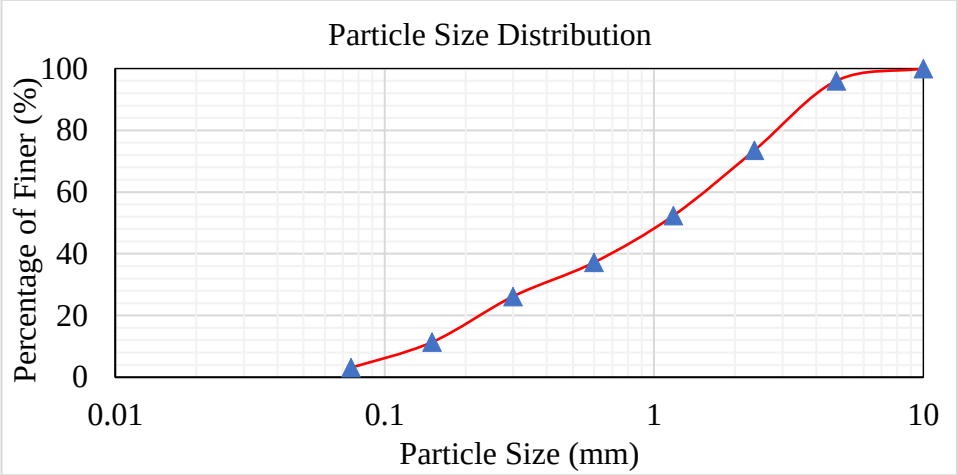

Figure 3.6: Particle size distribution curve – Manufactured sand

<u>Unified soil classification</u>

Manufactured sand was then classified based on unified soil classification system.

- D60 – 1.14mm (size of 60% finer particles)
- D30 – 0.38mm (size of 30% finer particles)
- D10 – 0.14mm (size of 10% finer particles)
- Coefficient of uniformity, Cu = D60/D10

  = 3
- Coefficient of curvature, Cc = $D30^2$/(D60*D10)

  = 0.9

Following the unified soil classification system analyzed manufactured sand can be classified as SP (poorly graded sand).

- **Saturated hydraulic conductivity**

The saturated hydraulic conductivity of the M-sand was determined through a constant head permeability test. The sample was placed inside the mould and compacted using a steel rod to ensure there were no voids in the filling. The estimated saturated hydraulic conductivity of the M-sand is $3.85*10^{-4}$m/s.

Although the saturated coefficient of permeability of M-sand ($3.8*10^{-4}$m/s) is greater than that of river sand ($2.1*10^{-4}$m/s), the values are in the same order. But for the formation of an effective capillary barrier effect, there should exist the proper contrast in their saturated hydraulic conductivity values, that is K_{s_coarse}/K_{s_fine} should be higher. Therefore, to increase the K_s of M-sand by several orders it was decided to remove some percentage of fine particles from the sample and make it much coarser. Since nearly half the percentage (47.6%) of particles is greater than 1.18mm, the suitability of particles that are retained on 1.18mm sieve was studied. Figure 3.7 shows the M-sand sample sieved and retained on a 1.18mm sieve. Based on UCS selected M-sand(coarse) is classified as SP.

Figure 3.7: M-sand sieved and retained on 1.1.8mm sieve

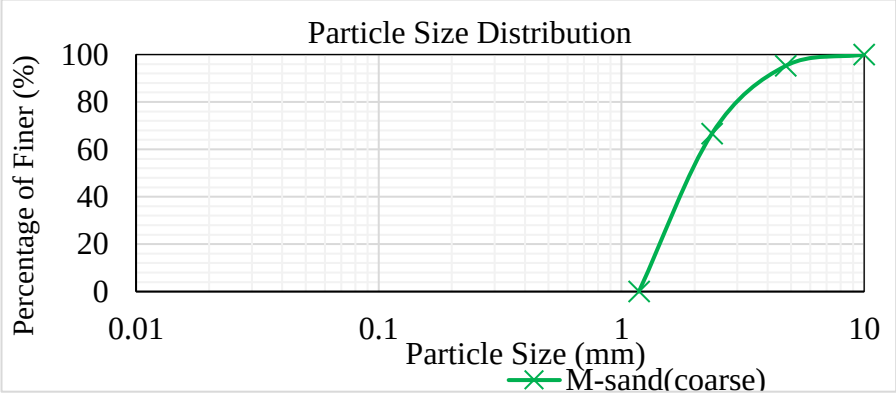

Figure 3.8: Particle size distribution curve - M-sand(coarse)

Saturated hydraulic conductivity of particles retained on 1.18mm sieve was determined using a constant head permeability test. The estimated saturated hydraulic conductivity of the M-sand is $2.8*10^{-2}$m/s. Since M-sand retained on 1.18mm have a saturated coefficient of permeability of higher order than the river sand, it can be utilized to form the effective capillary barrier cover.

- **Soil water characteristic curve**

SWCC of M-sand sieved and retained on 1.1.8mm sieve was established experimentally through the method of pressure plate apparatus, method of continuous measurements and empirically(Arya & Zapata method, Fredlund Xing method, Zapata method)(Muthuhetige & Kulathilaka, 2020). Figure 3.9 shows the SWCC obtained through experimental and empirical methods. It can be observed that SWCC from the method of continuous measurements agreed closely with the Fredlund Xing method as compared to the other methods.

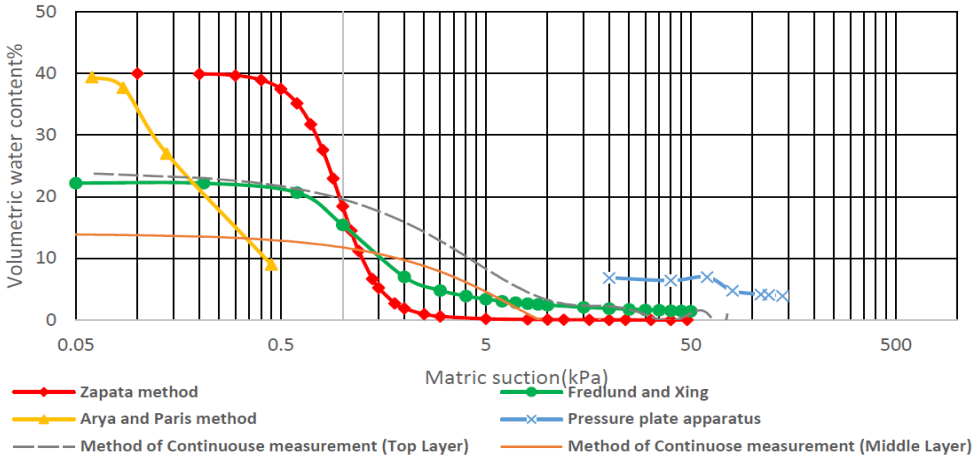

Figure 3.9: Established SWCC through various methods(Muthuhetige & Kulathilaka, 2020)

For the numerical simulations with Geoslope SEEP/W, the best fit parameter in Table 3.2 were used to reduces the possible errors in convergence.

Table 3.2: Fredlund Xing best fit parameters – M-sand(coarse)

Material	$\boldsymbol{\theta_s}$	**Best fit parameters**		
		a(kPa)	m	n
M-sand(coarser)	0.22	0.9	0.38	3.83

3.2.3 Sri Lankan Residual soil

In Sri Lanka majority of cut slopes are formed of residual soils the product of weathering of the parent rock. A representative sample of residual soil was used in both experimental and numerical study to resemble the field scenario. Engineering properties and SWCC of the soil were obtained by a previous research study on this material by Kulathilaka and Dhananjaya was used in this research study. Table 3.3 presents the basic properties of the residual used in this research(Dhananjaya & Kulathilaka, 2019).

Table 3.3: Basic soil properties – Residual soil

Basic soil properties	
Specific gravity	2.64
Maximum dry density	1589kg/m^3
Optimum moisture content	21.8%
LL	46.2
PL	41.6
PI	4.6
Saturated hydraulic conductivity	1*10^{-5}m/s

Fredlund & Xing best fit parameters were used in the establishment of SWCC of the residual soils in the numerical simulations with Geoslope SEEP/W. Table 3.4 presents the best-fit parameters used in the study.

Table 3.4: Fredlund Xing best fit parameters – Residual soil

Material	$\boldsymbol{\theta_s}$	**Best fit parameters**		
		a(kPa)	m	n
Residual soil	0.55	13	4.8	0.97

3.3 Instrumentation in the physical model

Rainfall experiments were performed on the physical model that was fabricated. An experimental study was carried out for the capillary barrier covers with slope angles

15^0 and 30^0 made of river sand as a fine layer and M-sand as a coarse layer. Instrumentation was done to monitor the matric suction and moisture content. Three tensiometers and five moisture sensors were used for the monitoring. Volumetric water content variation in capillary barrier cover layers was measured using the moisture sensors (figure 3.10(a)). Continuous reading throughout the experiment was read and recorded using the Wisco DL2200 data logger (figure 3.10(b) 8-channelled logger). Then the recorded results were analyzed using an MS Excel spreadsheet. Prior to the experiment the used each moisture sensors were calibrated manually (discussed in the appendix) for the different type of soils including river sand, M-sand coarser and residual soil since data logged using the logger were in voltages. Pore water pressure variation in the capillary barrier layers was not measured because of the difficulty in installing the KU tensio meters in these layers with considerably smaller thickness.

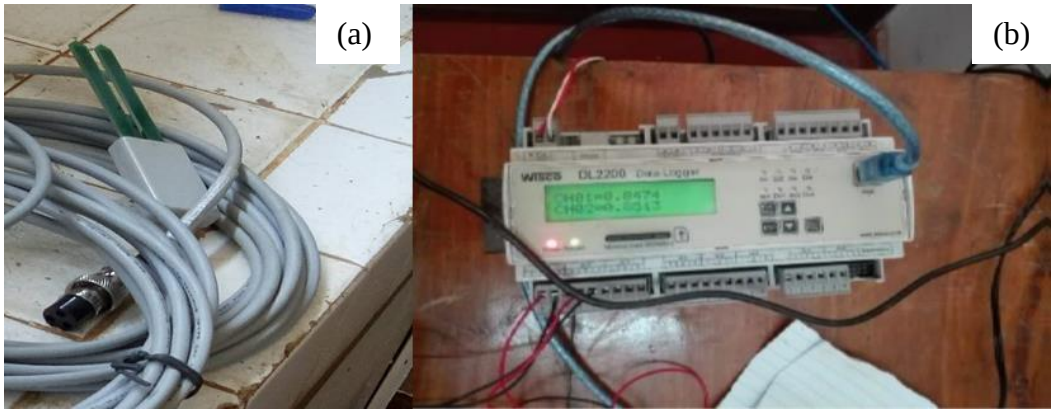

Figure 3.10: (a) moisture sensor, (b) Wisco DL2200 data logger

KU tensiometers(Jotisankasa, Porlila, Wissanupong Soralump, & Mairiang, 2007) were utilized to measure the pore water pressure variation in the residual soil slope beneath the capillary barrier cover. Three tensiometers were installed in the soil to measure the loss of matric suction due to any possible infiltration to the slope in case of any failure in the capillary barrier cover. Using the data logger continuous measurements were read and recorded throughout the experiment. Measured data were analyzed using an MS Excel spreadsheet. Installed tensiometers were properly sealed with a blue tag and adhesive tapes to avoid any possible desaturation that could occur due to contact of tensiometers with the air. As a precautionary measure tensiometer readings were monitored frequently to checked for potential desaturation. Figure

3.11(a) shows laboratory type KU tensiometer used in the measurement and figure 3.11(b) illustrates how the tensiometers were sealed from the outer atmosphere to avoid desaturation.

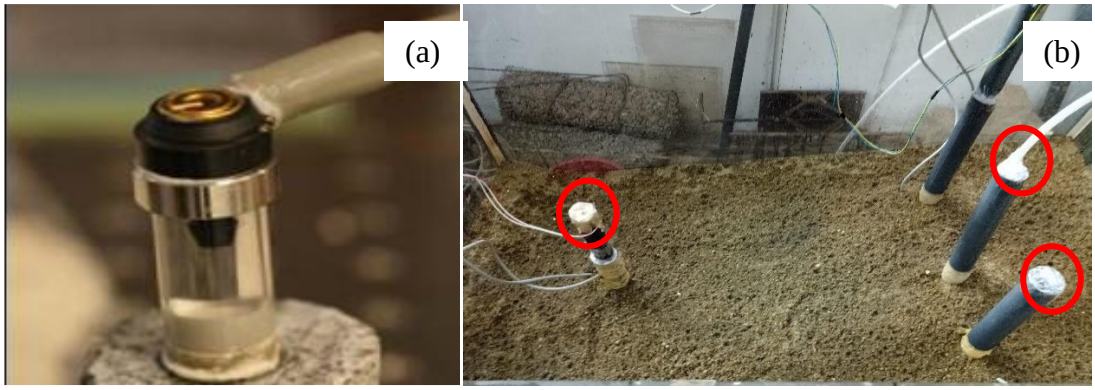

Figure 3.11: (a) KU tensiometer, (b) sealed end of tubes in which the tensiometers were installed

3.4 Development of the physical model with 15^0 slope angle

3.4.1 Building up of the model

Laboratory physical model was made at the slope angles of 15^0 and 30^0. The initial experiments were done with the model having a fine-coarse interface angle of 15^0. Capillary barrier cover was constructed with 20cm thick river sand over 10cm thick M-sand layer underline by residual soil layer. These layer thicknesses were decided based on the results of the numerical study presented in chapter 4. A 5cm thick aggregate layer was placed at the bottom of the model to drain out any infiltration that enters the system. Figure 3.12 illustrates the schematic diagram of the experimental model that was used in the study.

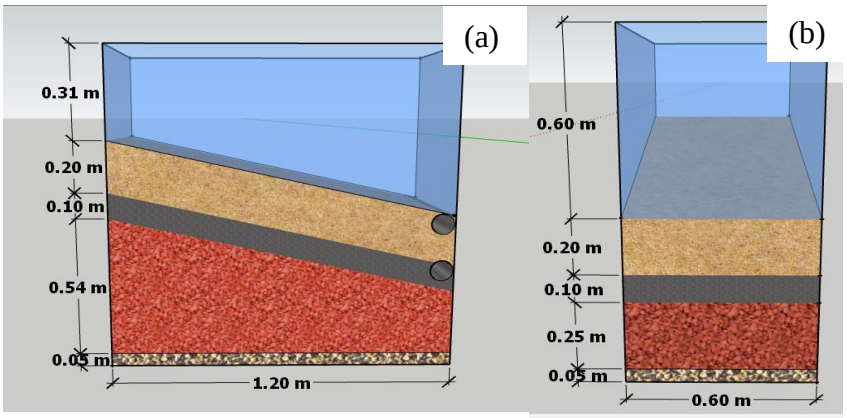

Figure 3.12: Schematic diagram of the constructed laboratory model, (a) side view, (b) front view

In the experimental model, geotextile was used in between each layer to avoid possible mixing of materials at the interface. Residual soil layer with slope angle 15^0 was placed over the aggregate layer and was compacted to a density of 1589kg/m^3. The soil sample was mixed with water and prepared to a moisture content of 15% before filing. The soil was placed in 20cm thick layers and compacted to a thickness of approximately 15cm using a wooden hammer. Rammer was not used in compacting any soil layers during the construction of the physical model to prevent damage to acrylic sheet walls.

River sand and M-sand were initially sufficiently air-dried before placing into the box to ensure that they were dry enough to form the capillary barrier effect when placed on top of each other. The moisture content of air-dried river sand and M-sand were 4% and 2% respectively. These layers were placed in 15cm thick layers and compacted to a 10cm thickness. Table 3.5 illustrates the density of each fill layers and the amount of soil mass that was placed and compacted to achieve each layer with the required thickness and density.

Table 3.5: Masses of each soil type used in the model

Soil	**Dry density (kg/m^3)**	**Moisture content (%)**	**Required weight (kg)**
Residual soil	1580	15	558.6
River sand	1580	4	236.6
M-sand	1577	2	115.8

Figure 3.13 illustrates the staged construction process involved in the development of a laboratory physical model. During the filling of the residual soil layer and other capillary barrier cover layers as shown in figure 3.14 along the top boundary with acrylic wall thin polythene sheet was placed to avoid any possible leakage into the soil layer through the soil wall interface.

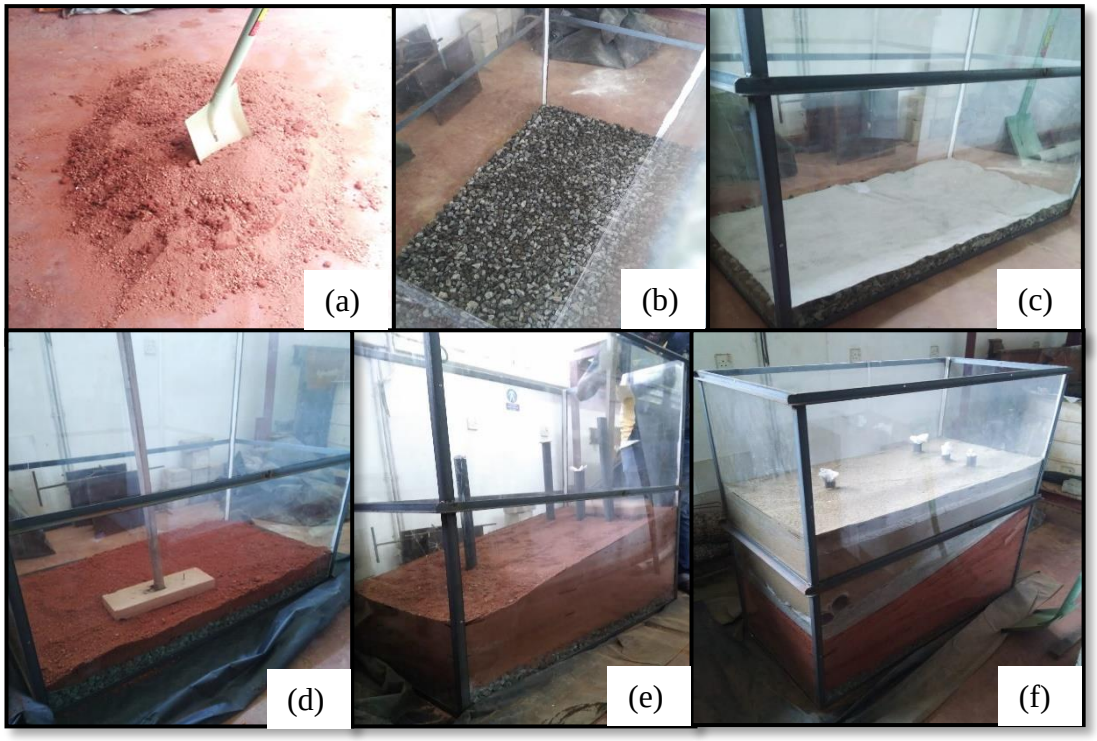

Figure 3.13: Construction stages, (a) sample preparation, (b) bottom drainage layer filling, (c) use of geotextile in between drainage and residual soil layer, (d) placing soil in layer and compacting using a wooden hammer, (e) installed PVC pipes for installing tensiometers at different depth in completed residual soil fill, (f) completely developed physical model

Figure 3.14: Installation of thin polythene layer along soil-acrylic sheet wall interface.

Also, 02 number of 5cm diameter perforated PVC pipes wrapped with geotextile were used at the toe of the model to enhance sufficient drainage in the capillary barrier cover. Figure 3.15 shows the perforated 5cm diameter drainage pipe.

Figure 3.15: Perforated PVC pipe used as a drain

Figure 3.16 shows the location where the toe drains were installed in the model to drain out any lateral diversion along the fine-coarse interface and to remove possible surface runoff from the fine sand layer. These drains will ensure that there is no accumulation of water at the down-dip part of the model.

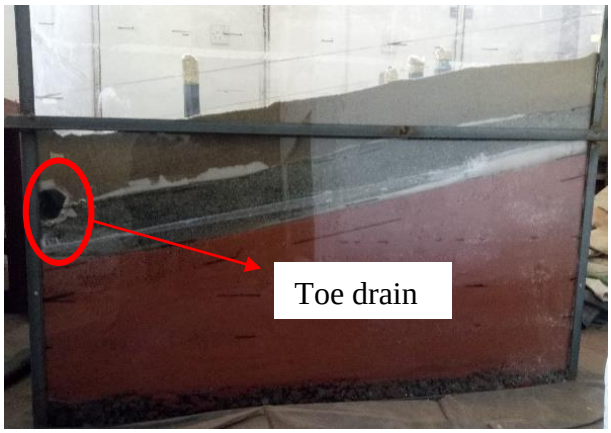

Figure 3.16: Installed toe drain in the model

3.4.2 Instrumentation layout for model with 15^0 slope

Locations where the tensiometers and moisture sensos were installed in the experimental model are denoted in figure 3.17. At the beginning of the rainfall experiments, a moisture sensor denoted by CH7 was installed at the mid-depth of the fine sand layer at the same cross-section as in the diagram. But later it was moved downwards to the fine-coarse interface because it is essential to measure the lateral diversion rather than the infiltration. Figure 3.18 shows the installation process of moisture sensors and a fully instrumented model ready for rainfall experiment.

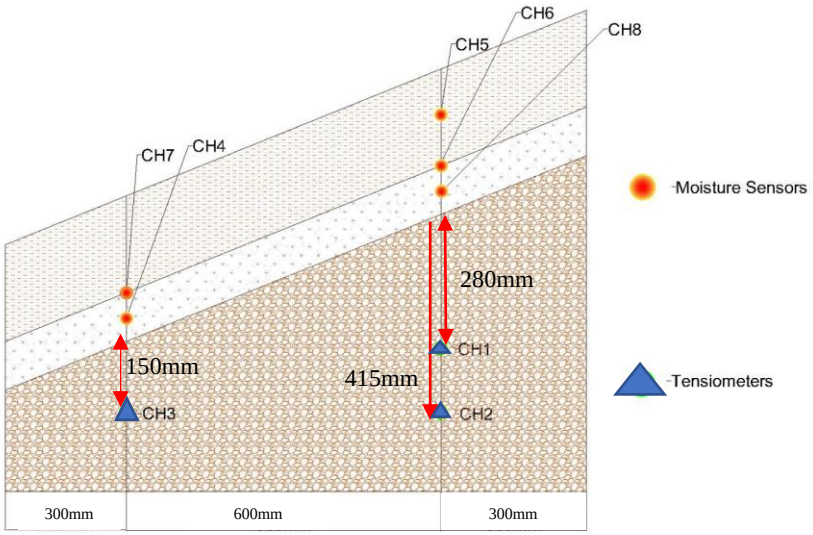

Figure 3.17: Locations where moisture sensors and tensiometers were installed in the model

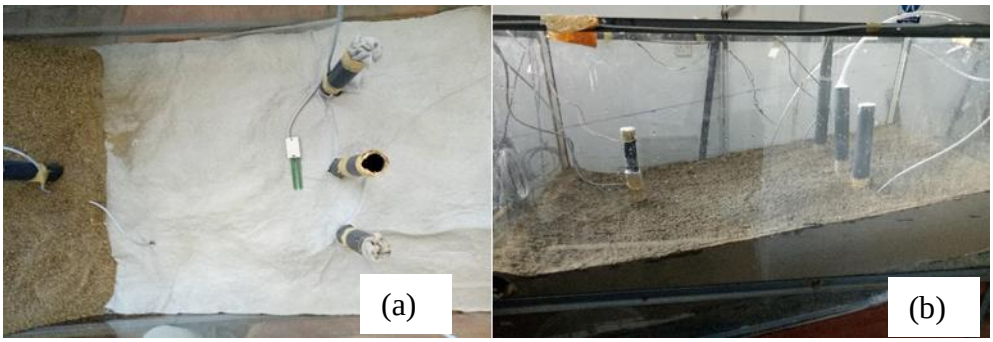

Figure 3.18: (a) installation of moisture sensor along mid of river sand (CH5), (b) fully instrumented model with moisture sensors and tensiometers.

3.4.3 Rainfall simulations used in the model with 15^0 slope

Experimental studies were carried out for slope with 15^0 for short duration low intense rainfall and prolonged intense rainfall to study the performance of capillary barrier cover under different circumstances.

- **Short term low intense rainfall**

The effect of short duration low intense rainfall on this capillary barrier model was studied by simulating a rainfall of intensity 5mm/hr into the model in the manner illustrated in figure 3.19. The maximum and minimum durations of rainfall applied were 8 hours and 1hour, respectively.

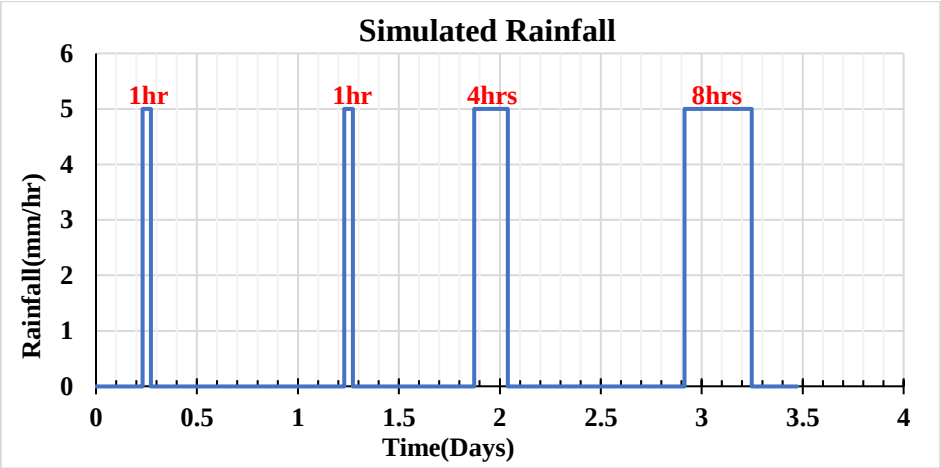

Figure 3.19: Simulated short-term rainfall pattern – 15^0 slope

Rainfall was applied to the model by the method of sprinkling water using a bucket from the adequate height above the surface of the model. Water was sprinkled at 15minutes interval to the model. The following method was used to estimate the volume of water that should be sprinkled at each time to stimulate 5mm/hr rainfall in the model.

- Surface area of the model = $0.745m^2$
- Total volume of water that enters the model for 1hour during 5mm/hr rainfall = 0.745×0.005
  $= 0.00373m^3$
  $= 3.72$ litres
- Volume of water to be sprinkled each time = 3.72/4 = 0.93 litres

Therefore 0.93 litres of water should be sprinkled each 15 minutes interval to simulate the 5mm/hr rainfall into the model.

- **Prolong intense rainfall**

Later after the first set of rainfall experiments to study the effect of short-term low intensity rainfall on the developed capillary barrier cover model, the system was allowed to dry sufficiently under the effect of lateral diversion and evaporation for the period of 03months. Then the second rainfall experiment was done on the model to check the effect of prolonging intense rainfall event. Applied rainfall intensity varies from 5mm/hr – 20mm/hr during this investigation. Simulated rainfall to the

experimental model during the second set of rainfall experiments is presented in figure 3.20.

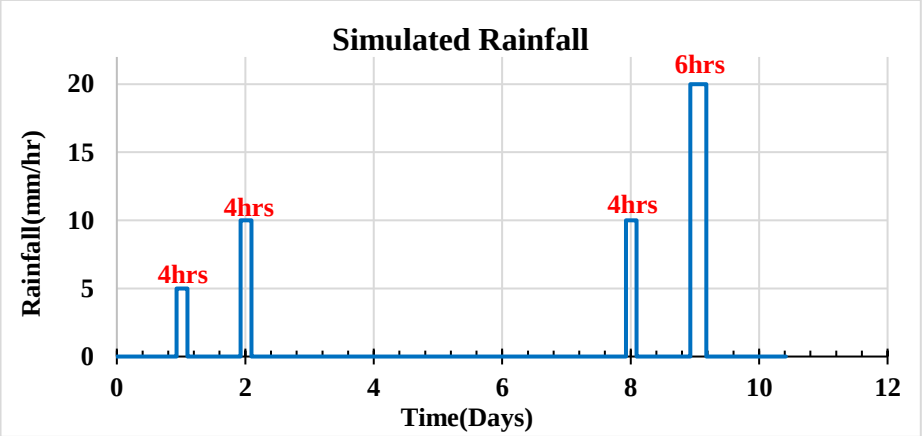

Figure 3.20: Simulated prolong intense rainfall pattern – 15^0 slope

As explained earlier method of sprinkling water using a bucket was used to apply the rainfall to the model. From the estimations, 1.86 litres of water was applied to the model in 15 minutes interval to stimulate 10mm/hr rainfall while 3.73 litres of water was sprinkled at 15 minutes interval for 20mm/hr rainfall.

3.5 Development of the physical model with 30^0 slope angle

3.5.1 Building up of the model

The model box was refilled from initial steps to develop the capillary barrier cover model with a slope angle of 30^0 so that the effect of increasing the interface angle on the performance of the capillary barrier cover with river sand and M-sand could be studied. Fine and coarse layers were removed from the earlier model and allowed to air dry for 2 weeks so that almost all moisture from the materials could be removed. The residual soil layer was also removed and prepared again to optimum moisture content and filled back in the model to form a 30^0 slope. Figure 3.21 shows the air-drying process of capillary barrier layer samples and a fully constructed and instrumented physical model for the rainfall experiments. As indicated in figure 3.21(d) toe drains were installed along the surface of the fine layer and fine-coarse interface at the toe end of the model to drain surface runoff and lateral diversion from the model. A schematic diagram illustrating the dimensions of the constructed experimental model is given in figure 3.22.

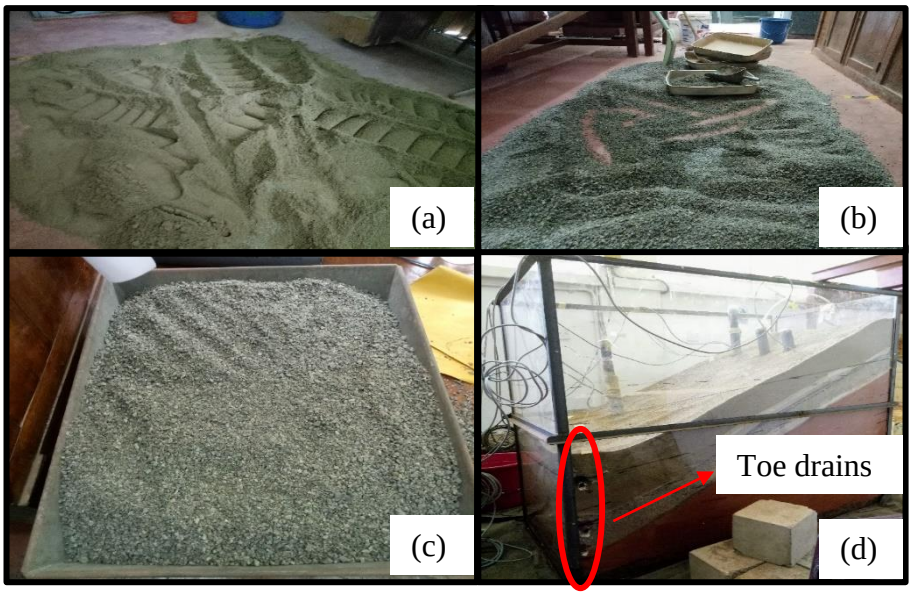

Figure 3.21: Construction stages, (a) air drying the river sand, (b) air drying the M-sand, (c) air dried M-sand sample ready for filling, (d) Fully constructed and instrumented 30^0 slope model

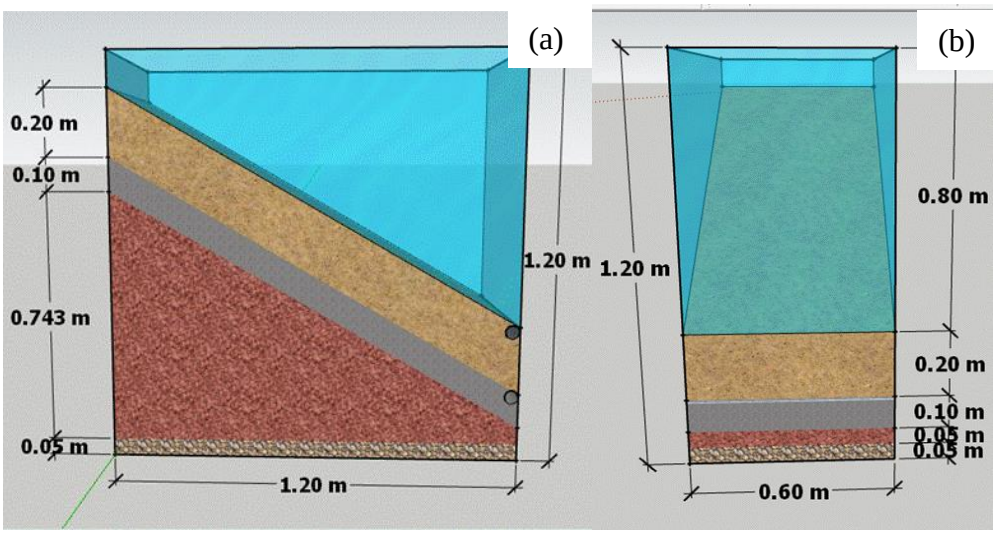

Figure 3.22: Schematic diagram of the experimental model, (a) side view, (b) front view

3.5.2 Instrumentation layout for model with 30^0 slope

Figure 3.23 shows the locations where the moisture sensors and tensiometers were installed in the model to monitor the behaviour during the rainfall experiment. In both experimental models with 15^0 and 30^0 slopes, volumetric water content variation in the residual soil layer was not measured due to limitation in the number of sensors that could be attached to the DL2200 data logger (only 8 channels were available in the used data logger) and shortage in moisture sensors.

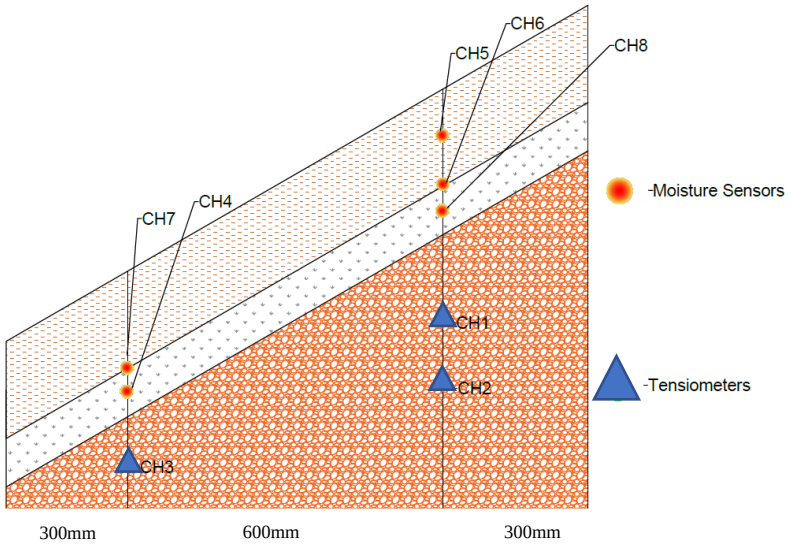

Figure 3.23: Locations where moisture sensors and tensiometers were installed in the model

3.5.3 Rainfall simulations used in the model with 30^0 slope

Performance of capillary barrier cover with fine-coarse interface angle 30^0 under prolong intense rainfall event was investigated by carrying out rainfall experiments for the given rainfall pattern in figure 3.24. Varying rainfall intensity from 5mm/hr to 20mm/hr was applied to the system for 7 continuous days. The maximum duration of rainfall for a single day was 8 hours and the worse rainfall event could be the 6 hours duration of 20mm/hr rainfall.

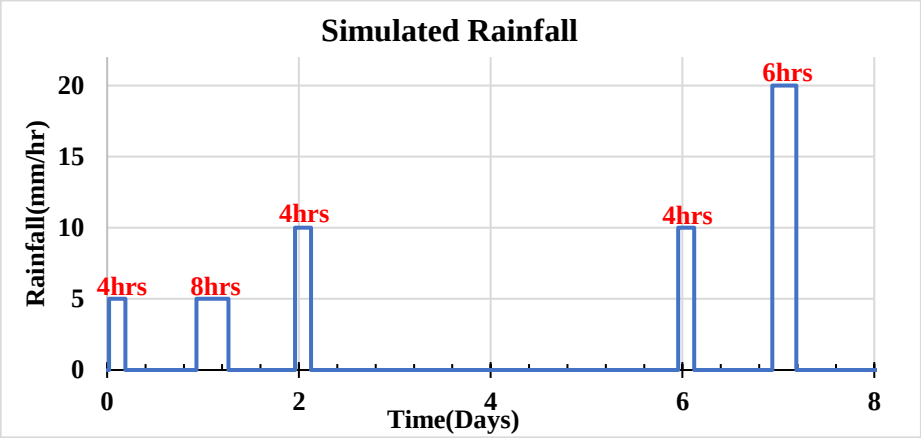

Figure 3.24: Simulated prolong intense rainfall pattern – 30^0 slope

The method of sprinkling water was used to simulate the rainfall. 1.86 litres of water was applied to the model in 15 minutes interval to simulate 10mm/hr rainfall while 3.73 litres of water was sprinkled at 15 minutes interval for 20mm/hr rainfall.

3.6 Results of the rainfall experiments

Moisture sensor readings and tensiometer readings which were read and recorded by the method continuous measurements were plotted against time. The measurements from the sensors were in the form of voltage values, these values were converted to matric suction and moisture content using suitable calibration factors established earlier.

3.6.1 Model with 15^0 slope angle

- **Changes during the short-term low intense rainfall**

Figure 3.25 presents the variation of volumetric water content along the mid depth of the fine layer determined from moisture sensors. Reading from CH5 (installed at upper part) shows that volumetric water content in the fine layer has increased from an initial value of 3.5% with each rainfall due to accumulation of infiltration into the fine layer (maximum recorded moisture content was 13.8% - during 8 hours rainfall). After the first rainfall increased moisture content to 8.5% has not reduced, but after all other rainfalls increased moisture content has reduced with time. Probably this may be due to the movement of moisture to the fine-coarse interface. CH7 was installed in the mid of the fine layer at the bottom of the model only during the first 2days, later it was moved to the fine- coarse interface. At the end of the second rainfall, the CH7 reading has reached to value of 7.6% from an initial value of 2%.

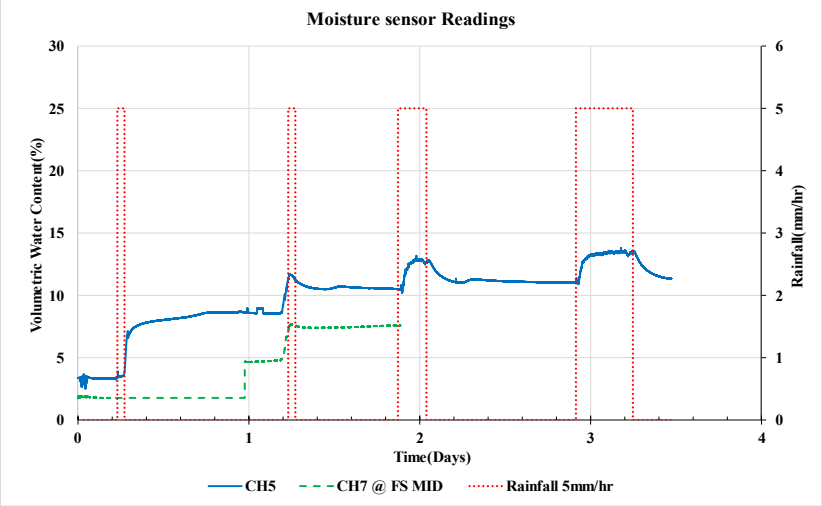

Figure 3.25: Variation of volumetric water content along mid of fine layer during low intense rainfall – 15^0 slope

Volumetric water content variation along the fine- coarse interface measured with CH6 (upper part of the model) and CH7 (bottom part of the model) is shown in figure 3.26. Reading from CH6 (upper part of the model) was stable around its value of 4% without any variation until the 6 hours rainfall on the third day. The infiltration has reached the fine-coarse interface at the upper part of the model after the third-day rainfall. At the end of the third-day rainfall moisture content at CH6 has raised drastically to a value of 25%. Thereafter the moisture content at CH6 at the interface remained constant and experienced another moderate increase during 6hrs long rainfall. At the end of rainfall, a reduction could be seen. and variation was considerably slow during the rainfall following that with a maximum of 22%. Reading of CH7 (at the lower part of the model0 increased to a value greater than that of CH6. It experienced a drop when the rainfall ended, and another increase could be seen at the 6hrs rainfall.

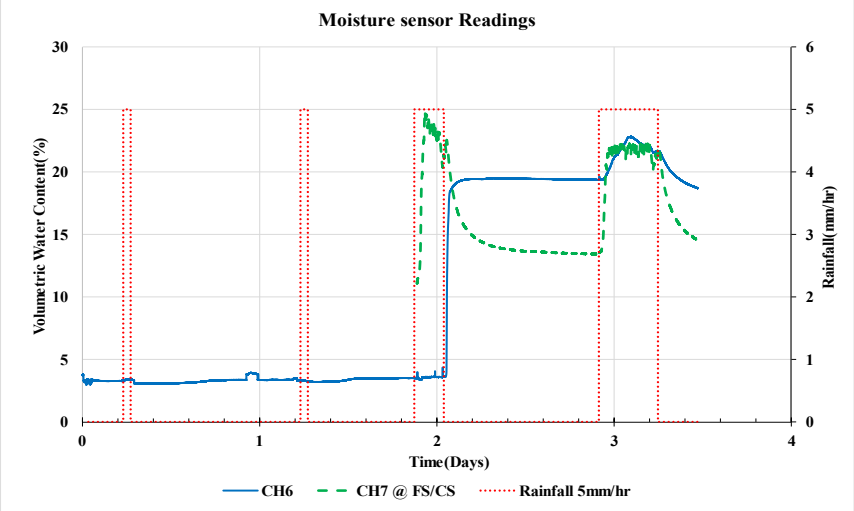

Figure 3.26: Variation of volumetric water content along the fine-coarse interface during low intense rainfall – 15^0 slope

Figure 3.27 presents the measured volumetric water content along the mid depth of the coarse layer. There was no change in the initial moisture content of 7% at CH8 (upper part of the model) until the 6 hours duration rainfall on the fourth day. But at CH4 a gradual increase of moisture content can be seen after the first rainfall. With each rainfall event, there is an increase in moisture content taking value from 10% to 16%. This may be due to failure in cover caused by the accumulation of infiltration and lateral diversion in the toe of the model.

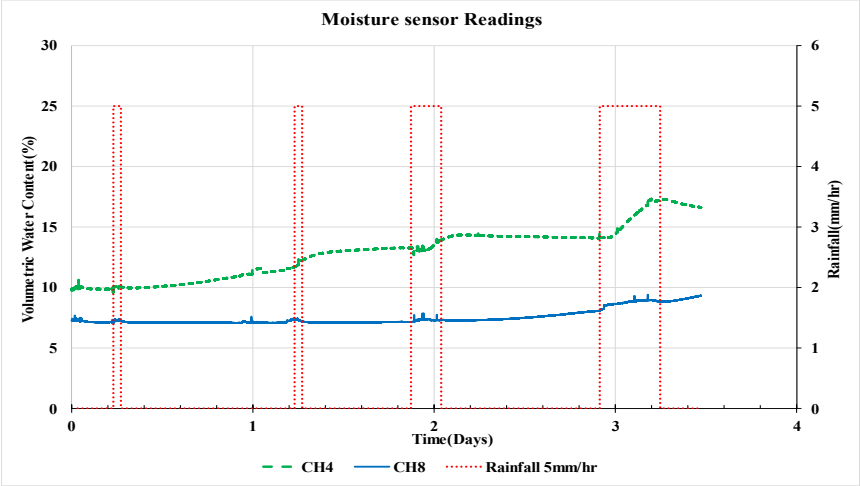

Figure 3.27: Variation of volumetric water content along mid of coarse layer during low intense rainfall – 15^0 slope

Matric suction variation measured by tensiometers installed in residual soil with time is shown in figure 3.28. Measured tensiometers readings remained almost the same during the first two-day rainfall for shorter durations. But the matric suction value has depleted in CH3 (at the lower level) and reached 18kPa from 22kPa after the second-day rainfall, this may be due to breakthrough in capillary barrier effect at downdip of model. Reading at the other two tensiometers has reduced from around 30kPa to 25kPa after the 4 hours duration rainfall on the third day. Reduced matric suctions then remained almost stable around 25kpa after that.

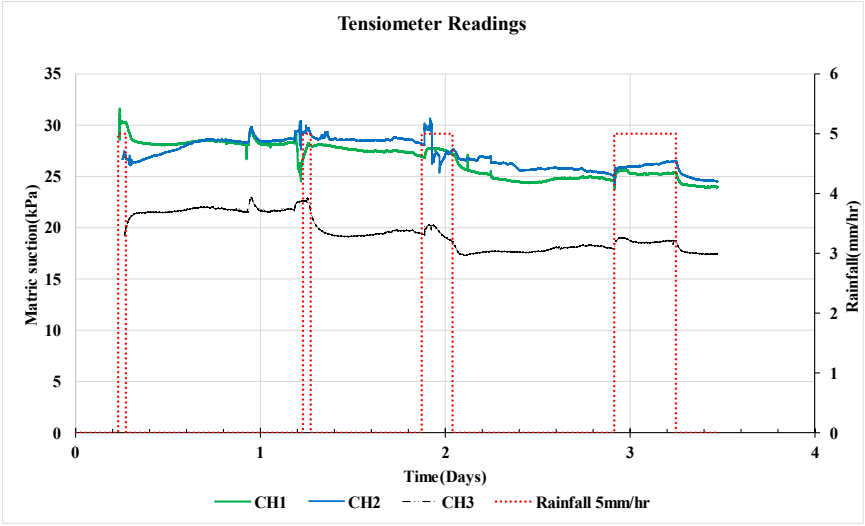

Figure 3.28: Variation of matric suction in tensiometers CH1, CH2 and CH3 during low intense rainfall – 15^0 slope

- **Changes during the prolong intense rainfall**

Effect of intense rainfall event with a maximum of 20mm/hr rainfall for a longer duration was studied with this rainfall event, where results discussed earlier were for low intensity (5mm/hr rainfall) shorter duration rainfall.

Figure 3.29 shows the variation in volumetric water content measured along the mid depth of the fine layer in the upper part of the model. Initial measured moisture content in CH5 was 4%. At each rainfall events, there is an increase in the moisture content. This increase was greater for rainfalls of higher intensity. At the end of rainfall events, the moisture content has reduced due to the downward movement of water along the fine layer. The measured maximum moisture content was 17% (during 20mm/hr rainfall).

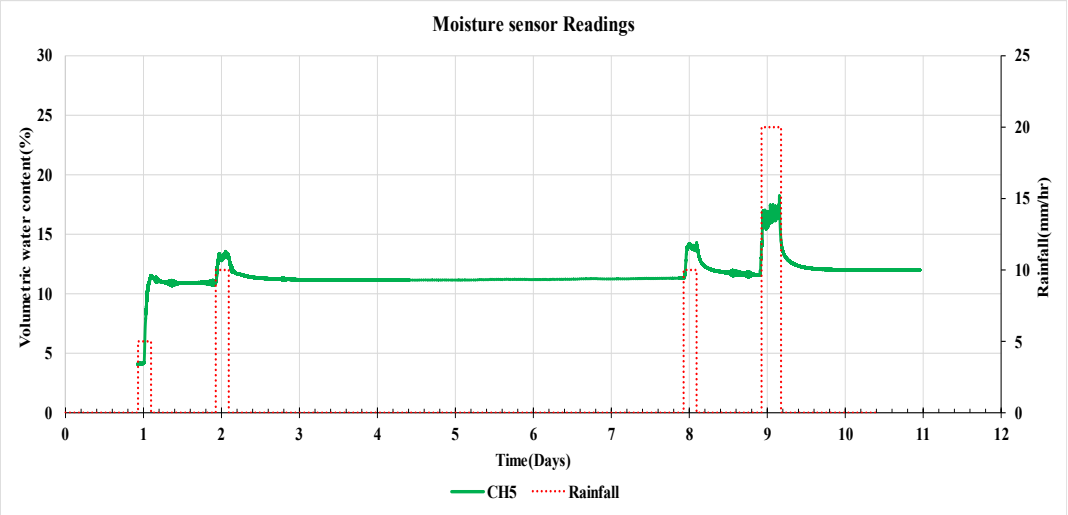

Figure 3.29: Variation in volumetric water content along the mid depth of the fine layer during prolong intense rainfall – 15^0 slope

Moisture content variation along the fine/coarse interface is presented in figure 3.30. CH6 installed at the upper part of the model has a slightly lower increase in moisture content than CH7 which was installed at the lower part of the model while their initial moisture content was around 5%. This was due to the accumulation of moisture in the down-dip direction through lateral diversion along the fine layer during the development of the capillary barrier effect. Maximum moisture content in CH7 reached 28% and at CH6 to 25% during 20mm/hr rainfall. In contrast to the rate of increase of moisture content during rainfall, the rate of reduction of moisture after each

rainfall was comparatively high in the bottom part of the model than the upper part. This is due to the removal of infiltration through provided toe drains.

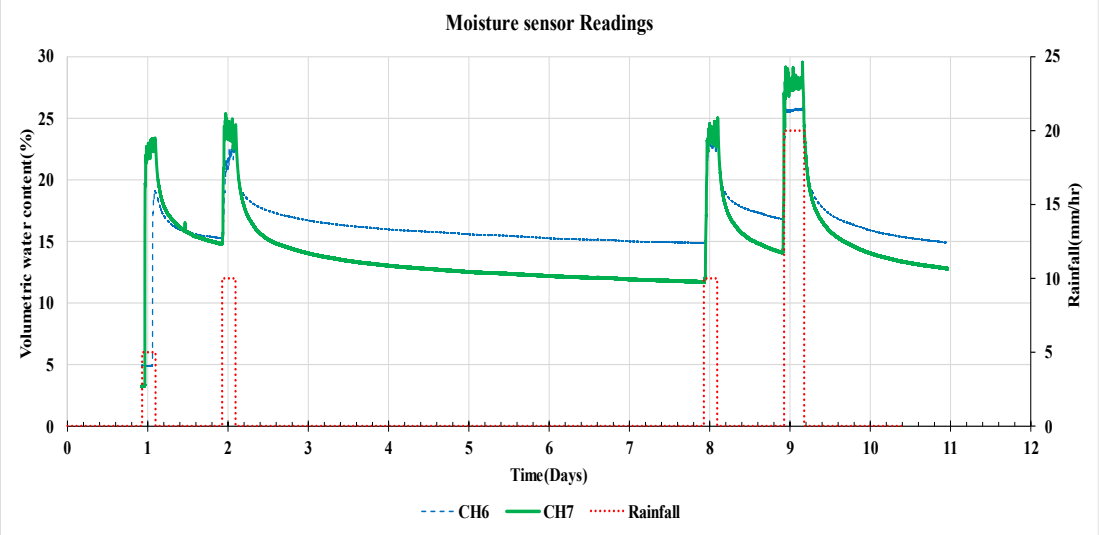

Figure 3.30: Variation in volumetric water content along the fine-coarse interface during prolong intense rainfall – 15^0 slope

Figure 3.31 shows the volumetric water content measured along the mid depth of the coarse layer.

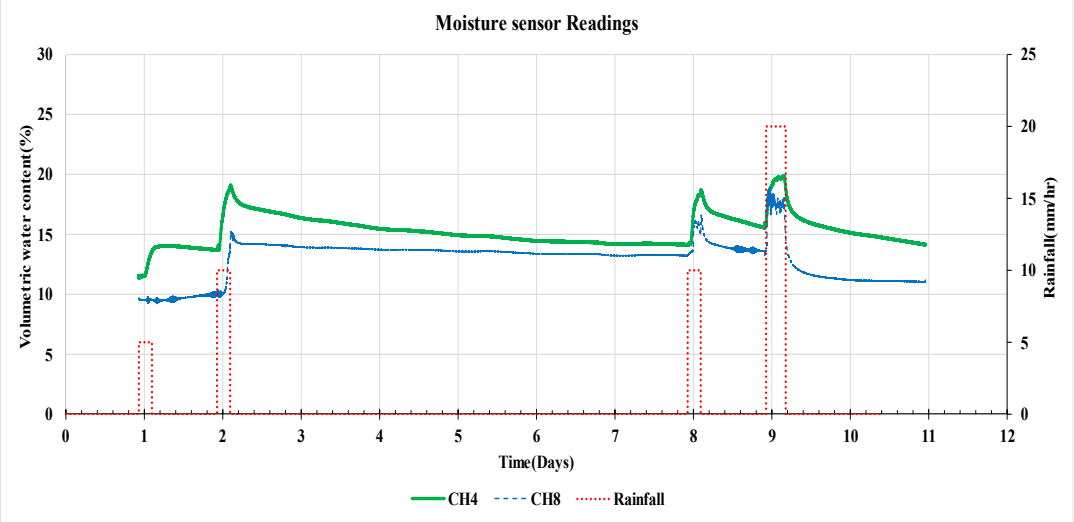

Figure 3.31: Variation in volumetric water content in mid of coarse layer during prolong intense rainfall – 15^0 slope

Initial moisture contents were 10% and 11.2% in CH8 and CH4, respectively. An increase of moisture content was observed in CH4 at the lower part of the model from the first rainfall itself. In CH8 at the upper part of the model, an increase could be seen

from second rainfall only. Throughout the experiment, the moisture content at the lower part (CH4) remained greater than that at the upper part (CH8). The reduction of moisture content at the end of each rainfall event was seen at both CH4 and CH8. The reduction rate was somewhat higher at the upper levels. Measured maximum moisture content in CH4 and CH8 were 20% and 17% respectively.

Variation of matric suction in residual soil prevailed in all three locations during prolong rainfall events are presented in figure 3.32. Initial matric suction measured in CH1, CH2, CH3 were18kPa, 25kPa and 19kPa, respectively. There was a reduction from 19kPa to 18kPa at CH1 with the first rainfall. Thereafter, the value remained constant until it went out of service 6 days later. Matric suction at CH2 and CH3 also have experienced a loss at the start of the rainfall events. However, throughout the 6days period matric suctions were remained at constant values.

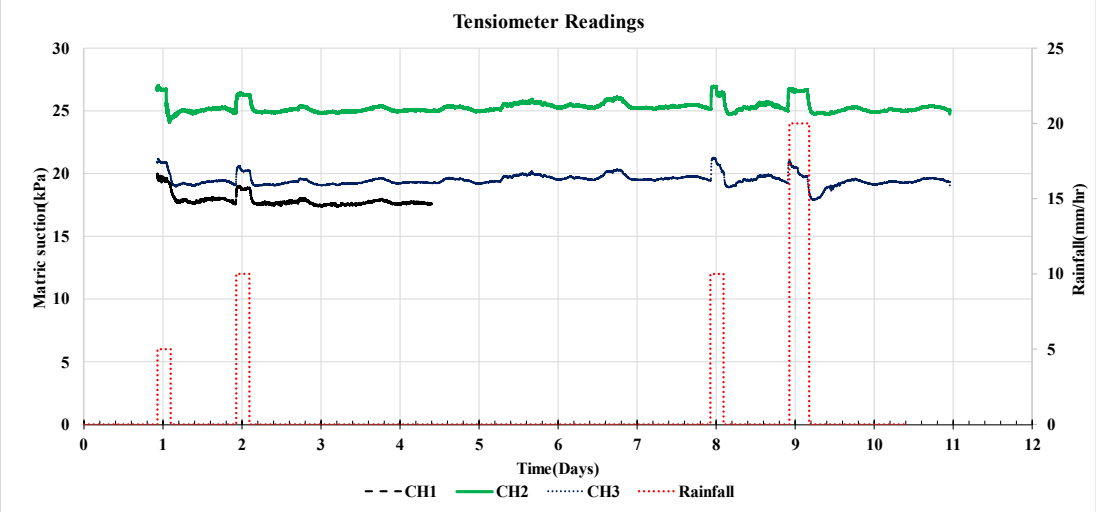

Figure 3.32: Variation in matric suction CH1, CH2, CH3 during prolong intense rainfall – 15^0 slope

3.6.2 Model with 30^0 slope

- **Prolong intense rainfall**

Only the effect of prolonging intense rainfall on capillary barrier cover built on 30^0 was studied here.

Figure 3.33 presents the variation of volumetric water content along the mid depth of the fine layer. Initially, the fine layer was sufficiently dry with a moisture content of 4%. With each rainfall, the moisture content had increased and there was a reduction

in moisture content value after the rain had stopped. But the moisture content did not reduce below a certain value (10%) even during a longer period of days without any rainfall. But during the 20mm/hr rainfall moisture content has reached a maximum value of 20%.

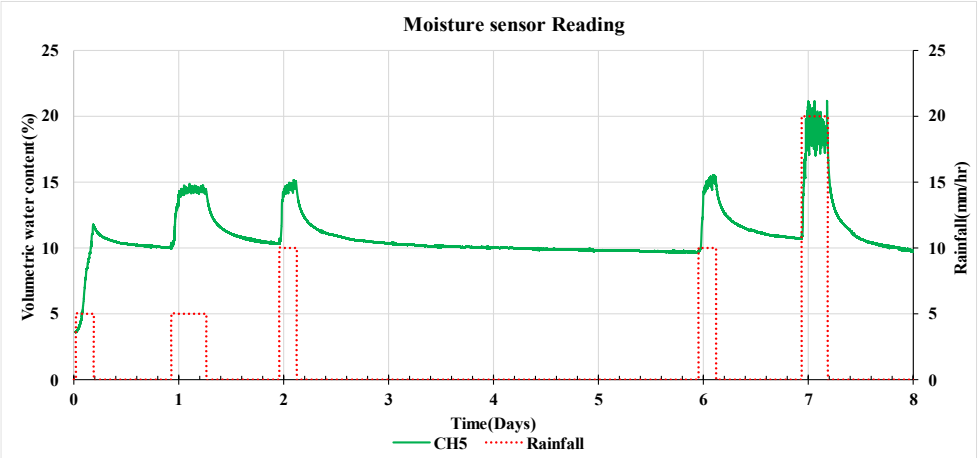

Figure 3.33: Variation in volumetric water content along mid depth of the fine layer during prolong intense rainfall – 30^0 slope

Moisture content variation measured along the river sand/ M-sand interface is presented in figure 3.34.

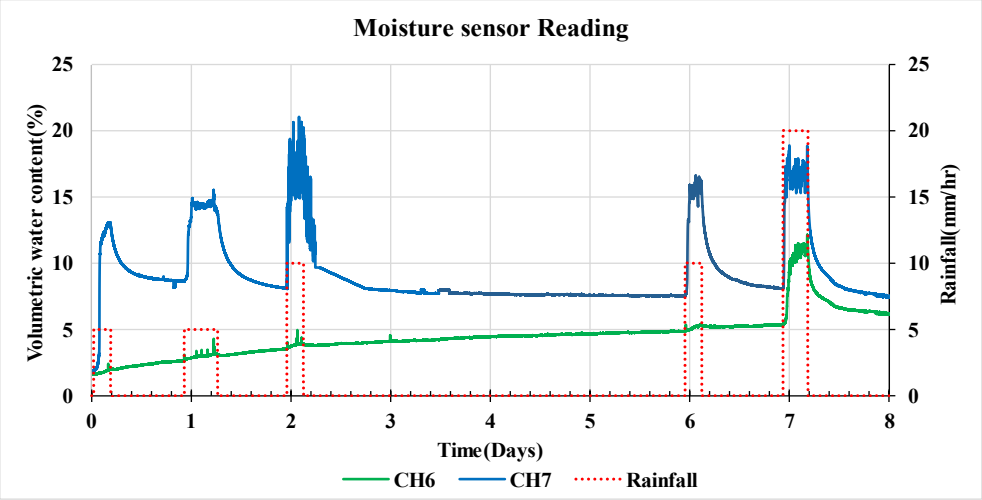

Figure 3.34: Variation in volumetric water content along the fine-coarse interface during prolong intense rainfall – 30^0 slope

Measured initial volumetric water contents at CH6 and CH7 were around 2.5%. With each rainfall CH7 (installed at the lower part of the model) showed a significant increase while the drastic increase in CH6 was seen only during 20mm/hr rainfall.

Maximum moisture content recorded in CH7 was 20% during the third day 10mm/hr rainfall and the maximum value measured in CH6 was 11% during 20mm/hr rainfall. At the end of all rainfall events when sufficient time is given for the removal of moisture from the system, the moisture content in the lower part of the model approached 8%.

Figure 3.35 illustrates the variation of volumetric water content along the mid depth of the coarse layer. The moisture content at CH4 and CH8 were 2.5% and 3% respectively. Until 20mm/hr rainfall event moisture senor readings remained almost steady with just a small variation, this may be due to moisture adjustment in the coarse layer. But there was a sudden increase in CH8 reading during the second rainfall event and this was due to leakage of moisture to the moisture sensor through its connectivity. Later this leakage was identified and sealed, after that moisture content remained steady around the value of 6.5%. During 20mm/hr rainfall for 6 hours duration, both sensors recorded maximum measurements. At the lower level (CH4) there was a gradual increase in moisture content during initial rainfall events. There was no reduction in moisture content at the end of a given rainfall event. CH4 had a maximum reading of 9% while CH8 had a maximum of 8.5%. The sudden increase of moisture content at the lower part (CH4) indicates the failure in the capillary barrier cover during 20mm/hr rainfall.

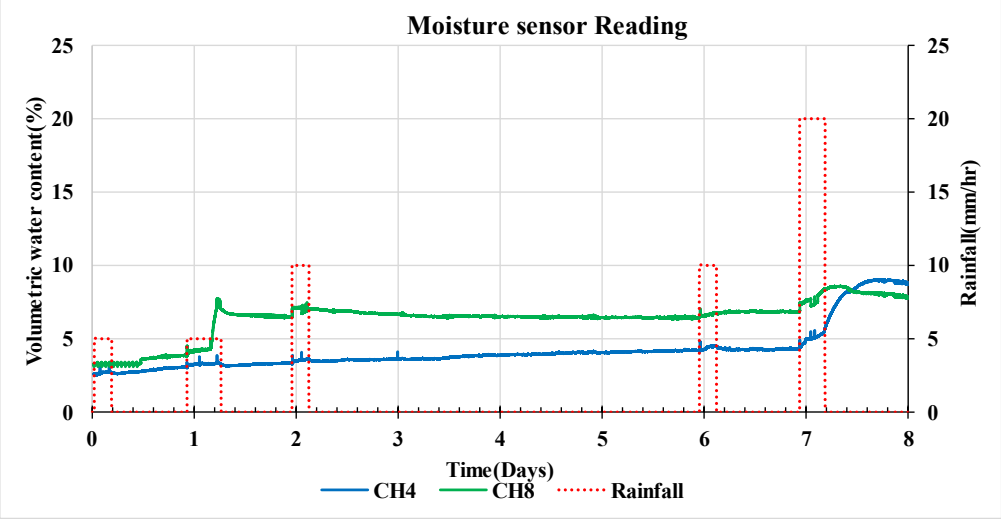

Figure 3.35: Variation of volumetric water content along the mid depth of the coarse layer during prolong intense rainfall – 30^0 slope

Variation of matric suction in residual soil layer is presented above in figure 3.36. Measured initial matric suction in CH1 was 20kPa and CH2 was 45Kpa. The graph shows that tensiometers readings were stable during all rainfall events despite their intensity and duration. As such, the provided capillary barrier cover with slope angle 30^0 has cutoff the infiltration into the slope fairly well. Measurements were not taken from CH3 installed at the bottom part of the model due to an error in readings from the tensiometer at that location.

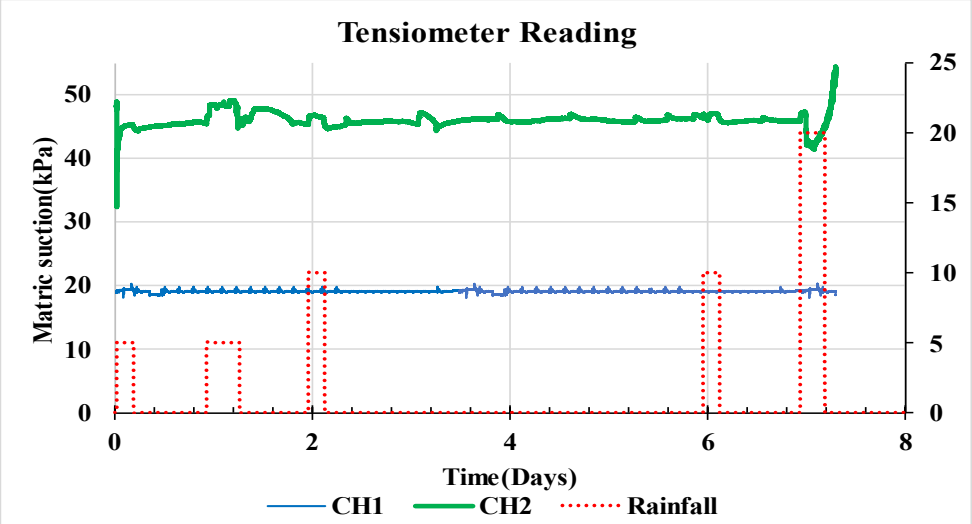

Figure 3.36: Variation in matric suction CH1, CH2 during prolong intense rainfall – 30^0 slope

3.7 Discussion

Rainfall experiments on laboratory physical model yield many findings on the capillary barrier cover constructed with river sand over M-sand. Experimental results from the study on the capillary barrier cover with an interface slope angle of 15^0 showed that it was effective in developing capillary barrier effect and cutting off infiltration into residual soil slope beneath it only during short duration low intensity rainfall (capillary barrier phenomenon was active during 5mm/hr rainfall for the 1-hour duration). The reason behind the failure of the capillary barrier during long duration rainfall can be identified as a low fine-coarse interface angle (15^0 slope) which was not enough to remove all the infiltrations that enter the system through lateral diversion and the model was not sufficiently dry enough to retain all the infiltration.

Capillary barrier cover has performed reasonably well after allowing to dry for a period of 3 months. It has almost cut off the infiltration into the slope even during two 10mm/hr rainfall with 4 hours duration. Although there was a failure in the capillary barrier effect only a slight drop (around 1kPa) in matric suction profiles in residual soil slope was noted at 20mm/hr rainfall following. Here since the saturated hydraulic conductivity of coarse layer is very much greater than residual soil, infiltration that enters the coarse layer after the failure was laterally diverted and drained through the drainpipe that was provided at the toe of the coarse layer. Therefore, the cover has recovered from its failure when it was allowed to dry out sufficiently under the combined effect of lateral diversion and evaporation.

Experiments on a model with a fine-coarse interface angle of 30^0 show that capillary barrier cover has performed satisfactorily during 10mm/hr rainfall events despite their duration. It has failed only during 20mm/hr rainfall for 6 hours duration. Although there was a sudden increase in recorded moisture content along the mid depth of the coarse layer in the upper part of the lope it can be neglected since it was due to leakage through senor's connectivity. The capillary barrier has not failed here because the moisture sensor reading installed along the mid-depth of coarse layer at lower part of slope has not shown any increase. During the lateral diversion moisture content increases along the fine-coarse interface in the downdip direction. The maximum moisture content recorded downstream is 20% while the upstream is 10%. Therefore, cover made with sufficiently dry layer materials on a slope angle of 30^0 performs well during prolonged intense rainfall events.

4 NUMERICAL STUDY OF CAPILLARY BARRIER THROUGH THE LABORATORY MODEL

4.1 Numerical study to establish model dimensions and fine & coarse layer thickness

As stated in chapter 3 a numerical modelling of the laboratory sized capillary barrier model was done initially. This also helped to finalize the dimensions of the experimental setup. The 2-D numerical modelling of the capillary barrier was done with GEOSLOPE SEEP/W software. In the study, the capillary barrier was made of fine sand and gravelly sand on top of the residual soil slope. Properties of materials used in the study are discussed in section 5.1.

4.1.1 Establishment of model parameters

Figure 4.1 illustrates the geometry and dimensions of the capillary barrier cover model used in the numerical study. Since the length and width of such confined models affect the development of the capillary barrier effect. In the first part of the study, the effect of varying the length of the model from 1000mm to 2000mm and the width of the model was investigated. Fine – coarse interface angles of 45^0 and 30^0 were used in capillary barrier cover model since most of the cut slopes angle varies up to 45^0 in Sri Lanka. Attention was paid especially to boundary effect on infiltration reported in similar model studies.

Studies reported in the literature guides that the moisture sensors and tensiometers should be placed 200mm distance away from wall of experimental setup to avoid boundary effect. Based on these studies and the available dimension of acrylic sheets (1.8m×1.2m boards, thickness 10mm) in the market the length of the model was decided to be 1200mm and the width was taken as 600mm. For these initial numerical studies, fine layer thickness was used as 30cm and coarse layer thickness as 30cm. The values reported in previous research and constructability was considered in selecting these dimensions for the analysis.

Thereafter numerical analysis was carried out to determine an effective fine and coarse layer thickness for this model.

For the investigations following fine and coarse layer thickness were considered,

- 100mm fine layer over 100mm coarse layer
- 200mm fine layer over 100mm coarse layer
- 300mm fine layer over 100mm coarse layer
- 100mm fine layer over 200mm coarse layer

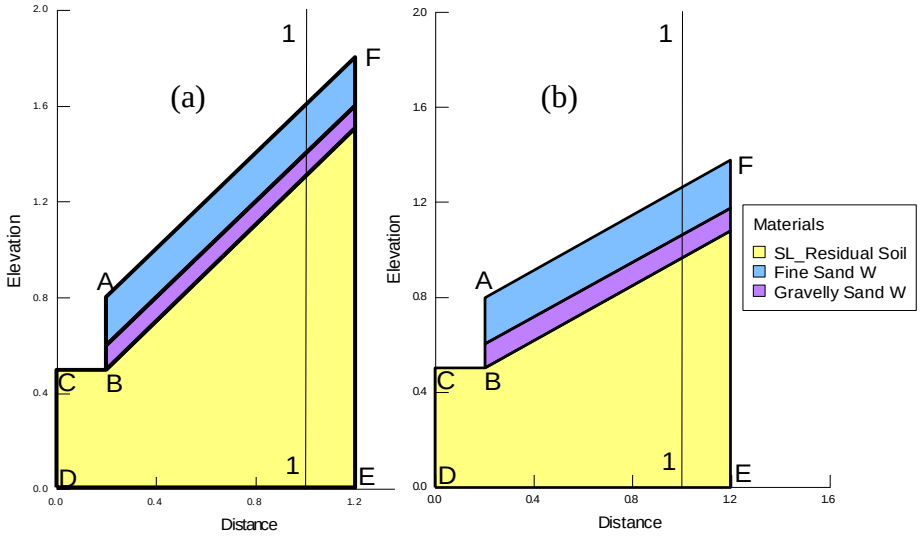

Figure 4.1: Geometry used in study to determine effective fine & coarse layer thickness, (a) model with 45^0 slope angle, (b) model with 30^0 slope angle

Following boundary conditions were used to simulate the field conditions in the model,

- CD, FE – no flow boundary (to create closed boundaries in the model)
- DE – initial ground water level (to introduce initial pressure head variation in the model)
- AF – flux boundary (to simulate rainfall to the model)
- AB – unit hydraulic boundary (to introduce drainage in the model)

4.1.2 Results

Pore water pressure variation along section 11 (x=1.0m) denoted in figure 4.1 was plotted to study the effect of different fine and coarse layer thicknesses combination on performance of capillary barrier under the rainfalls of intensity 5mm/hr and 20mm/hr.

4.1.2.1 Model with 45^0 slope angle

- **Fine/coarse layer thickness – 100mm/100mm**

The results of the analysis in figure 4.2 shows that water has infiltrated into the fine layer causing a loss of matric suction. There is some loss in matric suction in residual soil indicating a breakdown of barrier and some infiltration into the coarse layer. This effect was more significant for rainfall with an intensity of 20mm/hr. Therefore, the 100mm/100mm fine-coarse layer thickness combination appeared to be ineffective in cutting off the infiltration.

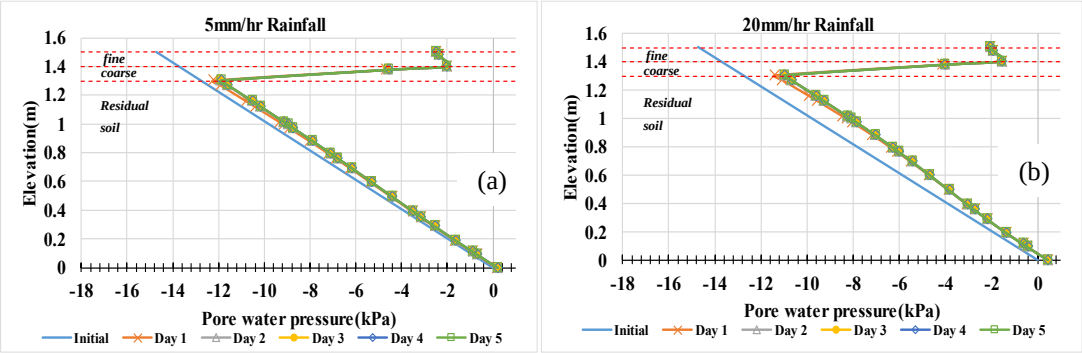

Figure 4.2: Pore pressure variation in 45^0 slope for fine/coarse layer thickness – 100mm/100mm, (a) 5mm/hr rainfall, (b) 20mm/hr rainfall

- **Fine/coarse layer thickness – 200mm/100mm**

Thereafter, the studies were extended to analyze the case of a fine layer of thickness 20cm over 10cm thick coarse layer. Figure 4.3 shows the pore pressure profile variation in the system when using the capillary barrier cover with fine and coarse layers of 20cm and 10cm thickness respectively.

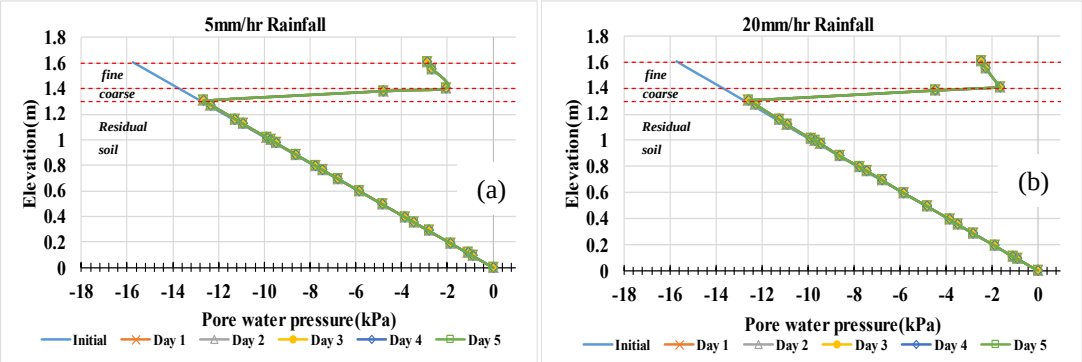

Figure 4.3: Pore pressure variation in 45^0 slope for fine/coarse layer thickness – 200mm/100mm, (a) 5mm/hr rainfall, (b) 20mm/hr rainfall

Analysis results show that loss in matric suction is only in fine layer and no change of matric suction has occurred at lower levels. This indicates that infiltration was diverted along fine- coarse interface without any breakthrough in capillary barrier effect. Infiltration of rainfall into the system is almost cut off when compared to the previously considered thicknesses.

- **Fine/coarse layer thickness -300mm/100mm**

Further numerical simulations were investigated to study the effect of increasing the fine layer thickness to 30cm while keeping the coarse layer thickness of 10cm. Figure 4.4 illustrates the variation of pore pressure for a system with fine layer with thickness of 30cm.

From the results, it can be seen that infiltration into the system has only entered the fine layer for 5mm/hr rainfall. But there is a slight change in the matric suction of underlying soil layers when rainfall has increased to 20mm/hr. The provided capillary barrier has almost cut off the infiltration into the system, but the performance of this combination is nearly similar to the previous system with a 20cm fine layer.

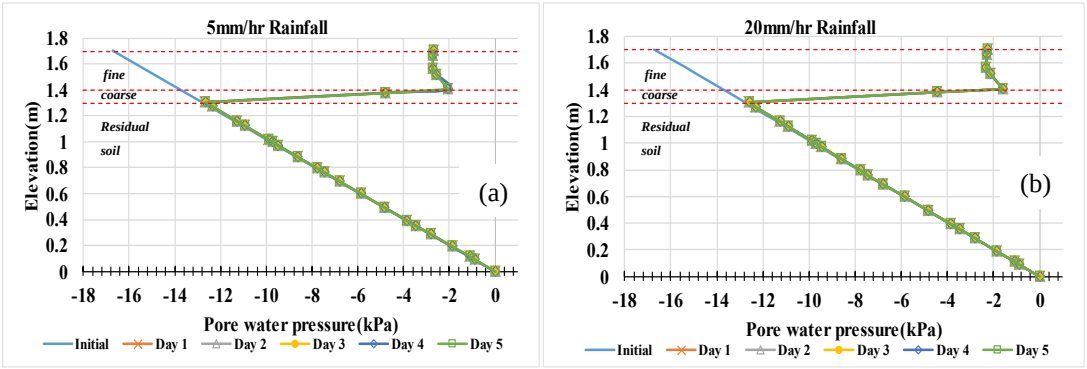

Figure 4.4: Pore pressure variation in 45^0 slope for fine/coarse layer thickness – 300mm/100mm, (a) 5mm/hr rainfall, (b) 20mm/hr rainfall

- **Fine/coarse layer thickness – 100mm/200mm**

Later the effect of varying thickness of the coarse layer on infiltration was studied by changing the coarse layer thickness to 20cm while keeping fine layer thickness to 10cm. Figure 4.5 gives the variation of pore pressure during 5mm/hr and 20mm/hr intensity rainfalls. Results of the analysis show that rainwater has infiltrated into the fine layer causing loss of matric suction in the fine layer for 5mm/hr rainfall. Further,

the infiltration has entered the underlying soil layers due to a breakthrough in the capillary barrier effect. This scenario is more significant for the increased rainfall intensity of 20mm/hr. Therefore, it appeared that increasing coarse layer thickness didn't improve performance of the capillary barrier effect.

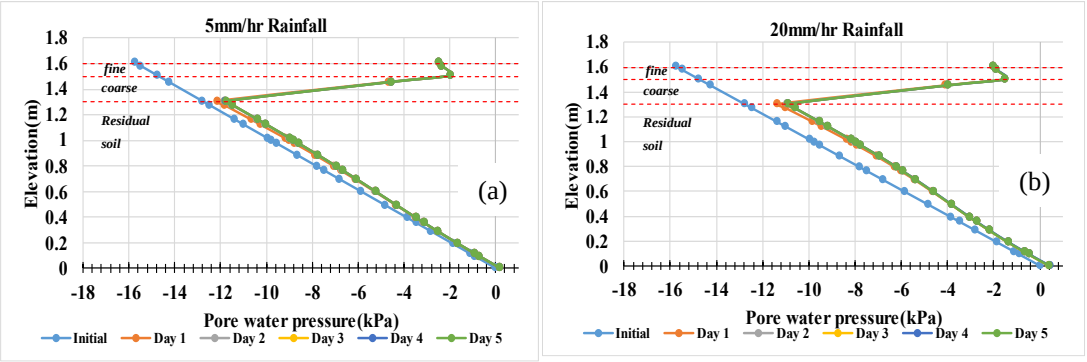

Figure 4.5: Pore pressure variation in 45^0 slope for fine/coarse layer thickness – 100mm/200mm, (a) 5mm/hr rainfall, (b) 20mm/hr rainfall

4.1.2.2 Model with 30^0 slope angle

Performance of the capillary barrier will change with the slope angle of the cut slope. Therefore, another series of parametric analysis was done for the 30^0 slope.

- **Fine/coarse layer thickness – 100mm/100mm**

Figure 4.6 shows that rainfall has infiltrated into the residual soil layer, indicating a breakdown of the capillary barrier cover. This effect was more prominent during rainfall with an intensity of 20mm/hr. Therefore, 100mm/100mm fine-coarse layer combination is not effective in cutting off infiltration in 30^0 slope also.

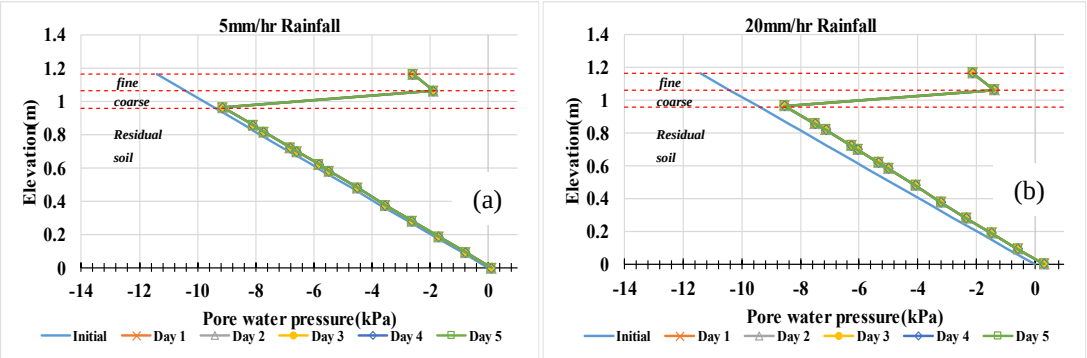

Figure 4.6: Pore pressure variation in 30^0 slope for fine/coarse layer thickness – 100mm/100mm, (a) 5mm/hr rainfall, (b) 20mm/hr rainfall

- **Fine/coarse layer thickness – 200mm/100mm**

Since there was a failure in the capillary barrier cover with a 10cm thick fine layer, later studies were extended to analyze the case of a fine layer of thickness 20cm over 10cm thick coarse layer. Figure 4.7 presents pore pressure variation profile in cover system when using the capillary barrier having a 20cm thick fine layer and 10cm thick coarse layer.

Results show that loss in matric suction is only in fine layer and there is no change of matric suction at lower levels. This indicates that infiltration was diverted along fine-coarse interface without breakthrough in capillary barrier effect. Infiltration of rainfall into the system is almost cut off when compared to the previously analyzed fine layer thickness.

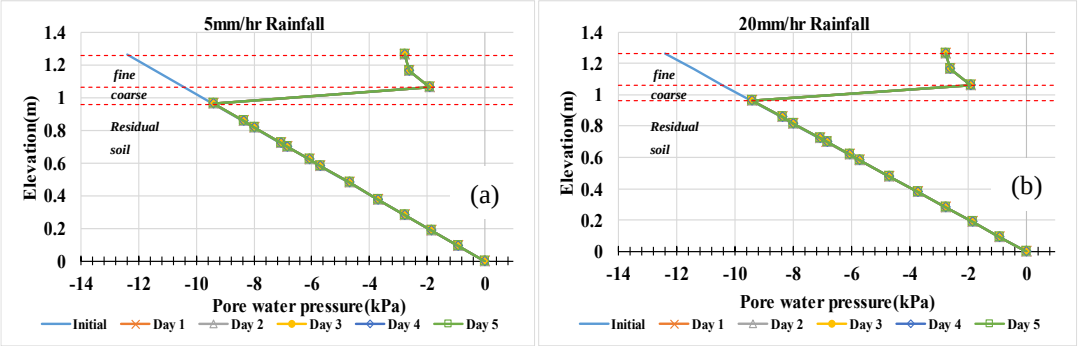

Figure 4.7: Pore pressure variation in 30^0 slope for fine/coarse layer thickness – 200mm/100mm, (a) 5mm/hr rainfall, (b) 20mm/hr rainfall

- **Fine/coarse layer thickness -300mm/100mm**

Numerical studies were extended further for investigating the effect of increasing the thickness of the fine layer to 30cm while keeping the coarse layer thickness of 10cm. Figure 4.8 shows the variation of pore pressure for capillary barrier cover with fine layer thickness increased to 30cm.

Results show that infiltration into the model has only entered the fine layer for 5mm/hr rainfall. But there is a slight change in the matric suction of underlying soil layers when rainfall has increased to 20mm/hr. The provided capillary barrier has almost cut off the infiltration into the system, but the performance of this combination is nearly similar to the previous system with a 20cm fine layer.

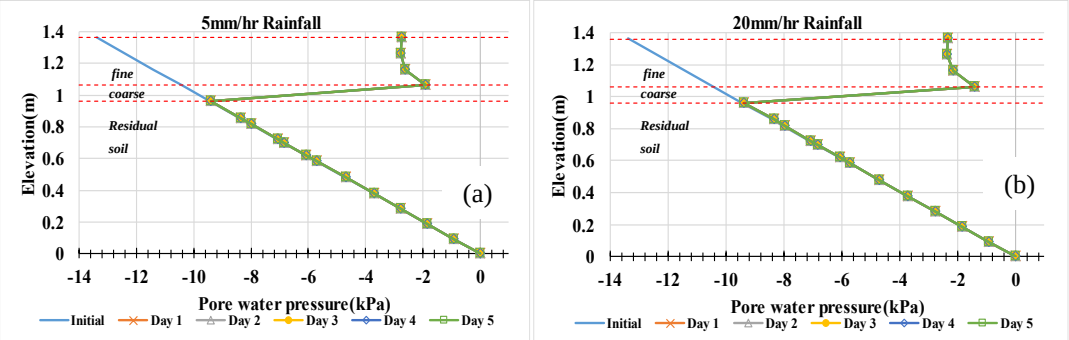

Figure 4.8: Pore pressure variation in 30^0 slope for fine/coarse layer thickness – 300mm/100mm, (a) 5mm/hr rainfall, (b) 20mm/hr rainfall

- **Fine/coarse layer thickness – 100mm/200mm**

Similar to studies with the 45^0 model the effect of varying thickness of the coarse layer on infiltration was studied by increasing the coarse layer thickness to 20cm while keeping fine layer thickness to 10cm. Figure 4.9 illustrates the variation of pore pressure during 5mm/hr and 20mm/hr intensity rainfalls. Results of the analysis show that rainwater has infiltrated into the fine layer causing loss of matric suction in the fine layer for 5mm/hr rainfall. Further, the infiltration has entered the underlying soil layers due to a breakthrough in the capillary barrier effect. whereas more infiltration has entered the residual soil layer during increased rainfall intensity of 20mm/hr. Therefore, it appears that increasing coarse layer thickness didn't affect the performance of the capillary barrier effect.

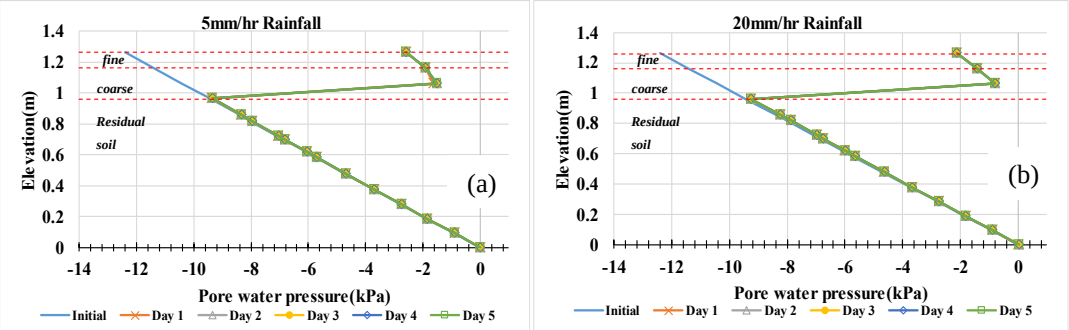

Figure 4.9: Pore pressure variation in 30^0 slope for fine/coarse layer thickness – 100mm/200mm, (a) 5mm/hr rainfall, (b) 20mm/hr rainfall

4.1.3 Discussion

Analysis results indicated that performance of capillary barrier cover increases with increasing fine layer thickness. In fact, the thickness of the coarse layer did not affect the functioning significantly as the water has moved along the boundary and not entered that layer. Performance of a capillary barrier cover system either with 45^0 or 30^0 slope angles with fine layer thickness 20cm and coarse layer thickness of 10cm found to be significant in cutting off the infiltration into underlying residual soil layer. A fine layer with thickness of 20 cm would be sufficient for the considered rainfall intensities. Therefore, it was decided to use a 20cm thick fine layer and a 10cm thick coarse layer in physical model of capillary barrier system. As discussed in chapter 3, river sand will be used as a fine layer and manufactured sand sieved and retained on a 1.18mm sieve will be used for coarse layer material in capillary barrier cover placed over a local cut slope of residual soil.

Figure 4.10 shows the flow vectors in the numerical model for infiltration of rainfall of intensity 20mm/hr. with a fine layer thickness of 20cm and a coarse layer thickness of 10mm. The results confirm that infiltration into the system is diverted through the fine layer at the fine-coarse layer boundary without allowing it to enter the coarse layer and provision of sufficient drainage at the down dip end of the cover will keep the cover sufficiently dry by removing the lateral diversion.

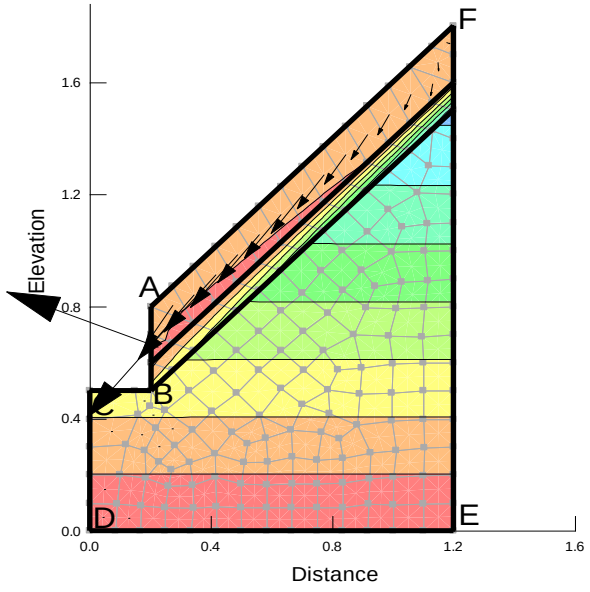

Figure 4.10: Flow vectors in the system with capillary barrier cover

4.2 Numerical verification of rainfall experiment

Results from rainfall experiments on 15^0 slope and 30^0 slope were verified using 2-D numerical analysis with SEEP/W program of GeoStudio software. Further analysis was not performed on a slope with 45^0 as it could not be constructed in the model box. Transient seepage analyses were simulated to investigate the capillary barrier cover develop with river sand over M-sand. 2-D numerical model resembling the laboratory physical model was used in the study. Similar to numerical investigations were done in the following two main phases,

- Numerical study of capillary barrier cover on 15^0 slope
    - Short-term low intense rainfall
    - Prolong intense rainfall
- Numerical study of capillary barrier cover on 30^0 slope
    - Prolong intense rainfall

4.2.1 Numerical study of capillary barrier cover on 15^0 slope

Figure 4.11illustrates the dimension of the numerical model used in the study and boundary conditions that were applied on model for resembling the laboratory model.

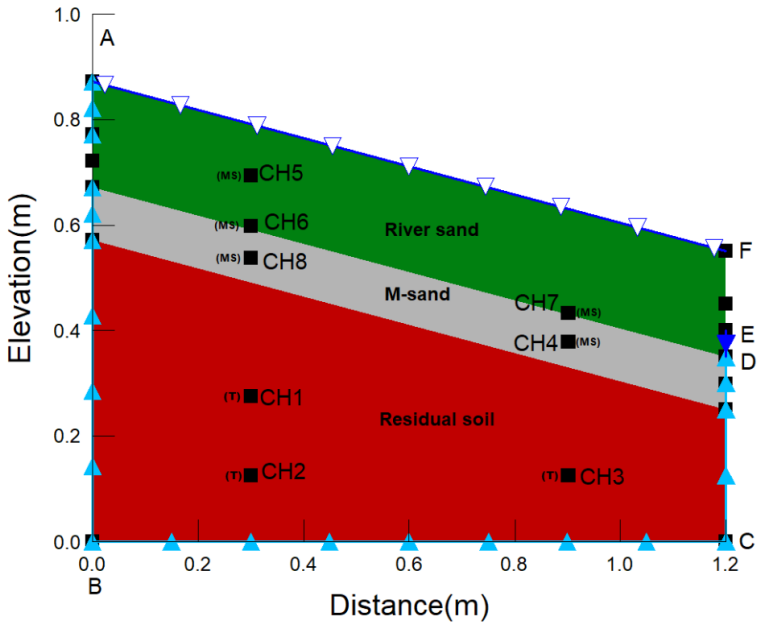

Figure 4.11: Geometry and boundary conditions used in numerical analysis – 15^0 slope angle

Capillary barrier cover layer was modelled with 20cm thick river sand as fine layer and 10cm thick M-sand (sieved and retained on 1.18mm sieve) as coarse layer. Matric suction variation was extracted from the nodes denoted as CH1, CH2, CH3 from the numerical analysis to verify the observations of tensiometers in the experiments. Volumetric water content variation was extracted from the nodes denoted as CH4, CH5, CH6, CH7, CH8 to verify the observations of moisture sensors in the rainfall experiments.

Material properties and SWCC of river sand, M-sand and residual soil that are described in chapter 3 were used in this numerical study.

The model was subjected to initial moisture content and pressure head variation similar to physical laboratory model. Initial pressure head variation in numerical model was input in the form of pressure head spatial function. Initial tensiometer readings and pore water pressure values determined from SWCC for measured volumetric water content along capillary barrier layers were used as spatial head values.

Following boundary conditions were applied to the model to create the field conditions to the numerical model,

- AB, BC, CD, EF - no flow boundary (to create a closed boundary in the model)
- DE – unit hydraulic boundary (to introduce drainage from the model)
- AF- flux boundary (to simulate rainfall into the model)

Transient seepage analyses for short-term low intense rainfall and prolonged intense rainfall were done with the numerical model corresponding to rainfall patterns used in the rainfall experiments.

4.2.2 Numerical study of capillary barrier cover on 30^0 slope

Dimensions of the 2-D numerical model used in the study and boundary conditions applied to model to resemble the laboratory experimental model is given in figure 4.12. Pore pressure variation in residual soil slope was extracted from numerical studies for nodes denoted as CH1 and CH2 while volumetric water content values in capillary barrier layers were obtained at nodes indicated as CH4, CH5, CH6, CH7, and CH8 in

the model. Later these results of numerical analyses were compared with experimental results.

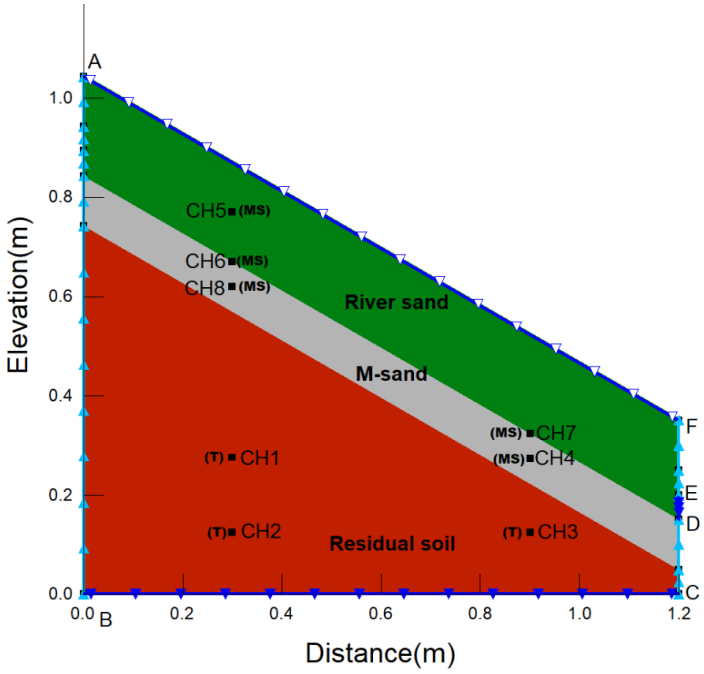

Figure 4.12:Geometry and boundary conditions used in numerical analysis – 30^0 slope angle

Following boundary conditions were applied on model to create field conditions to the numerical model,

- AB, BC, CD, EF - no flow boundary (to create a closed boundary in the model)
- DE – unit hydraulic boundary (to introduce drainage from the model)
- AF- flux boundary (to simulate rainfall into the model)

Material properties and SWCC of river sand, M-sand and residual soil that are described in chapter 3 was used in this numerical study.

Transient seepage analysis for prolonging intense rainfall was done with the numerical model corresponding to the rainfall pattern used in the experimental study. The spatial head function was used to input initial pore pressure state in model. Initial tensiometer readings and pore water pressure values determined from SWCC for measured volumetric water content along capillary barrier layers were used as spatial head values.

4.2.3 Results

4.2.3.1 Model with 15^0 slope angle

- **Short-term low intense rainfall**

Numerical validation of variation of measured volumetric water content in experimental model along mid of fine layer is given in figure 4.13. Numerical results at the upper level of the slope (graph (a)) show a clear increase of moisture content at all rainfall events. In the experimental results, a clear increase was noted only after the third rainfall event. Numerical results indicate a drop in moisture content after the cessation of the rainfall. At the lower level of the slope (graph (b)), a sharp increase of moisture content was seen in the numerical results with the third rainfall event. The experimental results also show a similar trend.

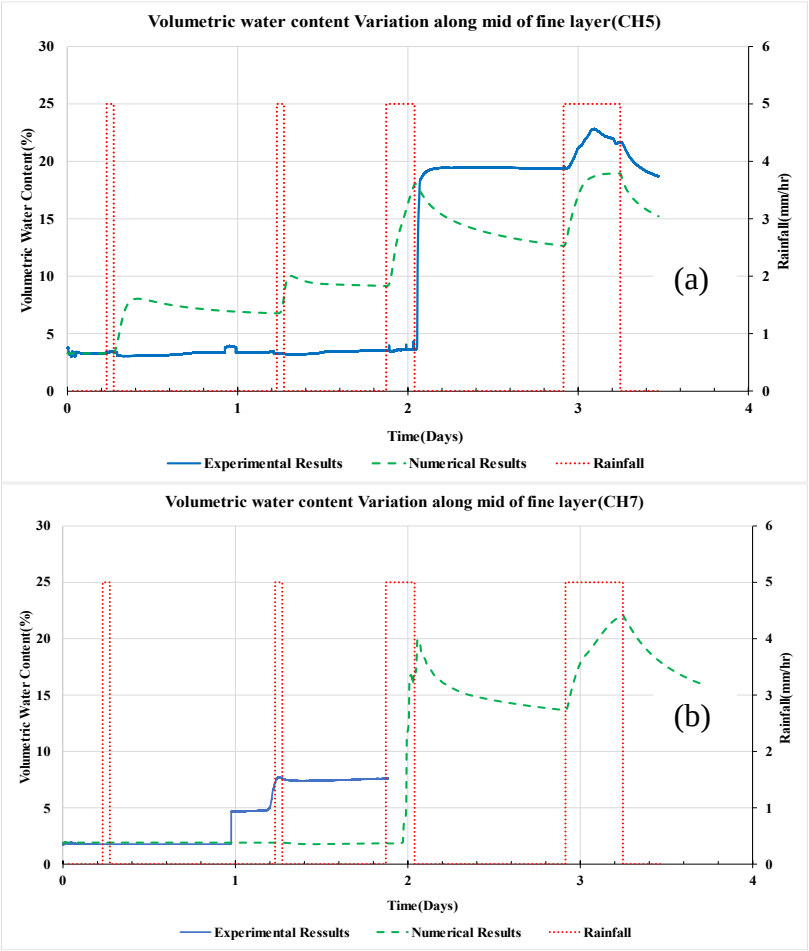

Figure 4.13: Comparison between experimental and numerical results – along mid of fine layer during low intense rainfall – 15^0 slope

Figure 4.14 presents the comparison between measured and numerically determined volumetric water content along the fine-coarse interface of the capillary barrier cover. Variation in both experimental and numerical results are similar although the numerically determined values are slightly lower than the measured values. In graph (67)(a) corresponds to the upper part of the model moisture content increase was noted with the third rainfall event in both numerical and experimental results. In graph (67)(b) corresponds to volumetric water content variation at lower part of model, where experimental values are slightly higher than the numerical results, but the trend is similar. At the end of the rainfall events, moisture content from both curves experienced a reduction.

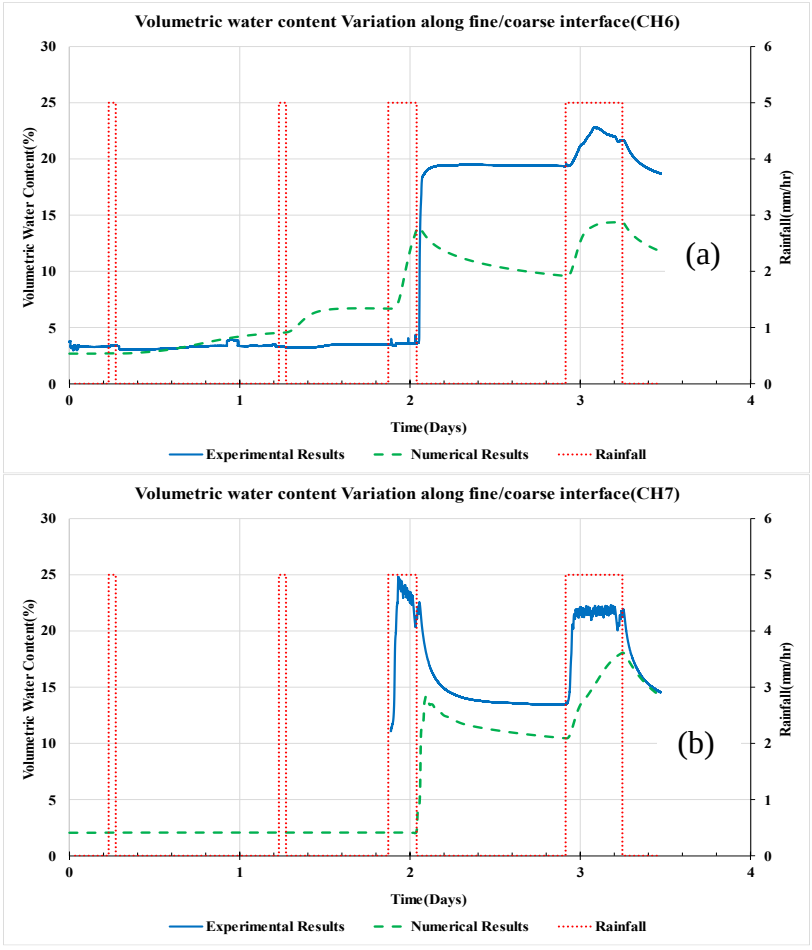

Figure 4.14: Comparison between experimental and numerical results – along fine/coarse interface during low intense rainfall – 15^0 slope

Comparison between experimental measurements and numerical results for the variation of volumetric water content along the mid depth of the coarse layer is

presented in figure 4.15. Experimental and numerical results determined at both upper and lower locations along mid of coarse layer comply with each other. The moisture content at the upper part of the model is presented in graph (a). It shows that there was no significant increase in moisture content in both curves up to the third rainfall event. A gradual increase in moisture content was seen after the third rainfall event. Graph (b) presents the moisture content values at the lower part of the slope. A much greater increase in moisture content was seen with all rainfall events in the physical model. Numerical analysis showed an increase after the third and fourth rainfall events.

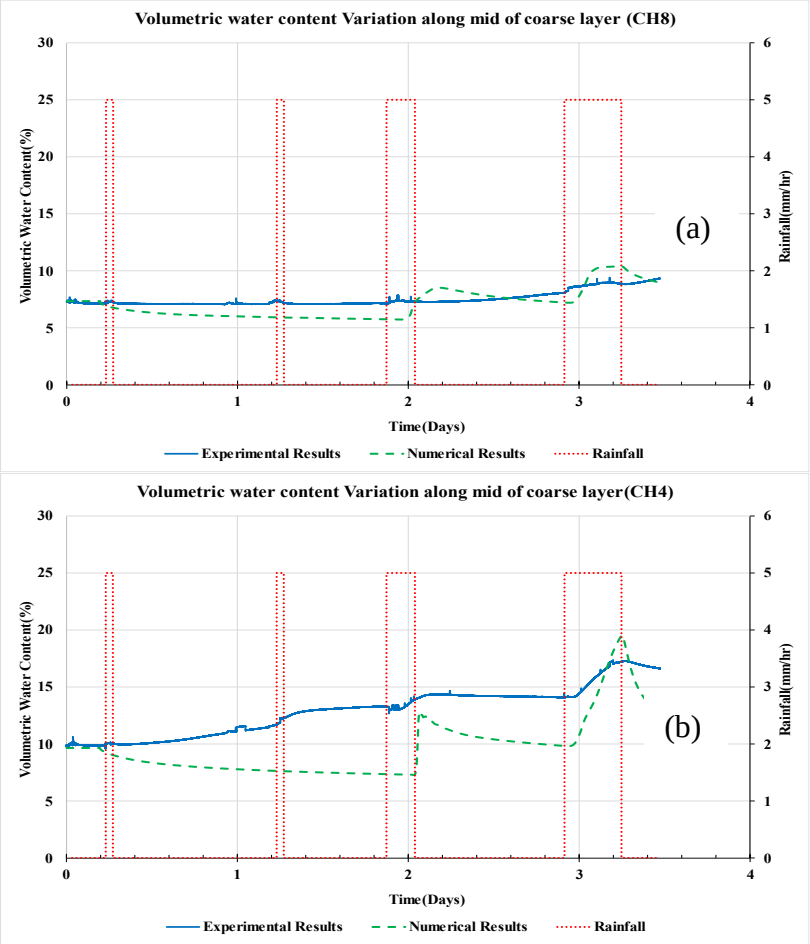

Figure 4.15: Comparison between experimental and numerical results – along the mid depth of the coarse layer during low intense rainfall – 15^0 slope

Figure 4.16 presents a comparison between the results of the rainfall experiment and numerical analysis. Measured matric suction profile variation in all three channels with tensiometers agreed well with the variation obtained from the numerical results. But

tensiometer readings were fluctuating with time may be due to the sensitivity of the sensors and the non-uniform nature of the given rainfalls.

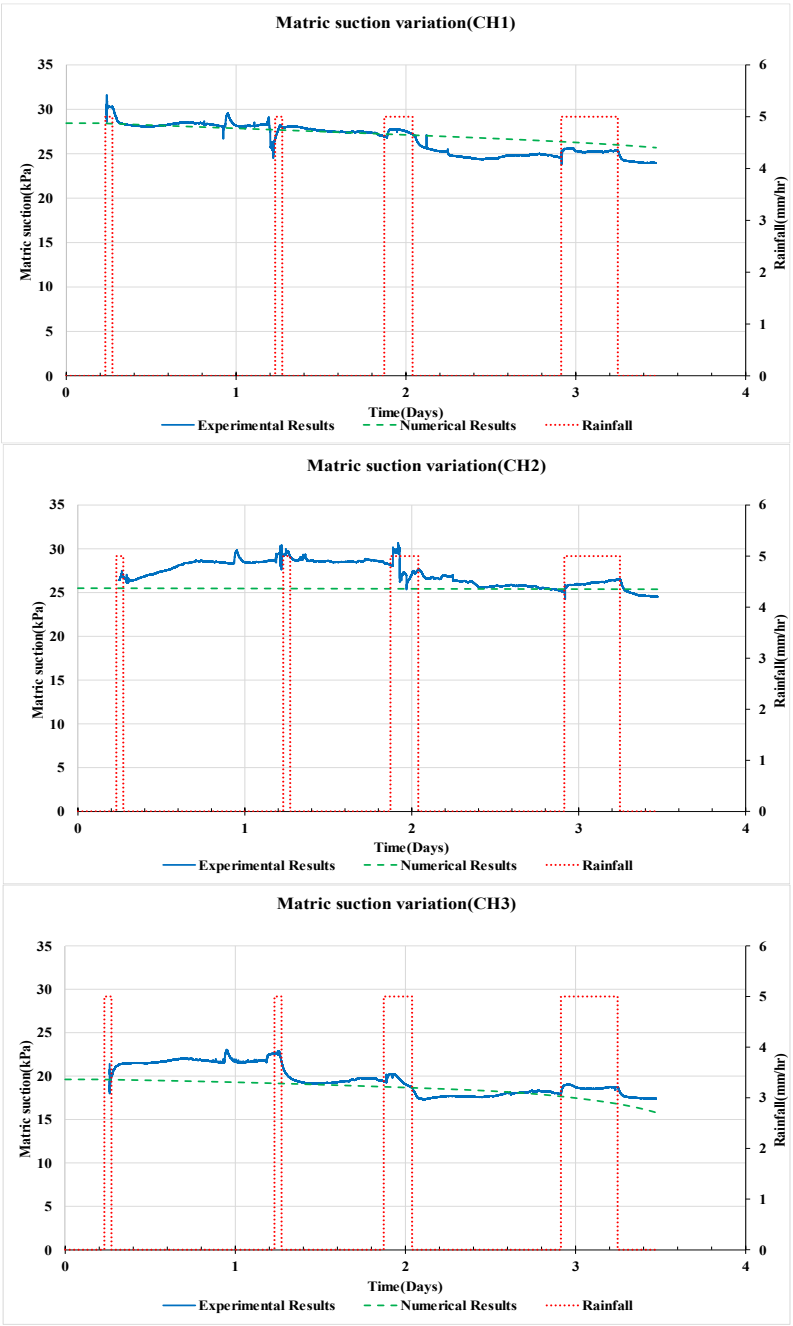

Figure 4.16: Comparison between experimental and numerical results during low intense rainfall – 15^0 slope

- **Prolong intense rainfall**

Figure 4.17 presents the comparison of experimental and numerical results of volumetric water content measured along mid depth of fine layer at upper part of cover.

The trend in variation of both results is similar at this point, but in numerical results, the increase of moisture content during the rainfall events is higher than the experimental observations.

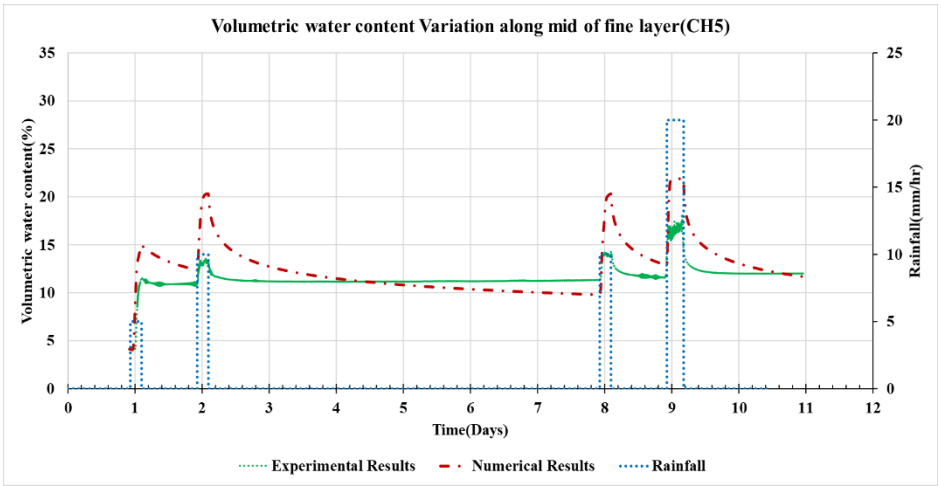

Figure 4.17: Comparison between experimental and numerical results – along mid of fine layer during prolong intense rainfall – 15^0 slope

Numerical verification of measured volumetric water content along the fine-coarse interface is given in figure 4.18 and 4.19. In both channels, experimental and numerical results follow the same trend in response to given rainfall. Experimental results were slightly higher than numerical values in CH6, but in CH7 the same moisture content was seen at end of rainfall events.

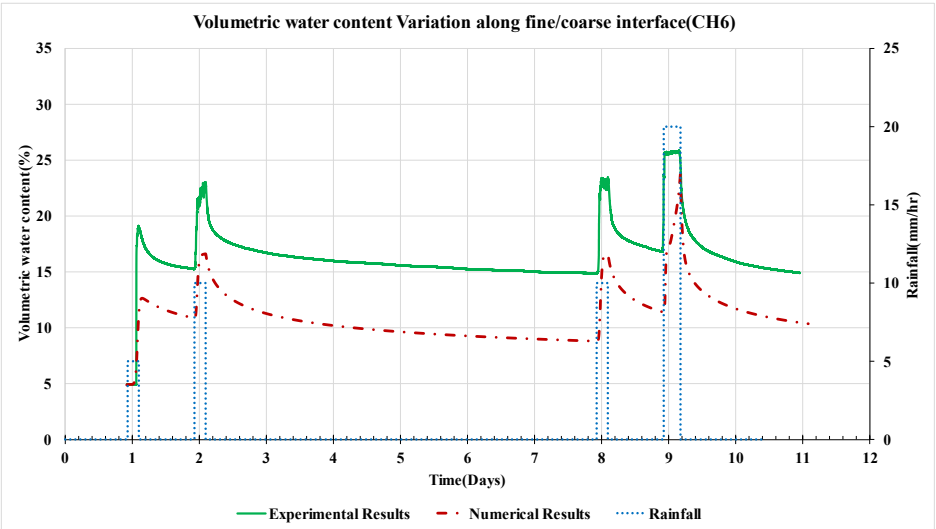

Figure 4.18: Comparison between experimental and numerical results – along fine/coarse interface(upper part) during prolong intense rainfall – 15^0 slope

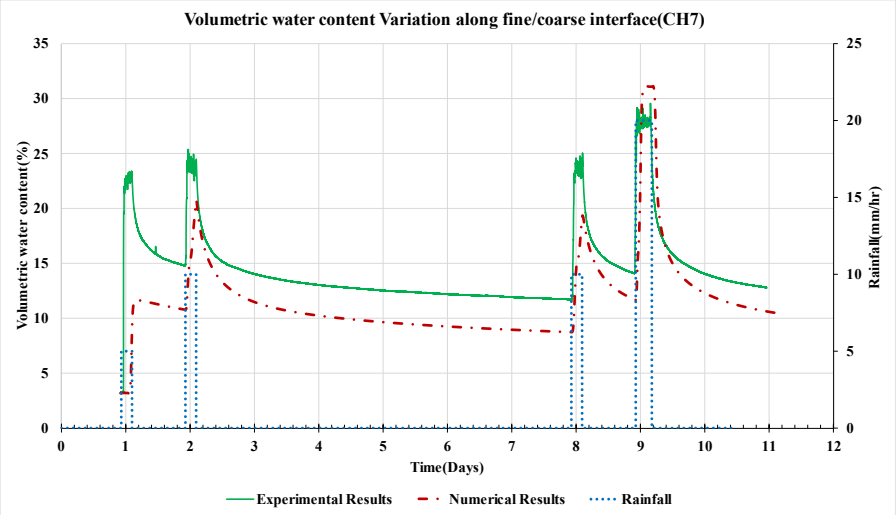

Figure 4.19: Comparison between experimental and numerical results – along fine/coarse interface (lower part) during prolong intense rainfall – 15^0 slope

Figure 4.20 presents the numerical validation of measured volumetric water content along mid depth of coarse layer. Variation of moisture content in experimental and numerical results was similar at both locations. CH4 at the lower part of the model recorded the maximum experimental measurement of 20% and the numerical value of 16% during 20mm/hr rainfall.

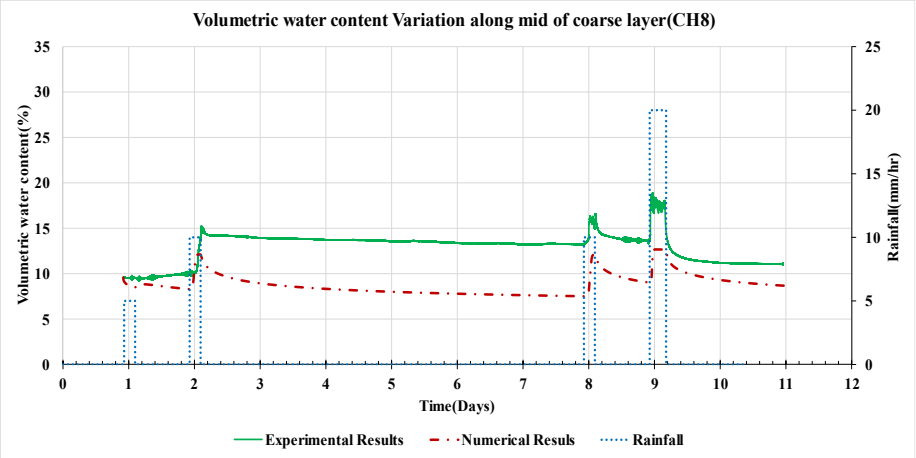

Figure 4.20:Comparison between experimental and numerical results -along mid of coarse layer(upper part) during prolong intense rainfall – 15^0 slope

Figure 4.21 presents the comparison between numerical and experimental results along the mid of the coarse layer. CH8 recorded a maximum experimental value of 18% and a numerical value of 13% during the same rainfall event. The increased moisture

content observed during a rainfall event in both numerical and experimental studies reduced to former values sometime after the end of the rainfall.

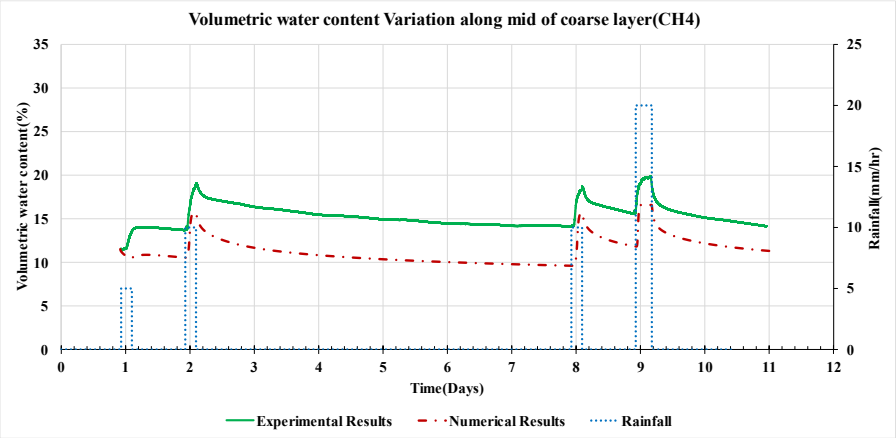

Figure 4.21: Comparison between experimental and numerical results – along mid of coarse layer(lower part) during prolong intense rainfall – 15^0 slope

Matric suction variation in residual soil layer measured from the experiment was verified with results of numerical simulation. Figure 4.22 presents the comparison of experimental and numerical results. Graph (a) corresponding to the upper level shows that trend in numerical results was similar to available experimental results. There is a gradual reduction (only 2kPa) over the whole rainfall period. Similarly, at CH2 (graph (b))(immediately below CH1) variation of matric suction in experimental data and numerical results are similar. There is a slight reduction of matric suction (only 2kPa) over the full period. But at CH3 (graph (c))at the lower part of the slope depletion in numerical results is higher than the experimental results at the end of given rainfalls. The reduction is around 4kPa which is about double that at the upper levels.

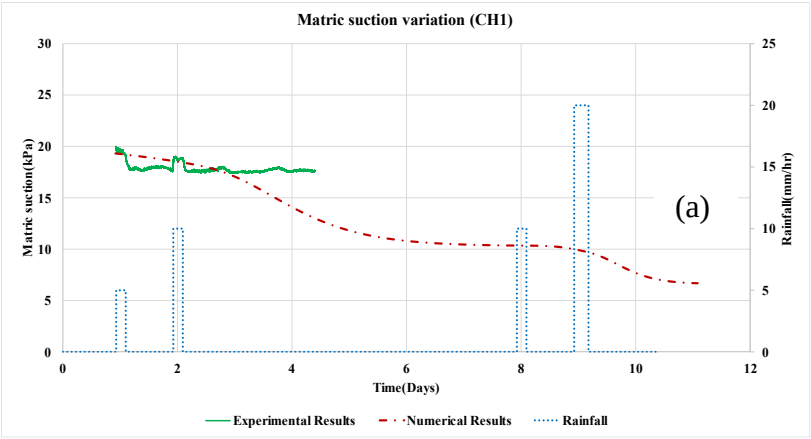

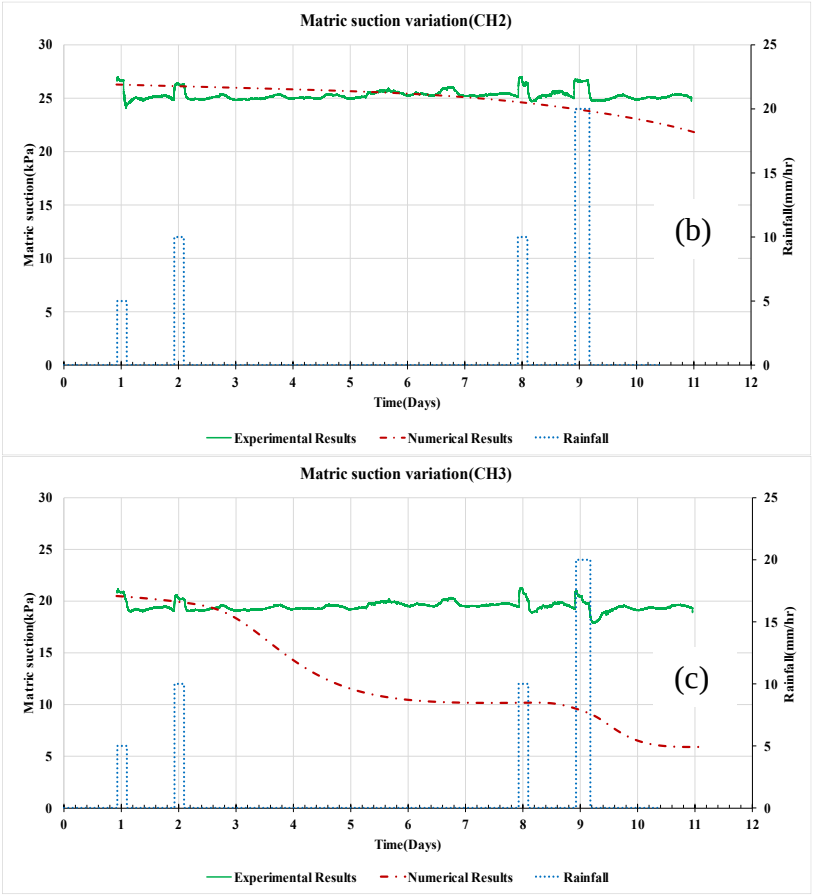

Figure 4.22: Comparison between experimental and numerical results during prolong intense rainfall – 15^0 slope

4.2.3.2 Model with 30^0 slope

- **Prolong intense rainfall**

Figure 4.23 presents the comparison of experimental and numerical results of volumetric water content measured along mid of fine layer.

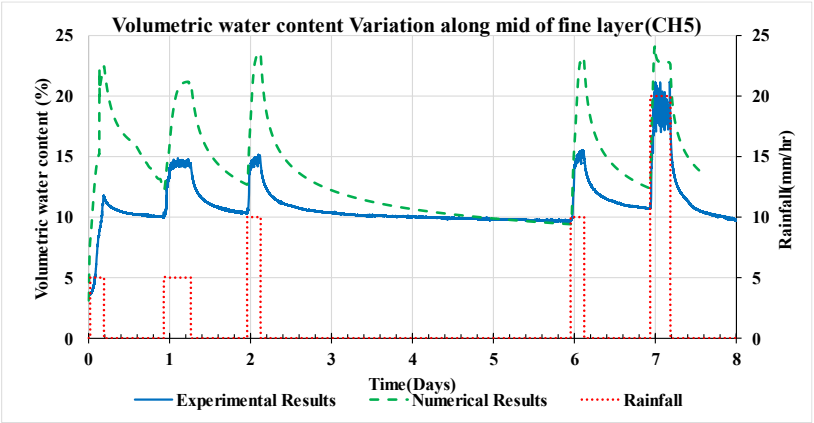

Figure 4.23: Comparison between experimental and numerical results – along mid of fine layer during prolong intense rainfall – 30^0 slope

The comparison shows that numerical values were slightly higher than experimental values during the initial four rainfall events, but during the last 20mm/hr rainfall both values were approximately the same around 22%. During all rainfall events, both curves showed a similar trend in variation. At the end of the third rainfall event, both experimental and numerical values approached moisture content of 10%.

Validation of experimentally measured volumetric water content along the fine-coarse interface is illustrated in figure 4.24. In CH6 (located at the upper part of the model) numerically determined moisture content variation curve shows a clear increase during all rainfall events and a reduction immediately afterwards. But the experimental results curve have a gradual increase up to final rainfall. Numerical results recorded a maximum moisture content value of 18% during 20mm/hr rainfall and the corresponding experimental value was 12%. In CH7 both experimental and numerical results were approximately the same throughout the rainfall. After the third rainfall, both experimental and numerical moisture content values approached 7.5%.

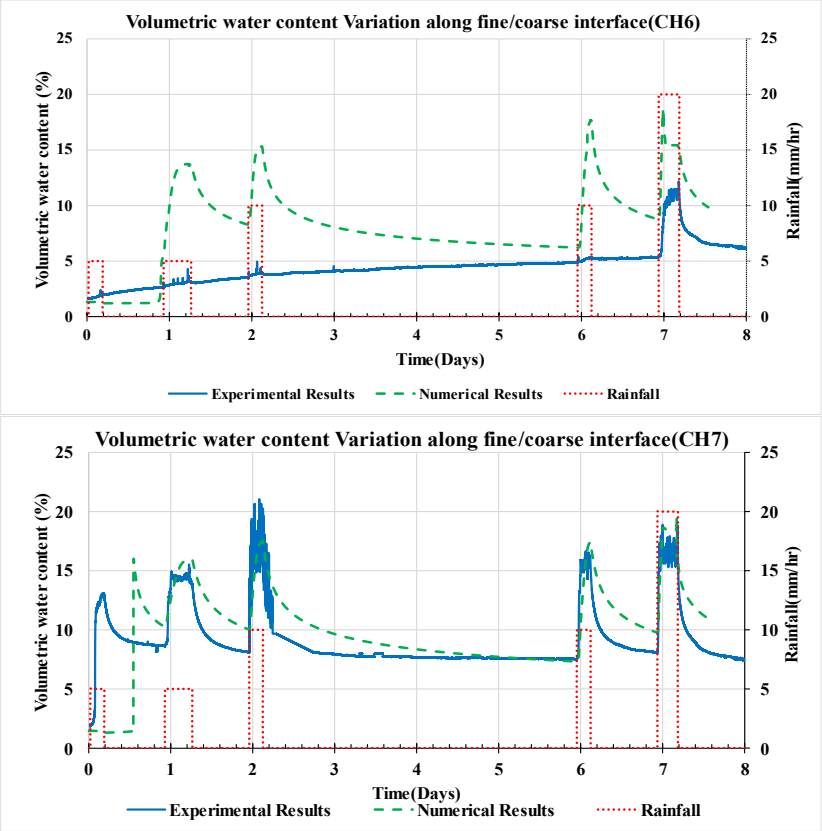

Figure 4.24: Comparison between experimental and numerical results – along fine/coarse interface during prolong intense rainfall – 30^0 slope

Figure 4.25 shows the comparison of numerical and measured volumetric water content along mid depth of coarse layer. Variation of moisture content in experimental and numerical results was similar at CH4 during the whole rainfall event. CH4 at the lower part of the model recorded a maximum experimental measurement of 9% and a numerical value of 11% during 20mm/hr rainfall. In CH8 at the upper part of the model up to the fourth rainfall event numerical curve remain steady, but in the experimental curve, there is a sudden hike during the second rainfall due to leakage through the connectivity of the moisture sensor. CH8 recorded a maximum experimental value of 8.5% and a numerical value of1 11%. Based on the results at CH4 and CH8 failure in the capillary barrier has occurred during intense rainfall of 20mm/hr.

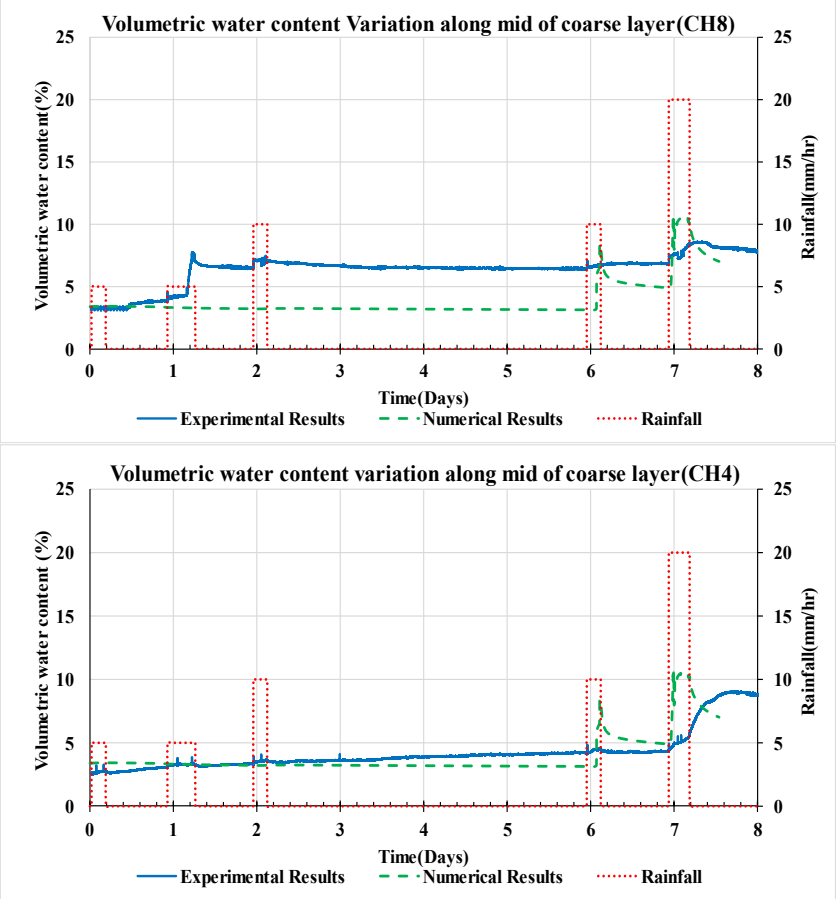

Figure 4.25: Comparison between experimental and numerical results - along the mid depth of the coarse layer during prolong intense rainfall – 30^0 slope

Comparison of experimental and numerical results is presented in figure 4.26. CH1 and CH2 recorded steady matric suction measurements throughout the rainfall

experiment. Both the numerical and experimental results indicate that the matric suction at two locations remained stable during all the rainfall events.

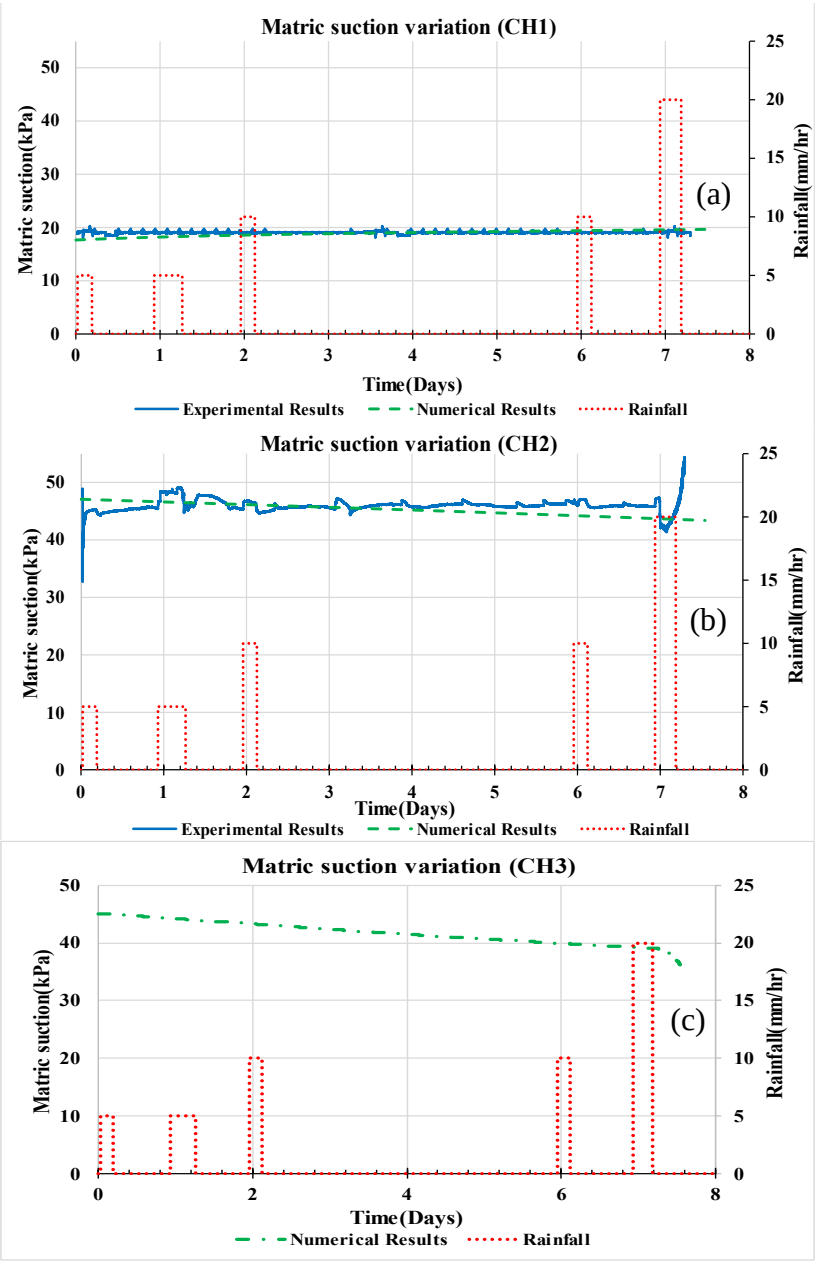

Figure 4.26: Comparison between experimental and numerical results during prolong intense rainfall – 30^0 slope

4.2.4 Discussion

The effectiveness of the capillary barrier in reducing the infiltration into the residual soil underneath was studied by laboratory experiment and verified by the numerical simulations of the model study. Three different rainfall events of increasing magnitude were applied on the models with slopes of inclination 15^0 and 30^0. Infiltration behaviour in the laboratory model was monitored using moisture sensors in the capillary barrier cover layers and tensiometers in the residual soil layer.

The trends shown by the experimental results and the numerical results are quite similar. During a rainfall event, the moisture content in the fine layer and along the fine/coarse interface has increased. But this increase has gradually diminished after the rainfall event. There is an increase in moisture content in the coarse layer during the higher rainfall event.

In both scenarios presented, capillary barrier has reduced the infiltration of rainfall into the underlying residual soil layer. Therefore, capillary barrier cover constructed with 20cm thick river sand over 10cm thick M-sand will reduce the rainfall infiltration into the slope beneath it when cover layers are sufficiently dry and proper drainage is provided.

Flow velocity vectors in the model with a slope angle of 15^0 at the end of prolonging intense rainfall simulations is given in figure 4.27. Magnitudes of flow velocity vectors are higher at the downdip part of the model indicating the lateral diversion along the fine-coarse interface. Magnitudes of flow vectors are almost zero in the upper direction of the model; this is due to existence of the capillary barrier effect in that region. The effect of capillary barrier in reducing the infiltration into residual soil layer is clearly illustrated in the diagram. With the failure of the capillary barrier during the fourth rainfall event of 20mm/hr at the end, water has entered the coarse layer at the lower part of the model, but due to the provision of a drain at the toe of the coarse layer, the infiltration into the residual soil layer was reduced significantly.

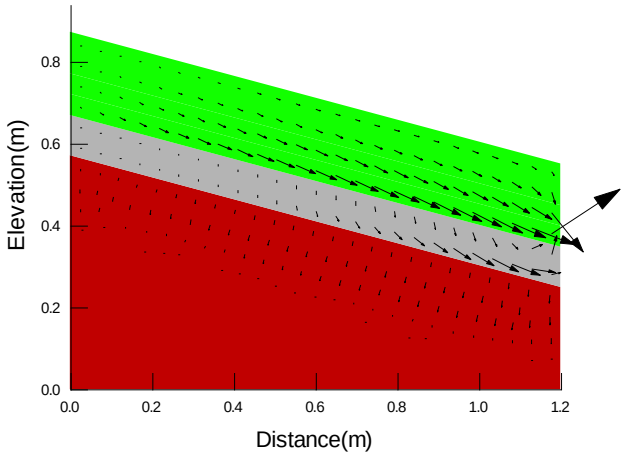

Figure 4.27: Flow velocity vectors in the capillary barrier model at the end of prolonging intense rainfall event - slope angle 15^0

Figure 4.28 illustrates the flow velocity vectors in the capillary barrier cover modelled on a slope with 30^0 inclination. Figure (a) shows the flow velocity in the model during the early rainfall events where the capillary barrier is completely effective. The effect of the capillary barrier in cutting off the infiltration into the system and laterally diverting all the infiltration that enters the fine layer is clearly illustrated in the figure. The magnitude of flow velocity vectors increases along the fine-coarse interface in the down-dip direction. From figure (b), the infiltration pattern into the system after the failure of the capillary barrier effect can be studied. Similar to earlier numerical studies here also coarse layer has laterally diverted moisture along it after the failure of capillary barrier cover. Therefore, infiltration into the residual soil layer is minimized significantly.

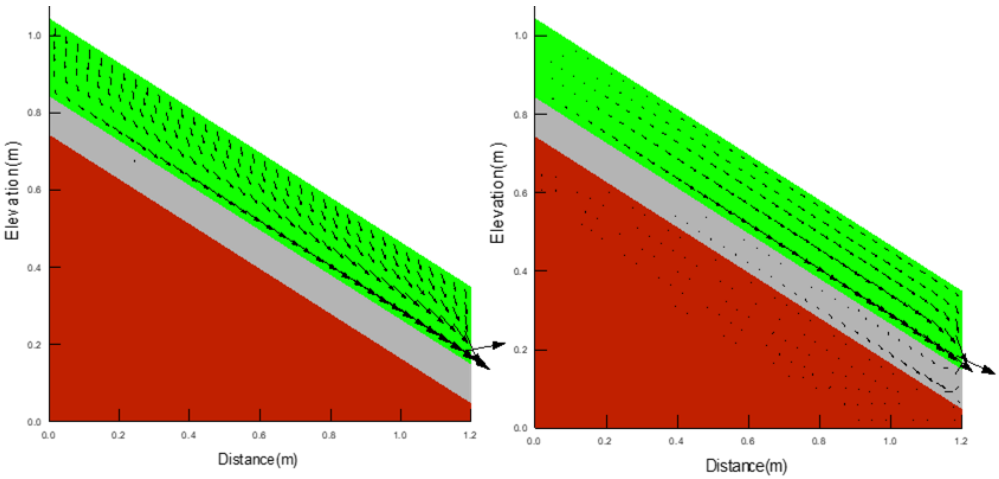

Figure 4.28: Flow velocity vector diagram (slope angle 30^0 during prolong intense rainfall), (a) during the presence of capillary barrier effect, (b) after the failure of the capillary barrier effect

5 NUMERICAL STUDY OF RAINFALL INFILTRATION INTO AN ACTUAL SLOPE WITH CAPILLARY BARRIER COVER

5.1 Numerical study on capillary covers on single level cut slopes in Sri Lanka

The use of capillary barriers to reduce infiltration into cut slops in residual soil formation have not been done so far. Hence in this research, the effect of the capillary barrier on the infiltration of rainfall into local cut slopes was investigated using the SEEP/W program of GeoStudio 2012 software. Generally, the cut slopes along various construction works are formed with multi-level cuts depending on their depth of the cut. But in the initial study cut slope with a single cut in a homogenous residual soil was considered to minimize the complexity in numerical analysis with the SEEP/W program. Figure 5.1 shows the geometry of multi-level cut slope and cut slope with a single cut (slope angle – 45^0) considered in these numerical simulations.

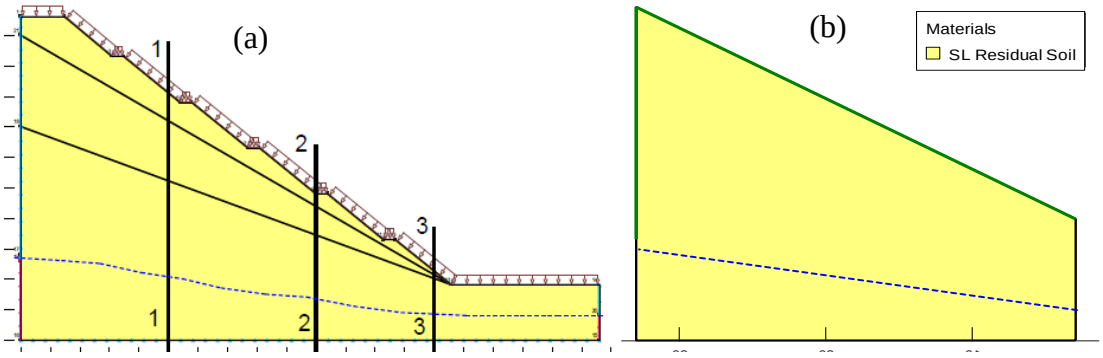

Figure 5.1: Geometry of cut slopes having, (a) multi-level cuts similar to field conditions, (b) idealized single level cut used in the numerical study

5.1.1 Properties of materials used in the numerical study

The slope was assumed to be made of local Lankan residual soil. Numerical investigations of infiltration were conducted on,

- Cut slope without any covers
- Cut slope with capillary barrier cover

In this preliminary study, the capillary barrier was considered to be made up of fine sand and gravelly sand. In this initial study, characteristics of constitutive materials were obtained from the literature(Tami et al., 2004a). Table 5.1 presents the Fredlund

and Xing best-fit parameters of residual soil, fine sand and gravelly sand and their saturated hydraulic conductivity used in the modelling.

Table 5.1: Best fit parameters & saturated hydraulic conductivity of materials

Material	K_s (m/s)	θ_s	θ_r	Best fit parameters		
				a(kPa)	n	n
Residual soil	1.0×10^{-5}	0.55	0.27	13	0.97	4.8
Fine sand	2.7×10^{-4}	0.41	0.03	1.94	6.3	0.87
Gravelly sand	7.6×10^{-2}	0.38	0.02	0.18	4.44	1.13

SWCC of the materials that were established and used in the SEEP/W program in the analysis are presented in figure 5.2. Graph (b) presents the hydraulic conductivity variation of materials with matric suction. From the graph, the contrast in the variation of hydraulic conductivity of fine material – fine sand and coarse material – gravelly sand with matric suction can be clearly seen. Capillary barrier effect phenomenon will form when these cover materials are placed at matric suction values greater than 0.5kPa, that is the cover should be sufficiently dry.

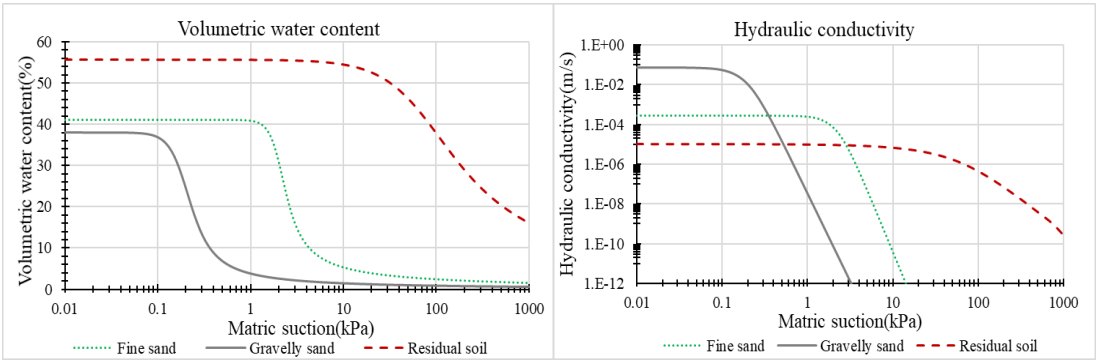

Figure 5.2: (a) Volumetric water content variation, (b) hydraulic conductivity variation

5.1.2 Geometry and boundary conditions

Cut slope section with depth 17m and width 30m as a single level cut having homogenous residual soil layer was used in the numerical study. Figure 5.3 presents the geometry and boundary conditions used in the analysis. Following boundary conditions were used to simulate the field condition,

- CD, DE, GF, HG – no flow boundary (to create closed boundaries in the model)

- DG – groundwater table with 100kPa cutoff boundary (to introduce initial pore water pressure condition in the model)
- CH – flux boundary (to simulate rainfall into the model)

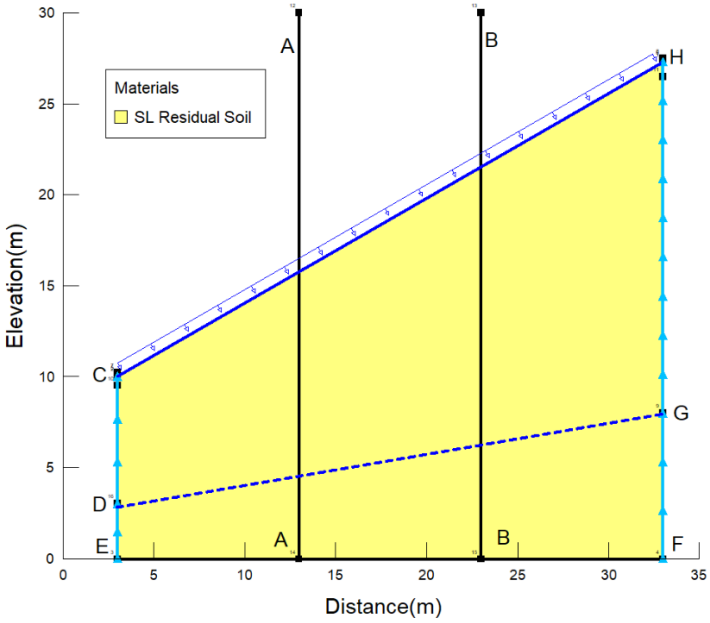

Figure 5.3: Geometry, boundary conditions used & studied sections – cut slope (45^{o})

For the analysis of the slope with capillary barrier cover same geometry and boundary conditions given in figure 5.3 were used. The capillary barrier cover consisting of a fine layer thickness of 200mm and coarse layer thickness of 100mm was simulated on the surface of the cut. Fine and coarse layer thickness were selected from the parametric study that was discussed in chapter 4 of the thesis. At the toe end of the capillary barrier layers, the zero-pressure condition was applied to simulate the drainage, that is to drain the lateral diversion along the fine-coarse interface in the model.

A very deep-water table with cutoff boundary of 100kpa was applied to the model in both analyses with & without capillary barrier cover. Rainfall infiltration for 10mm/hr. and 20mm/hr. rainfall intensity for prolong period of 05 continuous days was numerically simulated in both the analysis. The effect of rainfall infiltration into the slope was studied by establishing the pore water pressure profile along section AA and BB.

5.1.3 Stability analysis

The stability of the slope was analyzed at different stages for conditions of both; natural cut slope and cut slope with the capillary barrier incorporating the results of the pore pressure regime obtained through studies done with SEEP/W software to check the effect of capillary barrier in slope stabilization. In the stability analysis, it is difficult to check the stability of the capillary barrier cover, because in field constructions these layer materials are strengthened by filling them inside geocells. Therefore, the stability of only the cut slope was studied. Slope stability analysis was done using the Morgenstern and Price method using SLOPE/W software. Table 5.2 presents the strength properties of the residual soil used in the analysis. Mohr-coulomb model was used to model the soil.

Table 5.2: Mohr-Coulomb parameters used in the stability analysis

Material	γ	C’	$\emptyset^{'}$	θ_r
Residual soil	20kN/m^3	5kPa	32^0	0.27

5.1.4 Results

5.1.4.1 Cut slope without any covers

Pore water pressure distribution with time on the cut section was plotted along the sections AA & BB.

- **Behaviour during 10mm/hr rainfall**

Figure 5.4 shows the matric suction profile along section BB from the rainfall infiltration analysis. Initially maximum matric suction of 100kPa existed along this section, but from the graph, effect of infiltration into the slope can be seen. At the end of the fifth day, the maximum matric suction has reduced to 30kPa. Although the matric suction has depleted considerably, there is no significant rise in the groundwater table since the initial matric suction was high.

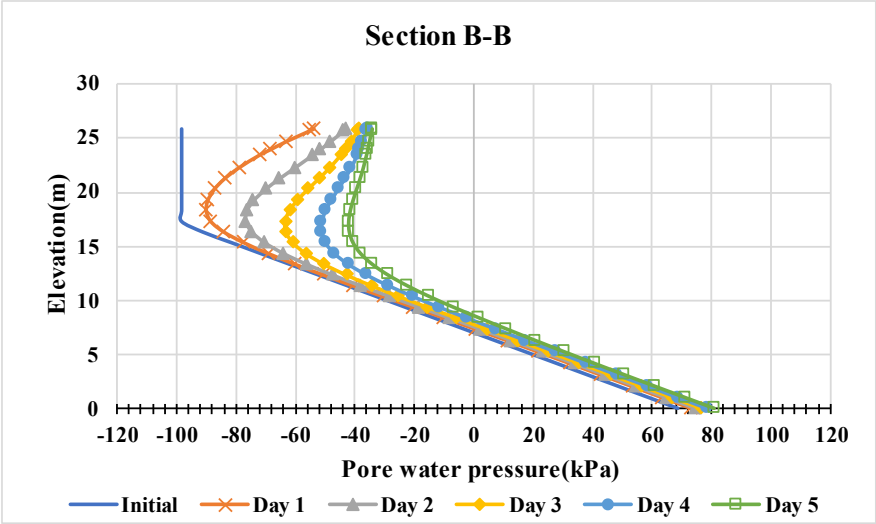

Figure 5.4: Pore water pressure profile variation during 10mm/hr rainfall – Section BB(without capillary barrier)

Pore water pressure variation along section AA was plotted to study the infiltration profile at the down dip direction of the slope where the existed initial matric suction was 110kPa is presented in figure 5.5. Due to a considerable amount of infiltration into the slope matric has depleted with time and maximum matric suction value has reached around 25kPa at the end of the fifth day. There is a significant rise in the groundwater table at this section as it is at the bottom of slope.

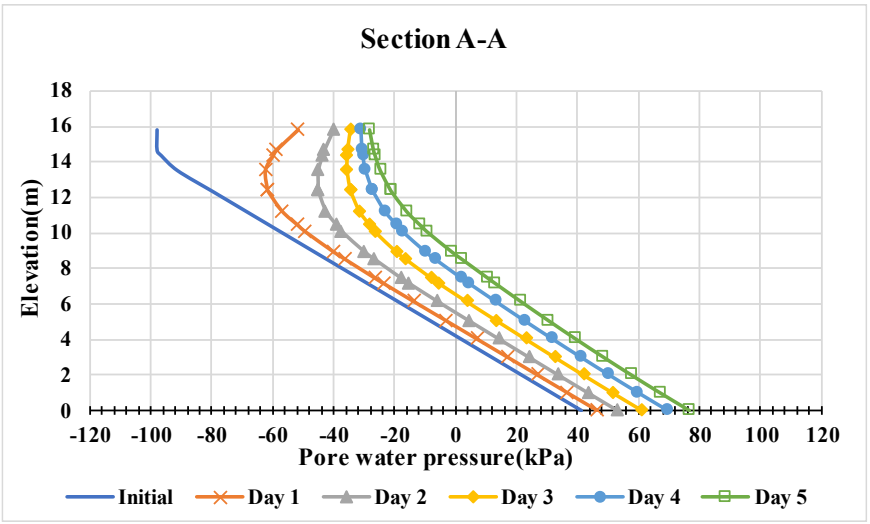

Figure 5.5: Pore water pressure profile variation during 10mm/hr rainfall– Section AA(without capillary barrier)

- **Behaviour during 20mm/hr rainfall**

Similar to analysis carried out for 10mm/hr intensity rainfall, the analysis was done for 20mm/hr rainfall in the same model and variation of pore water along sections AA and BB were plotted to examine the effect of intense rainfall on infiltration into a cut slope.

Figure 5.6 presents the variation of matric suction profile along section BB of the cut. From the graph, the effect of the increase in the intensity of rainfall on change in pore water pressure can be seen. The maximum matric suction value at the section has reached the value near 10kpa at end of the fifth day. That is the existed suction has almost diminished during 20mm/hr rainfall. Groundwater table which was steady up to day two has started to rise from the third day, and at the end of the fifth day, there is a clear rise in the water table.

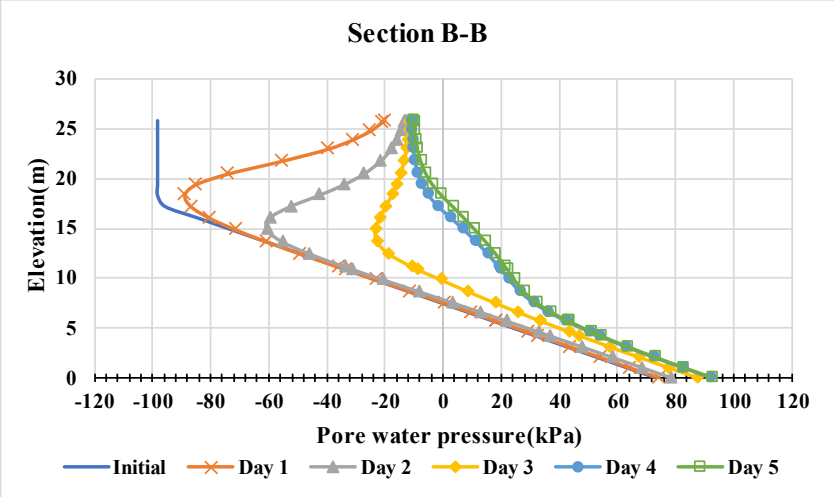

Figure 5.6: Pore water pressure profile variation during 20mm/hr rainfall – Section BB(without capillary barrier)

Figure 5.7 show the variation of pore water pressure plotted along section AA is given. The plotted profile shows that matric suction has reduced to zero value at the end of the third day. The water table has risen to the ground level when compared to the results of 10mm/hr rainfall. Because of this positive pore pressure has started to develop along the section which will results in a reduction of shear strength of the slope significantly.

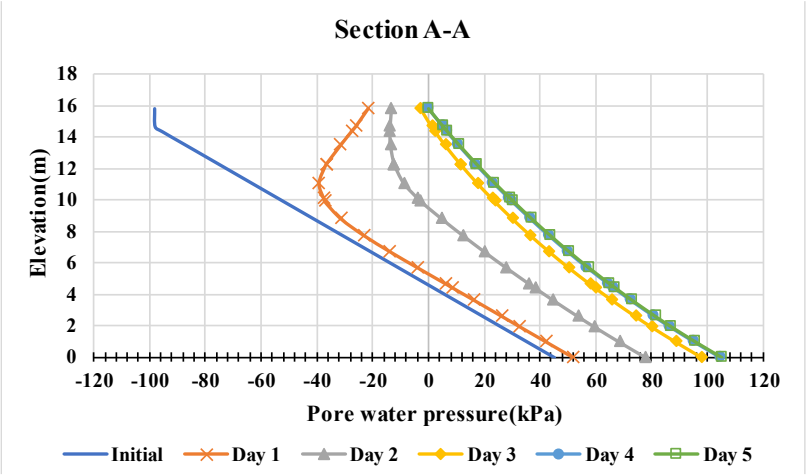

Figure 5.7: Pore water pressure variation profile variation during 20mm/hr rainfall – section AA(without capillary barrier)

5.1.4.2 Cut slope with capillary barrier cover

The effect of capillary barrier cover in the reduction of infiltration of rainfall into cut slopes was studied by plotting pore water pressure regime along section AA and section BB for rainfall of 20mm/hr intensity.

Pore water pressure variation along depth at section AA plotted with time for 20mm/hr rainfall is given in figure 5.8. Results show that provided capillary barrier has completely cut off the infiltration into slope at upper part of slope where existed initial matric suction was high (slope was sufficiently dry to form the capillary barrier effect). There is no rise of groundwater table even at the end of the fifth day due to the complete cutoff of infiltration at this section.

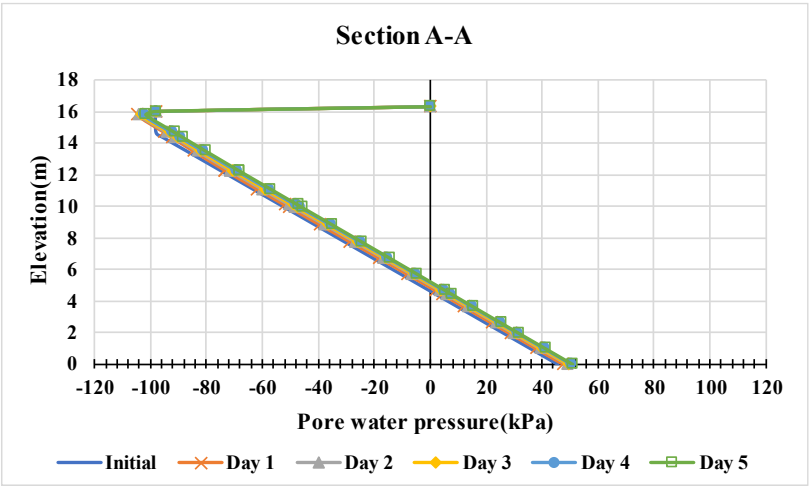

Figure 5.8: Pore water pressure profile variation during 20mm/hr rainfall– section AA(with capillary barrier)

Results in figure 5.9 show that there is a very small amount of infiltration to the slope along section BB which is located at the bottom part of the model. This may be due to the effect of boundary conditions at the toe end of the model since there is no notable breakthrough was spotted. But when compared with the matric suction profile variation for the slope without any covers this depletion of matric suction is negligible. Therefore, the provided capillary barrier cover was effective enough to cut off the infiltration completely during an intense rainfall event of 20mm/hr for 5days. As such infiltration into a slope with capillary for rainfall of intensity 10mm/hr rainfall was not carried out.

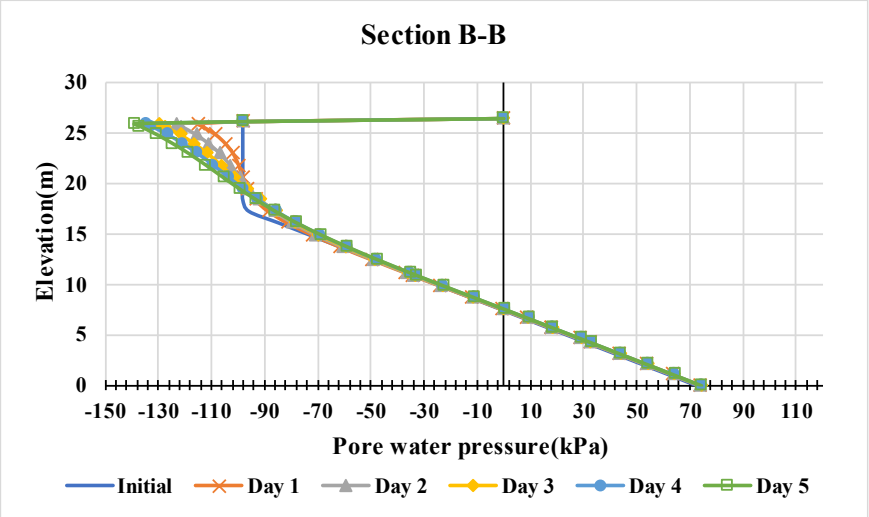

Figure 5.9: Pore water pressure profile variation during 20mm/hr rainfall– section BB(with capillary barrier)

5.1.4.3 Stability of slope

Figure 5.10 presents the variation of the factor of safety of the slope with time for the slope with and without capillary barrier cover.

The initial factor of safety of the slope before any rainfall was around 2.3, this shows that this slope stays stable during the dry season with the prevailing high matric suction. But factor of safety of the slope has reduced with infiltration into slope due to loss of matric suction and development of positive pore water pressure which causes a reduction in shear strength parameters of the soil. The loss of matric suction due to 10mm/hr rainfall and 20mm/hr rainfall has resulted in reduction of factor of safety. The matric suction loss is comparatively high for 20mm/hr rainfall and incidentally,

the factor of safety has reduced to a much lower value of 1.2 compared to the reduction with 10mm/hr rainfall. This depicts the potential risk of failure during intense prolonged rainfall events. When there is a capillary barrier cover, the infiltration was completely cut off and there was no reduction in FOS even with the 20mm/hr rainfall that prolonged for 5 continuous days.

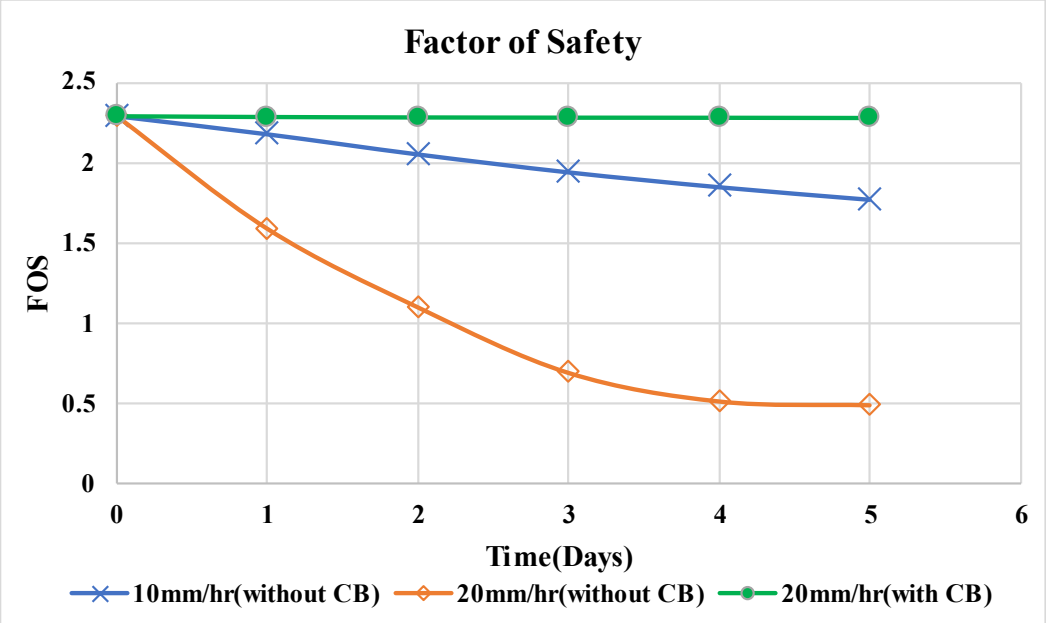

Figure 5.10: Factor of safety variation for 5 continuous days rainfall

5.1.5 Discussion

A preliminary numerical study on the effect of capillary barrier cover in Sri Lankan cut slope has many finding confirming the applicability of these covers in local cut slopes. From the results of the analysis for the slope without any covers, we can find that increase in rainfall intensity will lead to significant loss of matric. Even in some scenarios (during 20mm/hr rainfall) positive pore pressure had developed at downside of slope. From the numerical studies on slopes with capillary barrier covers it was found that infiltration into a natural slope with a single gradient cut slope can be very significantly reduced by a capillary barrier with,

- Proper constitutive fine and coarse material
- Fine and coarse layers of sufficient thickness

- Adequate drainage to remove laterally diverted flow along the fine-coarse interface

Capillary barriers are effective in completely cutting off any infiltration into the slope even during a rainfall of intensity 20mm/hr, wherein the case without capillary cover this rainfall has caused the development of positive pore water pressure in the slope. Hence, the stability of cut slopes can be maintained even under the conditions of extremely heavy prolonged rainfall with the provision of properly designed capillary barrier cover.

In the laboratory model studies with the capillary barrier, locally available river sand and M-sand(coarse fraction) were used as the fine and coarse layers, respectively. A series of analyses were done with the capillary barrier made of these materials.

In the reality, deeper cut slopes are made in road constructions and it is customary to do that with multiple berms. Numerous problems with convergence were observed when the capillary barrier on a multilevel cut slope was performed with SEEP/W. Hence it was decided to the further numerical studies with the MIDAS GTS NX software.

5.2 3-D Numerical study of laboratory level capillary barrier with MIDAS

Before carrying out the rainfall experiments on the developed laboratory physical model with river sand as a fine layer and M-sand (sieved and retained on 1.18mm sieve) as a coarse layer, the 3-D numerical investigation was done with Midas GTS-NX software to check the performance of the model under prolong rainfall for rainfall intensities of 5mm/hr, 10mm/hr and 20mm/hr. The model was subjected to high initial matric suction to make the capillary model sufficiently dry so that the performance of the capillary cover can be checked under prolong intense rainfall conditions.

5.2.1 Geometry and boundary conditions

Figure 5.11 illustrates the geometry of model that was used in the FEM analysis. Based on the physical model developed and layer thicknesses determined using previous 2-D numerical study, the analysis was done with capillary barrier cover made with 20cm thick fine layer over 10cm thick coarse layer underline by local residual soil. A fine-coarse interface angle of 15^0 was used in the investigations since the minimum slope angle intended to be used in the rainfall experiment was 15^0 degrees.

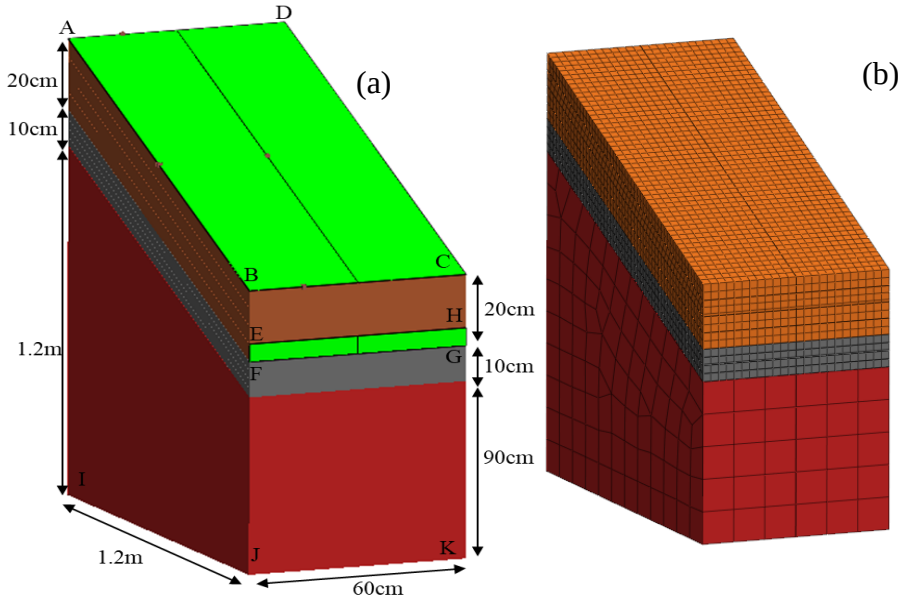

Figure 5.11: (a) 3-D geometrical model and boundary conditions, (b) Mesh used in the analysis

A fine mesh set of size 2.5cm was used in the meshing fine layer and coarse layer, while the coarse mesh set of size 18cm was used for residual soil. Here the fine meshing was used for capillary layers because their thicknesses were very small when

compared to residual soil layers, so the fine meshing is required to model the capillary effect precisely. Coarse meshing used in the residual soil layer to reduce the analysis time since its layer thickness was quite large and only seepage occurs through this layer.

Fredlund Xing best-fit parameters and saturated hydraulic conductivity of river sand, M-sand(coarse) and residual soil discussed in section 3.2 were used in modelling the material behaviour.

Following boundary conditions were used to resemble the field conditions in the model,

- ABCD – surface flux boundary (to simulate rainfall into the model)
- ABCD – review boundary (to simulate surface runoff on the surface of model)
- EFGH – zero pressure boundary (to introduce drainage from the model)
- IJKL – nodal head boundary -10m (to introduce initial pore water pressure condition in the model)

5.2.2 Results

Rainfall infiltration into the model was analyzed by plotting pore water pressure and volumetric water content variation along mid of fine sand layer and fine-coarse interface at different locations in the capillary barrier cover.

- **Pore water pressure head and volumetric water content variation**

Pore pressure and volumetric water content variation along mid of river sand layer, mid of M-sand layer and river sand-M-sand interface at x-30cm and x-90cm as shown in figure 5.12 in the first 10hours were plotted to study the infiltration profile into the capillary barrier cover system.

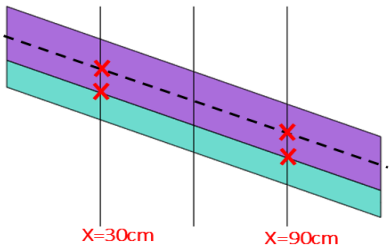

Figure 5.12: Locations where readings were taken

Figure 5.13 presents the pore water pressure variation along mid depth of fine layer, mid of coarse layer and fine-coarse interface at two different locations at the upper part and lower part of the model. Matric suction along mid of fine layer and fine-coarse interface has diminished completely from an initial value of 110kPa at the end of 10 hr simulation. But the matric suction along the mid of coarse layer has remained stable at 110kPa. Graphs for rainfall intensities of 5mm/hr, 10mm/hr and 20mm/hr show that infiltration has only entered the fine soil layer. This indicated the effectiveness of the capillary barrier made with river sand and M-sand. Also, the graphs show that the time taken for the loss of matric suction at these locations reduces with increasing rainfall intensity. For a given rainfall intensity rate of loss of matric suction increases along downdip direction of capillary barrier cover.

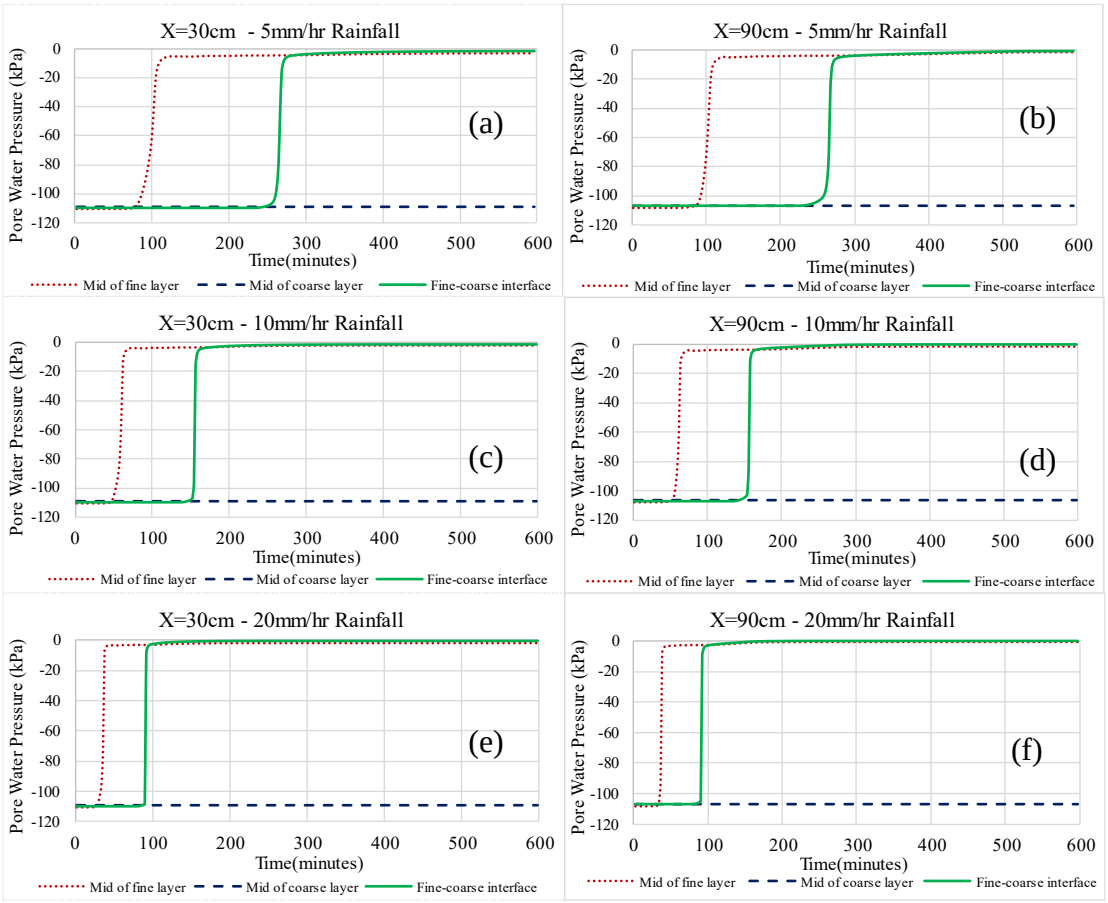

Figure 5.13: Pore pressure variation along the mid depth of fine & coarse layer and fine-coarse interface

Figure 5.14 presents the change in volumetric water content along mid depth of fine layer, mid depth of coarse layer and fine-coarse interface at two different locations.

Comparing graphs (example (a) & (b)) plotted at x-30cm and x-90cm for a given rainfall intensity it can be found that volumetric water content at lower part of model is higher than that at the upper part of the model (example – moisture content at mid of fine layer during 5mm/hr rainfall is 24% at the upper part and 30% in the lower part). This scenario is due to the collection of lateral diversion from upper part of cover along fine-coarse interface at the downdip direction. Later this lateral diversion is removed through drainage provided at toe of model. Similar to pore water pressure variation in model with capillary barrier cover the time taken to increase in volumetric water content along the plotted locations reduces with increasing intensity of rainfall.

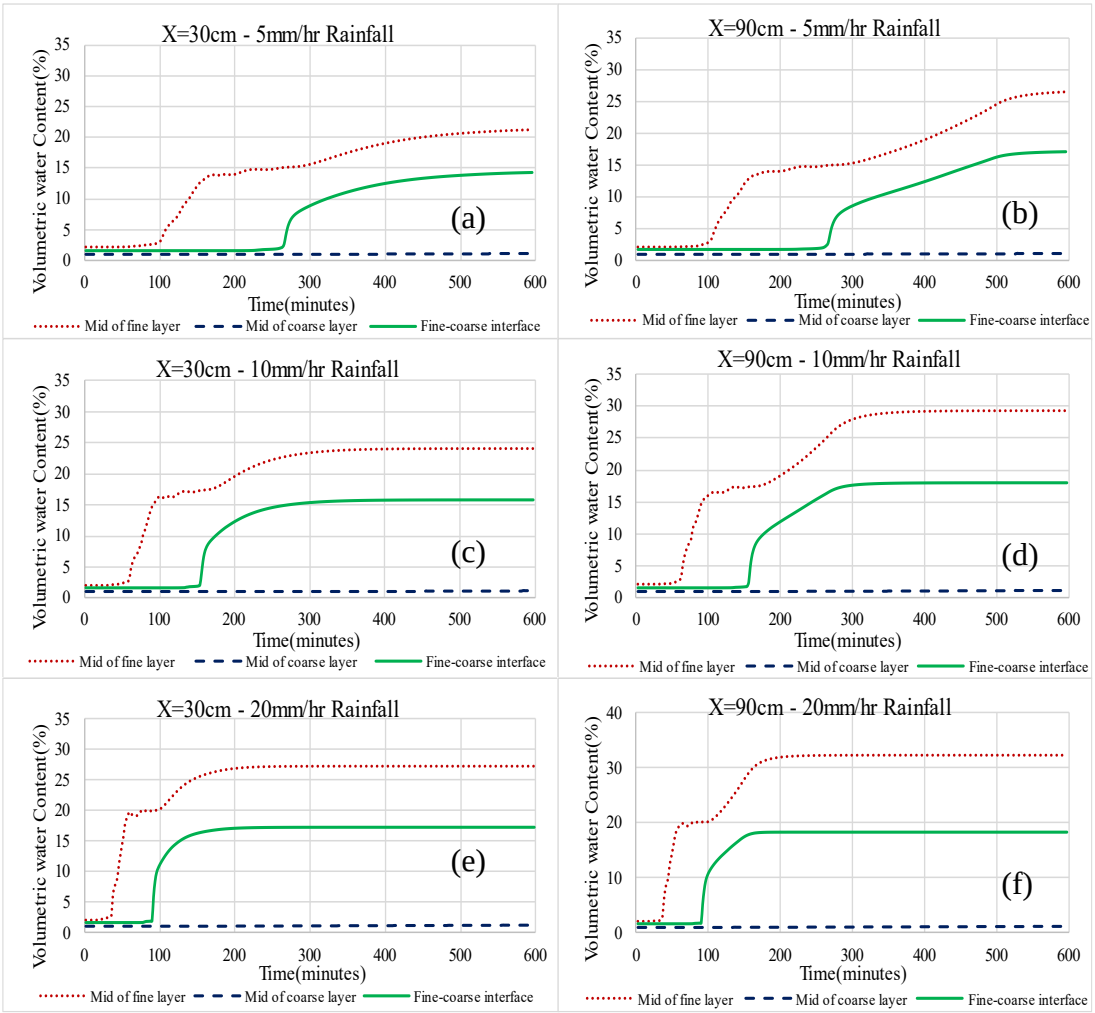

Figure 5.14: Volumetric water content variation along the mid depth of fine & coarse layer and fine-coarse interface

5.2.3 Discussion

From the 3-D numerical analysis results, it is found that cover made with placing 20cm thick river sand over 10cm thick M-sand (sieved and retained on 1.18mm sieve) form the capillary barrier effect under high matric suction range even during intense rainfalls varying from 5mm/hr -20mm/hr. Capillary barrier cover has performed well in prolonging intense rainfall events without any breakthrough as shown by the numerical study.

Figure 5.15 illustrates the flow velocity vectors in the capillary barrier cover at the end of 1hr duration. Flow vectors have not reached the fine-coarse interface during this period and infiltration has started to accumulate in the fine layer.

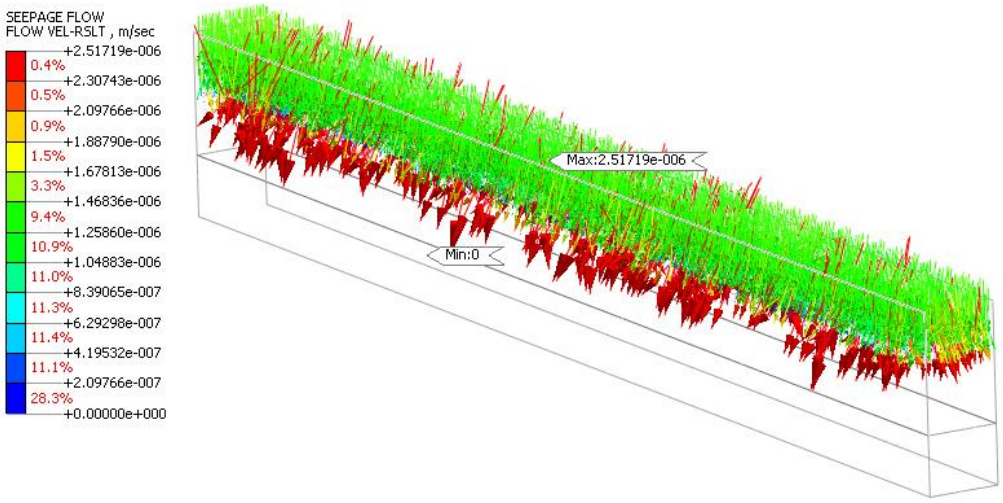

Figure 5.15: Flow velocity vectors – at end of 1hr rainfall

Figure 5.16 presents how the infiltrated water is being laterally diverted along the fine-coarse interface without any breakthrough in the capillary barrier effect at the end of 10hr rainfall. The magnitude of the flow increases along the down dip direction due to the collection of infiltration from the fine layer.

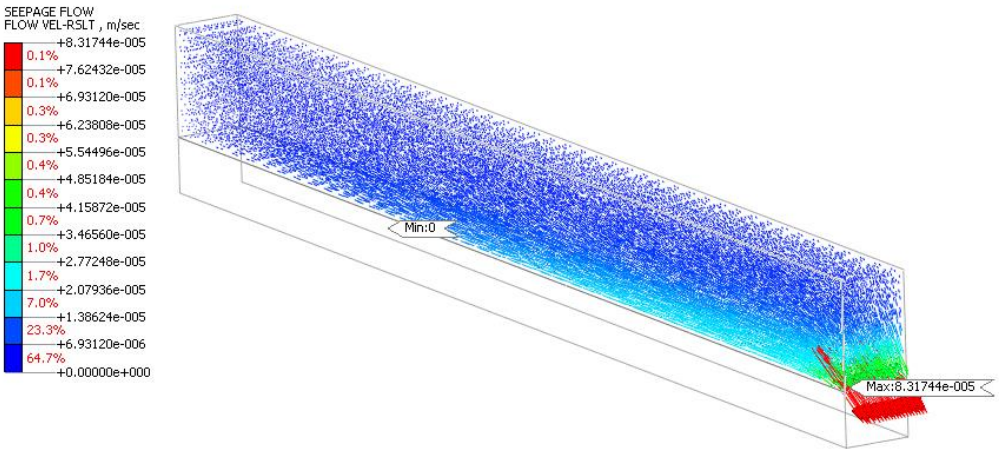

Figure 5.16:Flow velocity vectors – at end of 10hrs rainfall

In an effective capillary barrier cover during rainfall infiltration, the upper part of the cover remains sufficiently dry while the bottom part becomes wet due to lateral diversion. The fine layer along the fine-coarse interface at the downdip direction gets almost fully saturated when the capillary barrier performs with its full capacity. But the coarse layer beneath the fine layer remained dry indicating that there was no failure in the capillary barrier cover. Figure 5.17 shows that degree of saturation along fine-coarse interface has reached 100% at the toe of the model while the coarse layer remains sufficiently dry with almost 0% degree of saturation.

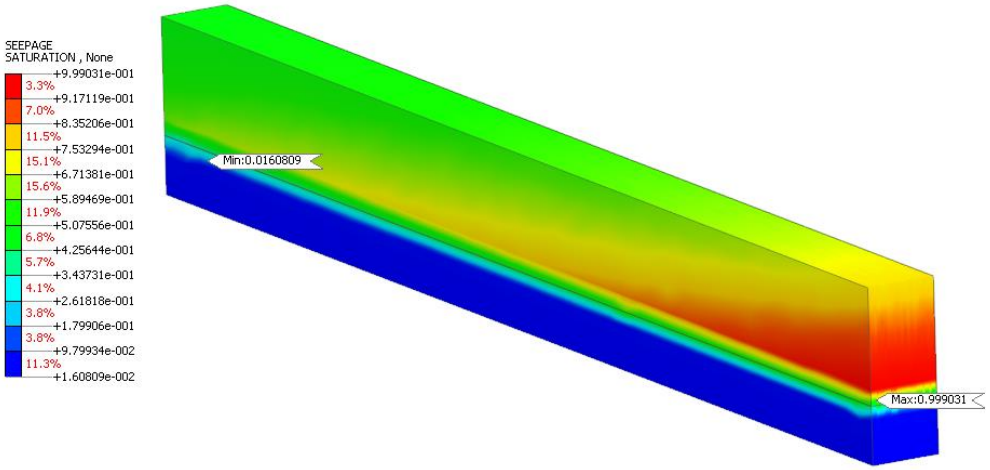

Figure 5.17: Degree of saturation in capillary barrier cover – at end of 10hrs rainfall

Therefore, it appears that the selected combination of river sand and M-sand can be utilized to construct capillary barriers under different rainfall patterns for varying slope angles from 15^0 – 30^0.

5.3 3-D numerical study of a multi-level cut slope with MIDAS

Performance of capillary barrier cover constructed with river sand as a fine layer and M-sand as coarse layer was studied experimentally and experimental results were verified using 2-D numerical analysis with SEEP/W program of GeoStudio software. Through studies, it was found that these materials can be used as constitutive materials of capillary barrier cover on the local slopes made of residual soils. But all these studies were laboratory-based experiments and their numerical verifications. The applicability of the capillary barrier constructed with these materials on cut slopes of real dimension must be studied. With time and resource limitations, it was not possible to conduct an instrumental field study. As such, only a numerical study was done for the effectiveness of the capillary barrier for a multilevel cut slope. Midas GTS-NX software was used in this numerical investigation considering the complexity of the geometry and infiltration in cut slope with capillary barrier cover system.

5.3.1 Materials and boundary conditions

Numerical simulations were done for the following two conditions,

- Cut slope without capillary barrier cover
- Cut slope with capillary barrier cover

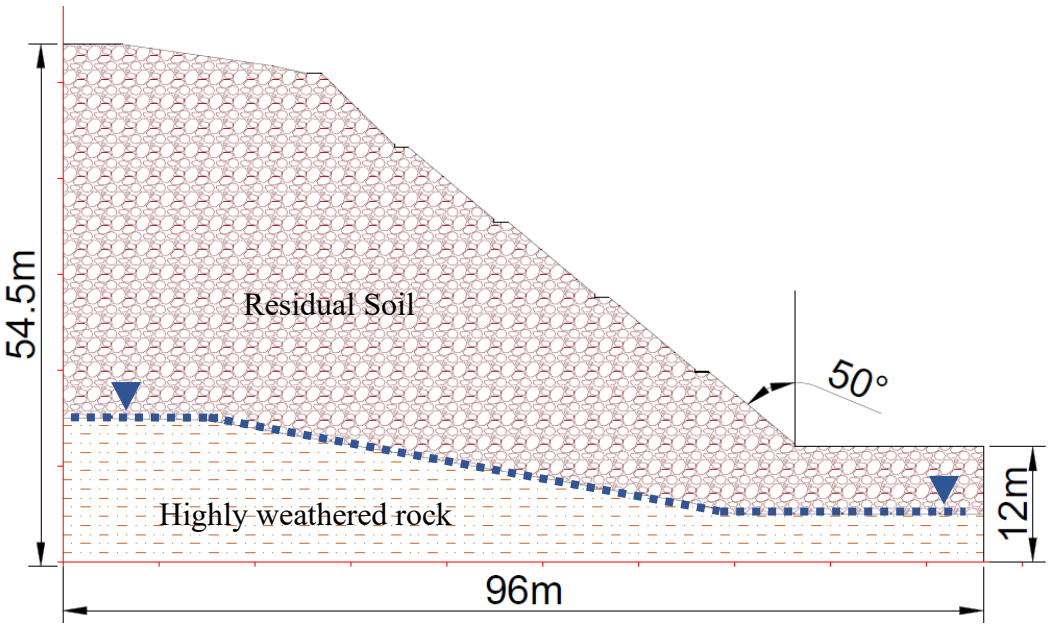

Figure 5.18: Geometry of cut slope used in the study

In both simulations' berm drains were applied to the model to facilitate the surface runoff out of the cut slope. Figure 5.18 illustrates the cut slope geometry resembling the real field conditions used in the study. The slope was assumed to be made of a thick residual soil layer overlying a highly weathered rock. In the study model with multiple levels cuts, a slope angle of 40^0 was used. A deep water table as indicated in the figure was used in the analysis and a maximum matric suction limit of 100kPa was applied to the model, so the real scenario of frequent wetting and drying of slopes can be simulated in the model. Performance of capillary barrier cover under prolong intense rainfall was studied by considering a sufficiently dry cover system. Investigations were done for 05 continuous days rainfall of intensities 5mm/hr, 10mm/hr and 20mm/hr.

Capillary barrier cover with 20cm thick river sand over 10cm thick M-sand layer was applied on the slopes to study the effectiveness of cover in reducing rainfall infiltration into the slope. Fredlund Xing best-fit parameters and saturated hydraulic conductivity of materials discussed in chapter 3.2 were used in this numerical study. In modelling the material behaviour of highly weathered rock best-fit parameters of residual soil was used and a value of 1×10^{-7}m/s was used as saturated hydraulic conductivity(Sujeevan & Kulathilaka, 2011). Berm drains were modelled using impervious material property available in the software to model the structural items.

Following boundary conditions were used to simulate the field conditions in the model,

- On the surfaces of slope and capillary barrier cover – surface flux boundary (to simulate rainfall into the model)
- On the surface of berm drains, slope, and capillary barrier cover -review boundary (to simulate surface runoff on the surfaces)
- Toes of capillary barrier covers – zero pressure boundary (to introduce drainage in the model)
- Along residual soil – highly weathered rock interface – groundwater table (to introduce initial pore pressure condition in the model)

Figure 5.19 illustrates the slope modelled with capillary barrier cover and berm drains to study infiltration profile into the slope with capillary barrier cover system.

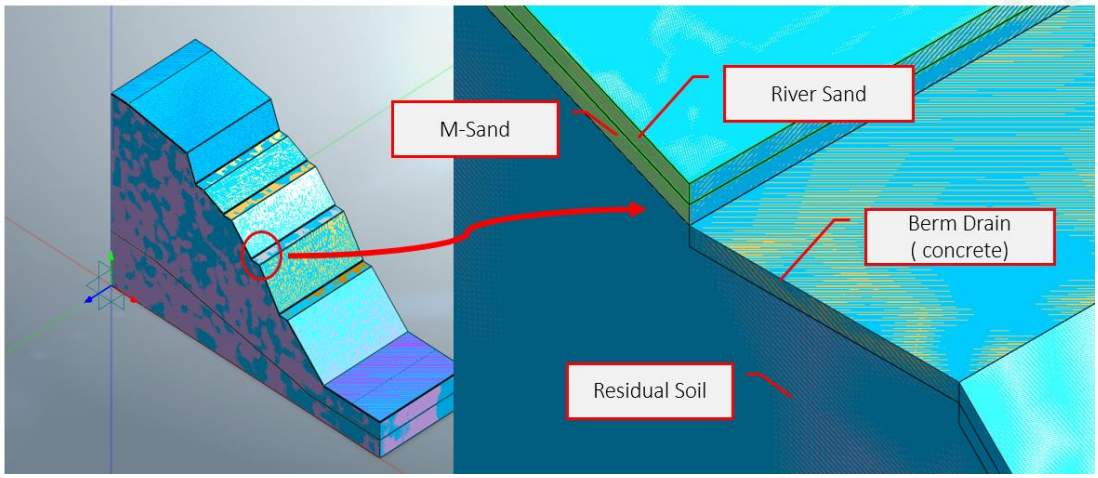

Figure 5.19: Capillary barrier cover and berm drain used in the numerical study

5.3.2 Results

Pore water pressure variation along section AA, BB, CC were plotted from results of numerical analysis to investigate the performance of the capillary barrier cover system in the real scenario. Figure 5.20 presents the sections along which the pore pressure regimes were obtained.

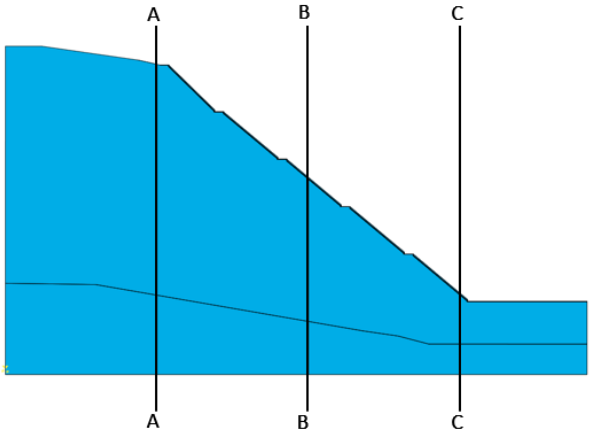

Figure 5.20: Sections along which the pore water pressure graphs were plotted

5.3.2.1 Cut slope without capillary barrier cover system

- **Behaviour during 5mm/hr rainfall**

Figure 5.21 shows the variation of pore pressure along section AA during 5mm/hr rainfall. Initially, maximum matric suction of 100kPa has prevailed in this section

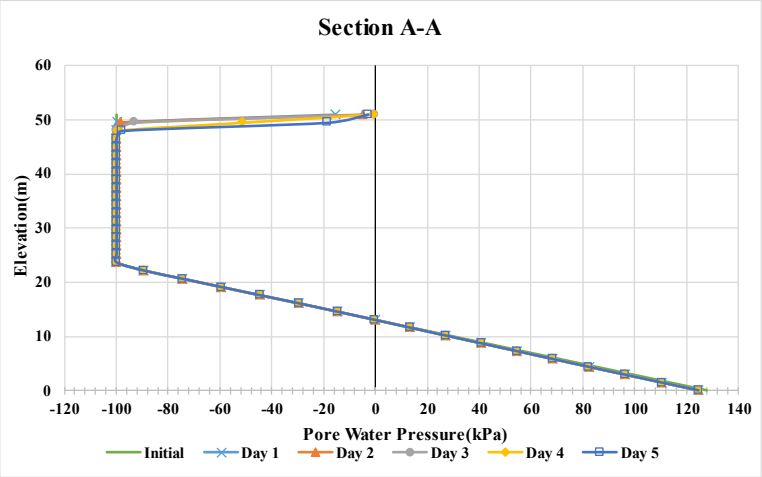

Figure 5.21: Pore pressure variation (5mm/hr rainfall) – section AA(without capillary barrier)

Pore pressure variation along section BB is presented in figure 5.22. Matric suction has lost in only to about 5m depth due to rainfall infiltration. At the surface level, matric suction has depleted completely.

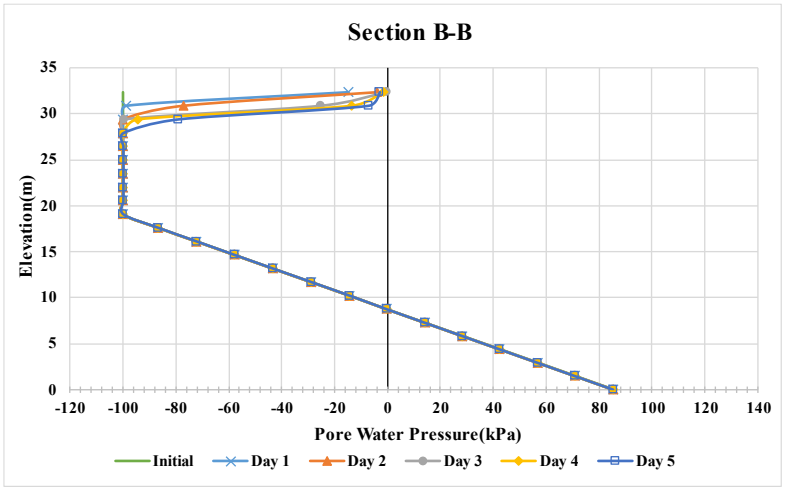

Figure 5.22: Pore pressure variation (5mm/hr rainfall) – section BB(without capillary barrier)

Figure 5.23 shows the pore water pressure variation along section CC of the slope. Matric suction has depleted to a greater depth in this section when compared to other upper sections since existed initial matric suction was low with the value of 80kPa. With time infiltration has reached greater depth along the section.

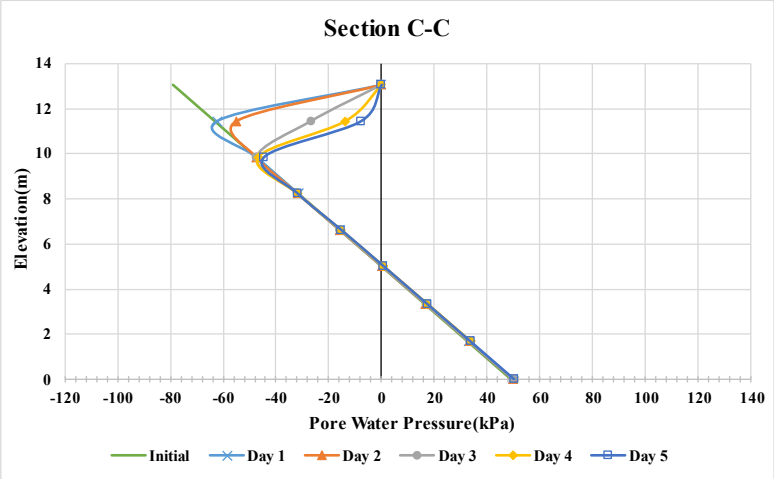

Figure 5.23: Pore pressure variation (5mm/hr rainfall) – section CC(without capillary barrier)

- **Behaviour during 10mm/hr rainfall**

Figure 5.24 shows the variation of pore pressure along section AA during 10mm/hr rainfall. Initially, maximum matric suction of 100kPa has prevailed in this section, but with time due to rainfall matric suction near the surface has depleted significantly.

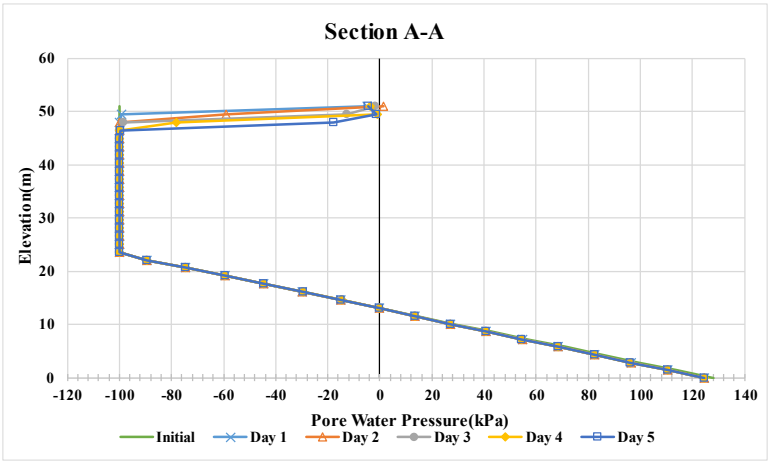

Figure 5.24: Pore pressure variation (10mm/hr rainfall) – section AA(without capillary barrier)

Pore pressure distribution along section BB is given in figure 5.25. Due to the continuous rainfall prevailed initial maximum matric suction of 100kpa was lost along the depth with time. Rainwater has infiltrated to a depth of 5m into this section causing loss of matric suction.

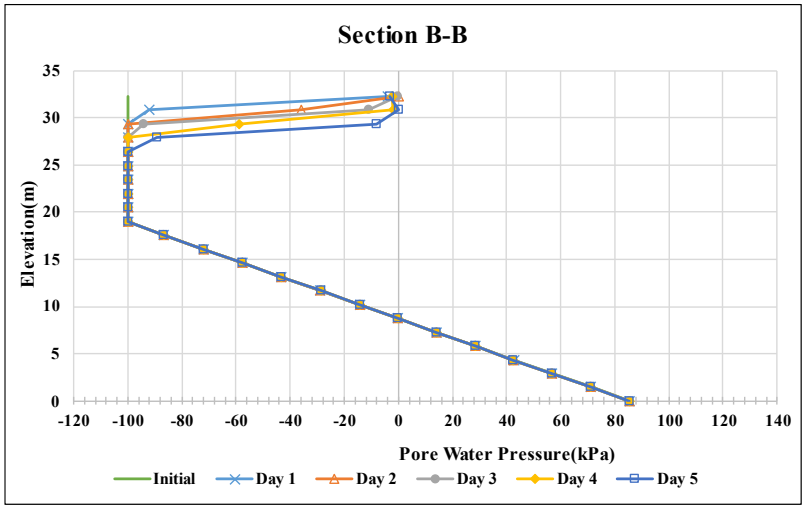

Figure 5.25: Pore pressure variation (10mm/hr rainfall) – section BB(without capillary barrier)

Distribution of pore water pressure along section CC during 10mm/hr rainfall is presented in figure 5.26. Matric suction has depleted in this section to a greater depth when compared with other sections. Prevailed maximum matric suction of 80kPa has completely lost up to 6m depth in this section.

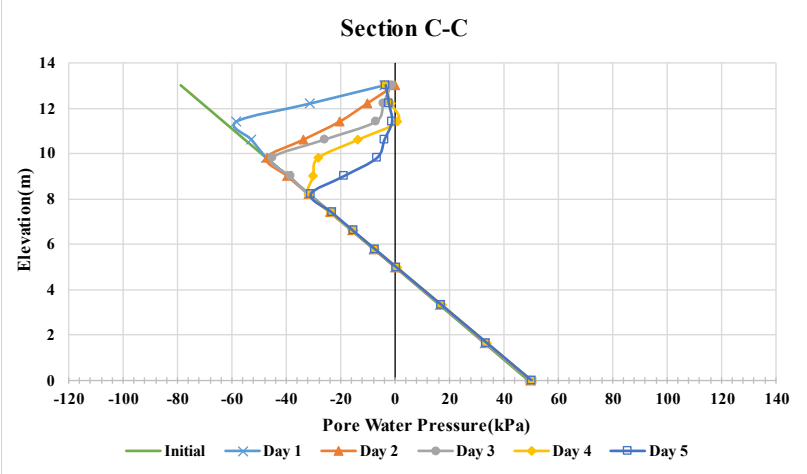

Figure 5.26: Pore pressure variation (10mm/hr rainfall) – section CC(without capillary barrier)

- **Behaviour during 20mm/hr rainfall**

Figure 5.27 shows the variation of pore pressure along section AA during 20mm/hr rainfall. Initially, a maximum matric suction of 100kPa prevailed in this section, but with time due to rainfall matric suction has depleted significantly and at end of the fifth day positive pore pressure has developed up to considerable depth.

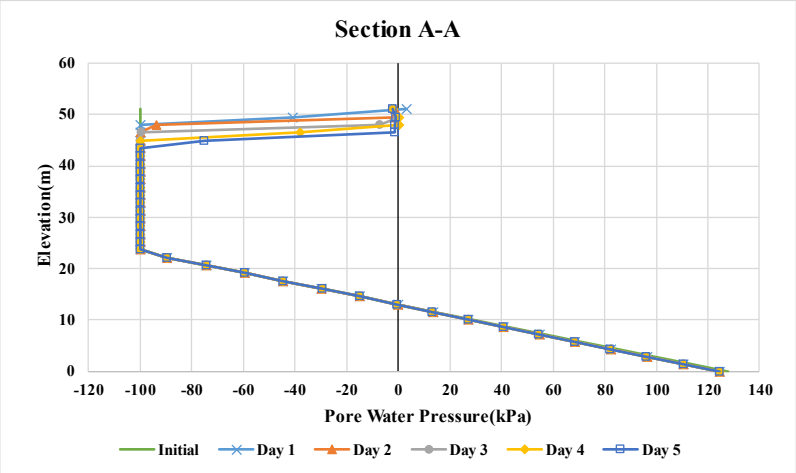

Figure 5.27: Pore pressure variation (20mm/hr rainfall) – section AA(without capillary barrier)

Pore water pressure distribution along section BB is presented in figure 5.28. The continuous rainfall has caused the development of positive pore pressure near the surface - a perched water table. Rainwater has infiltrated 10m deep into this section causing considerable loss of matric suction.

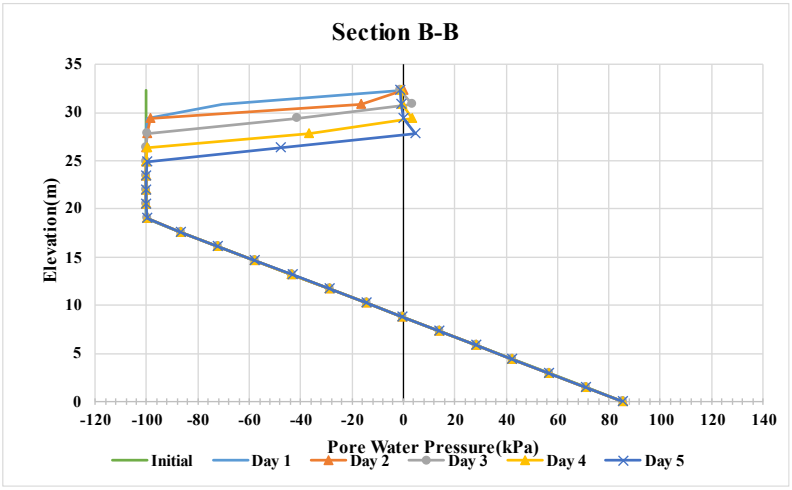

Figure 5.28: Pore pressure variation (20mm/hr rainfall) – section BB(without capillary barrier)

Variation of pore water pressure along section CC during 20mm/hr rainfall is given in figure 5.29. Matric suction has depleted in this section to a greater depth and even positive pore pressure has developed up to a significant depth of the section at the end of the fifth day.

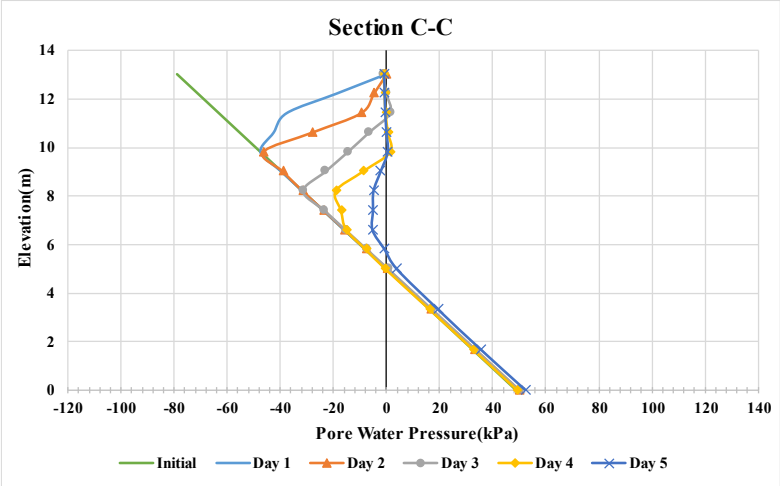

Figure 5.29: Pore pressure variation (20mm/hr rainfall) – section CC(without capillary barrier)

5.3.2.2 Cut slope with capillary barrier cover system

- **Performance during 5mm/hr rainfall**

Figure 5.30 shows the variation of pore water pressure along section AA during 5mm/hr rainfall. Since this section at the uppermost part of the model capillary barrier cover was not applied considering the field construction process. Initially, maximum matric suction of 100kPa prevailed in this section, but with time due to rainfall matric suction has lost considerably for a depth of 5m.

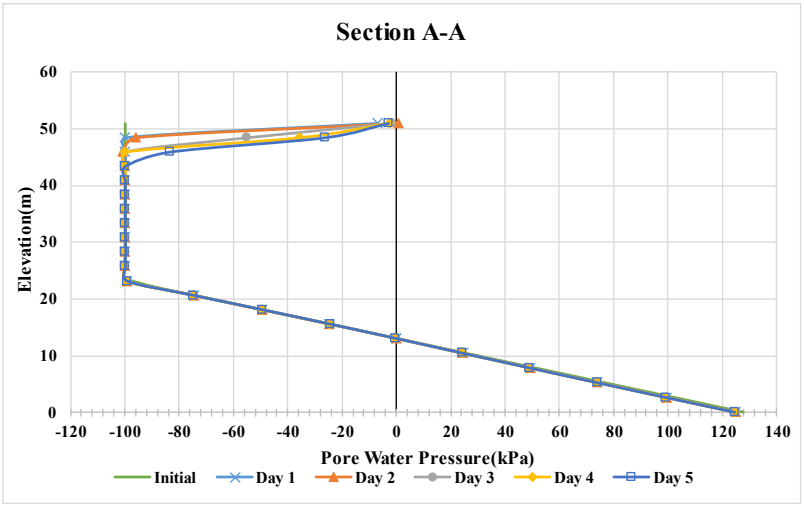

Figure 5.30: Pore pressure variation (5mm/hr rainfall) – section AA(with capillary barrier)

Pore water pressure variation along section BB is given in figure 5.31. Due to presence of capillary barrier cover on surface of slope along this section even during the

continuous rainfall prevailed initial maximum matric suction of 100kPa has remained the same without any loss. This shows the effect of the capillary barrier cover system in cutting off rainfall infiltration during 5mm/hr rainfall.

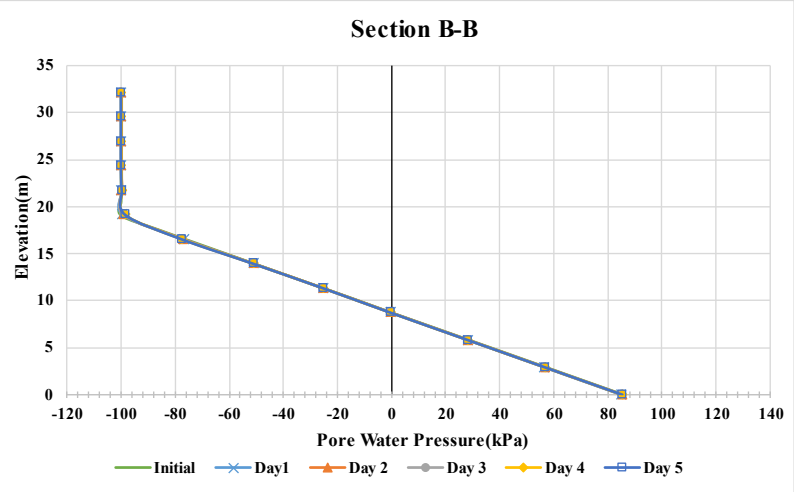

Figure 5.31: Pore pressure variation (5mm/hr rainfall) – section BB(with capillary barrier)

The distribution of pore water pressure along section CC during 5mm/hr rainfall is shown in figure 5.32. Matric suction has depleted in this section to a considerable depth when compared with the model without a capillary barrier cover system. Even at the end of the fifth day, the matric suction loss was about 50kPa.

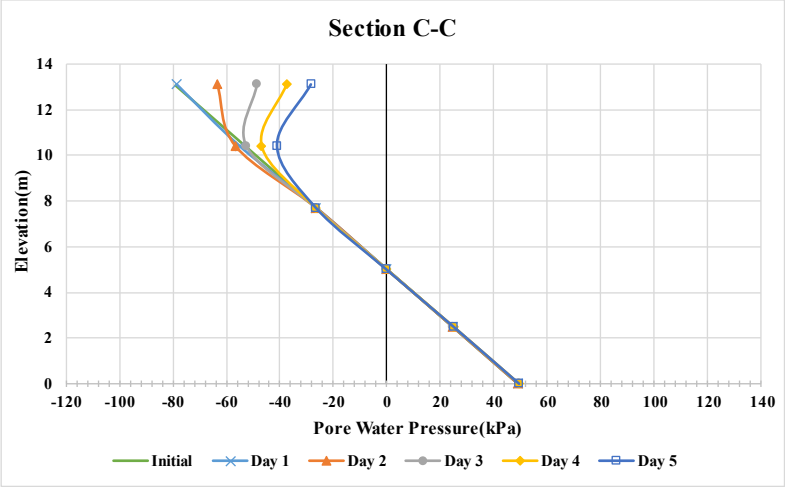

Figure 5.32: Pore pressure variation (5mm/hr rainfall) – section CC(with capillary barrier)

- **Performance during 10mm/hr rainfall**

Figure 5.33 presents the variation of pore water pressure along section AA during 10mm/hr rainfall. Considering similar construction in the field, the capillary barrier cover was not applied to this section. Initially, maximum matric suction of 100kPa prevailed in this section, but with time due to rainfall matric suction has depleted significantly

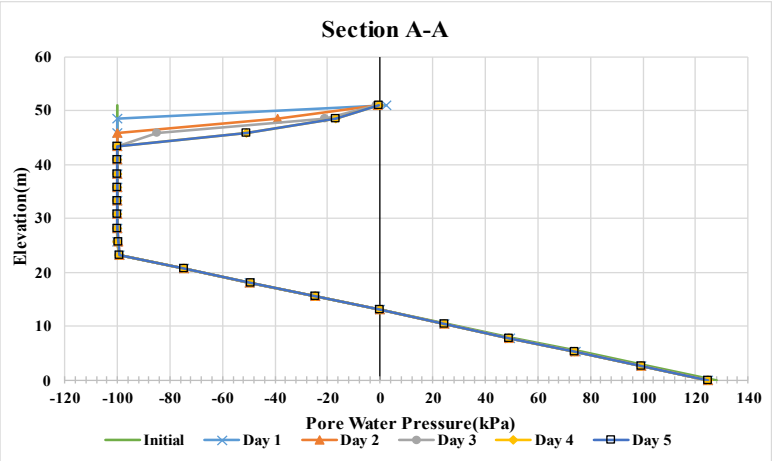

Figure 5.33: Pore pressure variation (10mm/hr rainfall) – section AA(with capillary barrier)

Pore water pressure variation along section BB is presented in figure 5.34. Since capillary barrier cover is provided on surface of slope along this section even during the continuous rainfall prevailed initial maximum matric suction of 100kPa has remained the same without any loss. This indicates the effect of capillary barrier cover system in cutting off rainfall infiltration even during 10mm/hr rainfall.

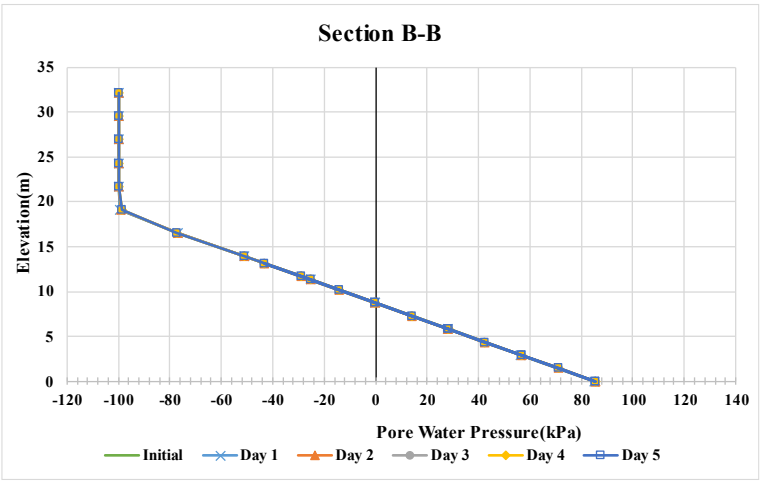

Figure 5.34: Pore pressure variation (10mm/hr rainfall) – section BB(with capillary barrier)

Variation of pore water pressure along section CC during 10mm/hr rainfall is given in Figure 5.35. Matric suction has depleted in this section in a considerably low amount when compared with the model without a capillary barrier cover system. Even after 5 continuous days, matric suction loss was about 60kPa while positive pore water pressure has developed in model without capillary barrier cover.

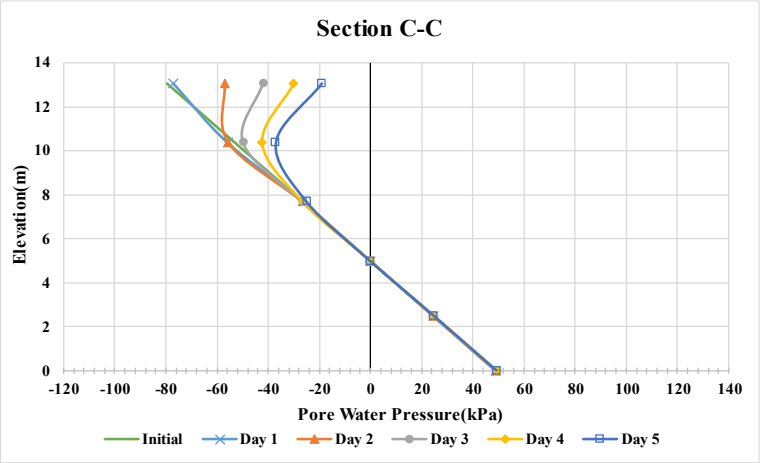

Figure 5.35: Pore pressure variation (10mm/hr rainfall) – section CC(with capillary barrier)

- **Performance during 20mm/hr rainfall**

Figure 5.36 presents the variation of pore water pressure along section AA during 20mm/hr rainfall. On this uppermost part of the model considering similar construction of field capillary barrier cover was not applied. Initially, maximum matric suction of 100kPa prevailed in this section, but with the rainfall, matric suction has depleted significantly. Positive pore pressure has developed at end of the fifth day under the slope surface.

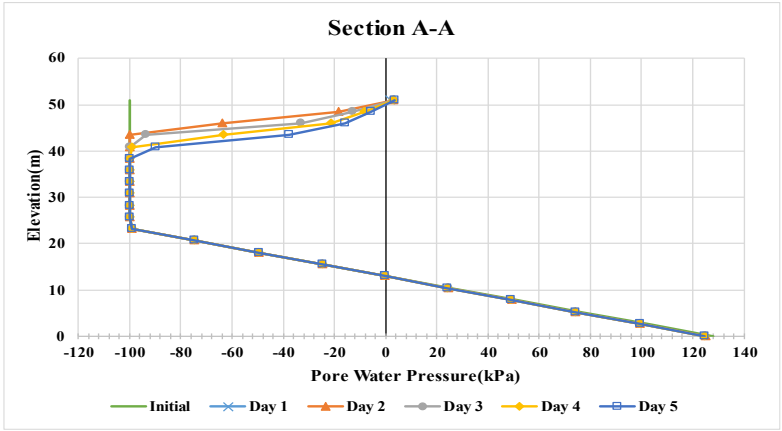

Figure 5.36: Pore pressure variation (20mm/hr rainfall) – section AA(with capillary barrier)

Pore water pressure variation along section BB is presented in figure 5.37. Since capillary barrier cover was there on the surface of the slope along this section even during the continuous rainfall prevailed initial maximum matric suction of 100kPa has remained the same without any loss until the fourth day, but at end of the fifth day, matric suction has lost significantly. This shows that the capillary barrier cover system cut off rainfall infiltration sufficiently during 20mm/hr rainfall.

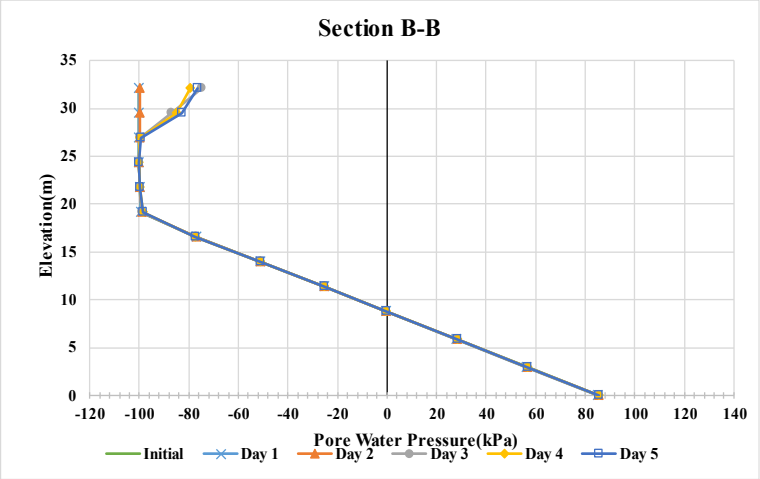

Figure 5.37: Pore pressure variation (20mm/hr rainfall) – section BB(with capillary barrier)

Pore water pressure variation along section CC during 20mm/hr rainfall is given in figure 5.38. Loss of matric suction along this section is significantly low when compared with the model without a capillary barrier cover system. Even after 4 continuous days, matric suction loss was about 75kPa while positive pore water pressure has developed in model without capillary barrier cover.

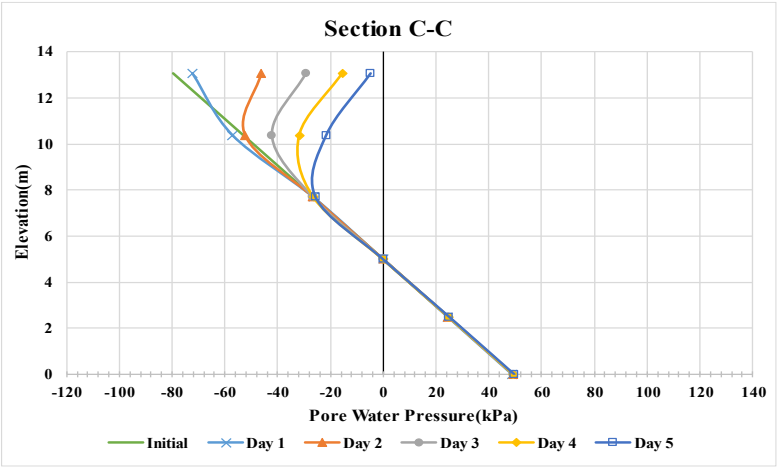

Figure 5.38: Pore pressure variation (20mm/hr rainfall) – section BB(with capillary barrier)

5.3.3 Discussion

A 3-D numerical analysis was done with the intention of studying the field applicability of capillary barrier cover constructed with 20cm river sand over 10cm thick M-sand(coarse) in a slope of 40^0 angle in Sri Lankan residual soil. Initial analysis on a cut slope without capillary barrier cover for rainfall intensity varying over 5mm/hr, 10mm/hr and 20mm/hr for continuous 5 days show that infiltration into the system increases with the rainfall intensity causing loss of matric suction. Even positive pore water pressure has developed in some sections during 10mm/hr and 20mm/hr rainfalls. Perched water table conditions were developed near the surface of the slope during prolong intense rainfall and a rise of the groundwater level was seen at the lower section of the slope. Figure 5.39 shows the infiltration profile (variation of pore water pressure head) into the slope without capillary barrier cover at the end of 20mm/hr rainfall.

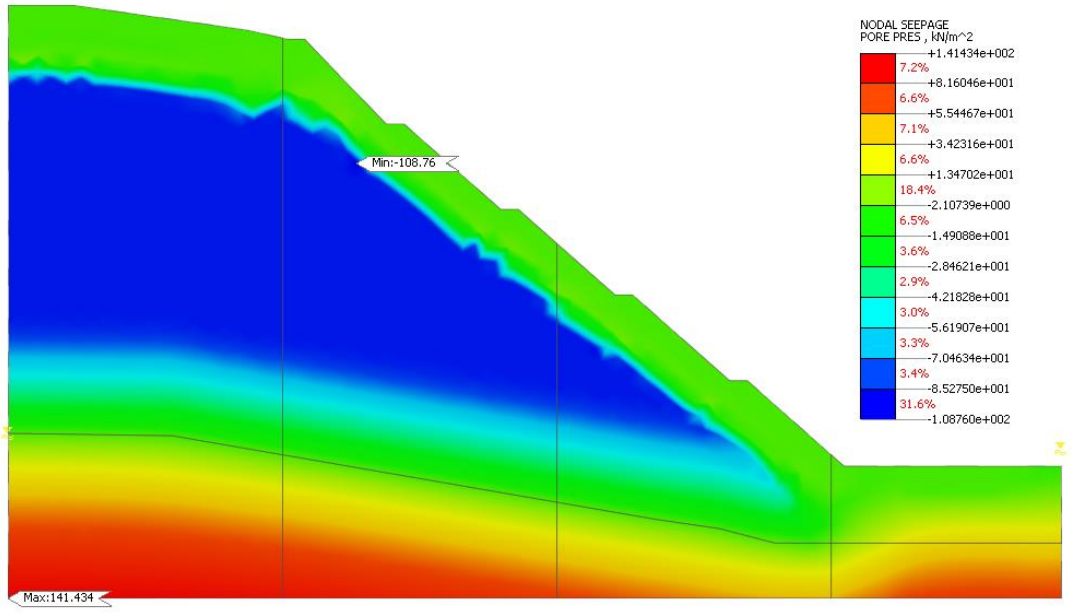

Figure 5.39: Pore water pressure distribution diagram after 5continuous days rainfall of 20mm/hr (slope without capillary barrier cover)

Figure 5.40 shows the infiltration profile (variation of pore water pressure head) into the slope with capillary barrier cover at the end of 20mm/hr rainfall. Numerical investigation shows that constructed capillary barrier cover on the cut slope has cut off the infiltration into the slope almost completely. Cover has completely cut off the

infiltration into the slope during low intense rainfall of 5mm/hr. Provided capillary barrier cover performed well even during prolong 20mm/hr rainfall. Therefore, Capillary barrier cover constructed with river sand and M-sand is effective in completely cutting off any infiltration into the slope. Hence, a properly designed capillary barrier cover with these materials can be applied on fields to maintain the stability of cut slopes even under the conditions of extremely heavy prolonged rainfalls.

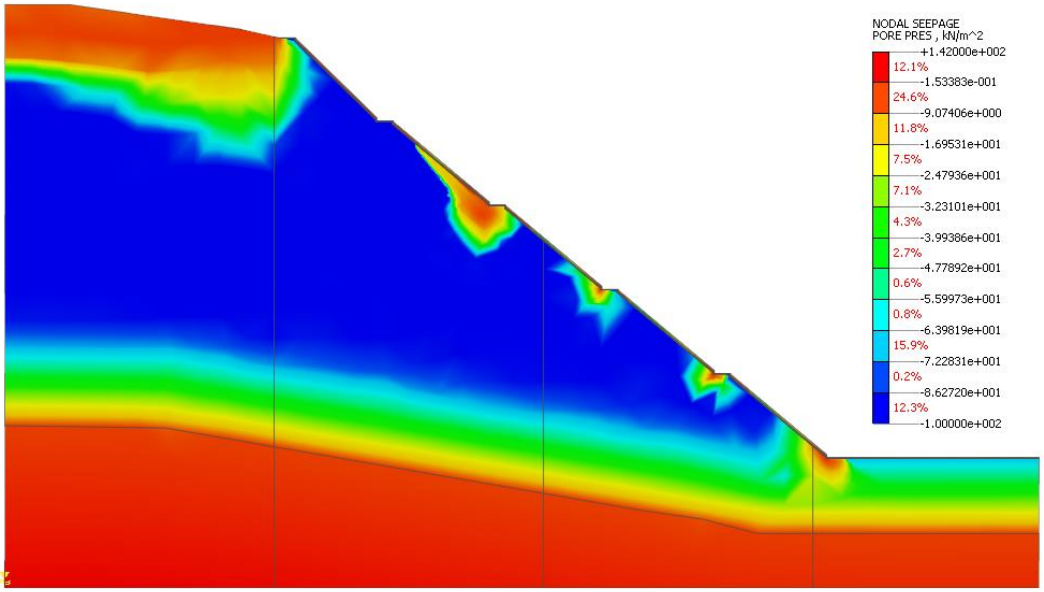

Figure 5.40: Pore water pressure distribution diagram after 5 continuous days rainfall of 20mm/hr (slope with capillary barrier cover)

6 CONCLUSIONS AND RECOMMENDATIONS

6.1 Conclusions

Rain induced slope failures are a major challenge to Sri Lankan Engineers involved in infrastructure development. When natural slopes are cut to somewhat steep angles their safety margins reduce with the infiltration of rainwater during the prolong heavy rainfalls. Hence, improvement of surface and subsurface drainage is essential to minimize the risk. In some cases, structural interventions in the form of slope reinforcements and toe retaining structure are also to be done. In this research, an alternative technique – the use of capillary barriers on the reduction of landslides risk was studied.

The possibility of using capillary barrier covers in reducing landslide risks on cut slopes in Sri Lanka is a unique study area. In this research study possibility of using locally available fine and coarse materials to construct a capillary barrier cover was investigated. Preliminary numerical studies were done with constitutive materials from literature to check the effect of capillary barrier cover on local cut slopes made of residual soil. The study showed a promising effect of the capillary barrier in reducing rainfall infiltration into local cut slopes. As such, the research was extended to study the effectiveness of the capillary barrier cover formed with local constitutive materials.

Local river sand and M-sand were selected as study materials in this research. Initially, the basic material properties and SWCC of these materials were determined through laboratory experiments. Later these material properties and best-fit parameters through Freudlund & Xing model were used in the study.

A Laboratory physical model was constructed to analyze the performance of capillary barrier cover with river sand and M-sand under different slope angle and varying rainfall intensities and duration of rainfall. Since it was found that the influence of boundary on the development of a capillary barrier effect is less than 200mm, measurements were taken from rainfall experiments in the model beyond this influence distance. Effective combination of fine and coarse layer thickness was also determined as 20cm and 10cm respectively from these numerical studies. It was also found that

only the thickness of the fine layer affects the performance of the capillary barrier cover.

Rainfall experiments and their numerical verifications show that the capillary barrier with local materials performed well to reduce the rainfall infiltration into the residual soil slope beneath it. Following conclusions were arrived from this experimental and numerical study,

- Fine-coarse interface angle affects the performance of the capillary barrier effect. The cover with slope angle 30^0 cut off the infiltration for a longer duration than the cover with 15^0 slope angle. Therefore, lateral diversion increases with an increase in the fine-coarse interface angle.
- Effectiveness of cover increases when it is sufficiently dry. Capillary barrier cover constructed on 15^0 slope performed effectively in reducing rainfall infiltration for a longer duration when it was allowed to dry for a period of three months.
- Performance of the capillary barrier reduces with the increase in rainfall intensity and duration.

3-D numerical analysis to check the field applicability of the capillary barrier lead to many findings. Positive pore water pressure may develop in cut slopes during prolong intense rainfall events, which will lead to failures of these slopes due to loss of shear strength. But when applying the capillary barrier made up with local constitutive materials on the surface of these cuts along with sufficient surface drainage (berm drains) rainfall infiltration can be cutoff significantly even during intense prolong rainfall events.

Therefore, the locally available materials; river sand and M-sand(coarse) can be used to construct capillary barrier covers which will perform to cut off the rainfall infiltration into local cut slopes and reduces the risk of cut slope failures during intense rainfalls. Both these materials fall into the UCS classification of SP but with different percentage of finer and coarser particles.

6.2 Recommendations

This study focused only on the use of river sand and M-sand as capillary barrier fine and coarse layer materials. But during real construction works these materials may not be readily available at the site. On that occasion's constructor may have to look up to use different materials. As such further studies should be done to check the suitability of other different materials. Especially the possibility of using local materials at the site have to be focused on to reduce the construction cost.

Drainage layers provided along the fine-coarse interface affects the performance of the capillary barrier covers significantly. Literature suggests the possible use of different soil materials and synthetic materials as drainage layers. These drainage layers increase the lateral diversion along the capillary barrier. Therefore, effect of different drainage layers on the performance of the capillary barrier should be analyzed. Further, the effect of using a geotextile layer as a separation medium between soil layers should also be studied. These geotextile layers perform as transportation layers and contribute to lateral diversion.

Meanwhile, the field applicability of capillary barriers on local cut slopes was investigated through only numerical simulations. An instrumented capillary barrier constructed on the field has to be monitored over the period of the dry season and rainy season to investigate its performance in the long run under field conditions and in different climatic conditions. The stability of capillary barriers on steep slopes should be studied along with the effect of erosion of fine soil layer during intense rainfalls. Studies on possible adoption of mitigations measures such as use of geomat layer on top of capillary barrier cover to prevent people accidentally removing the part of fine soil should also be done.

Surface covers such as vegetation covers are widely used on cut slopes to reduce the erosion and infiltration of rainfall. The vegetation cover will be essential to minimize erosion of slope surface. Therefore, further studies should be done to investigate the effectiveness of the combined performance of surface covers and capillary barrier covers on local cut slopes in reducing the infiltration.

REFERENCES

Ahmad-adli, M., Huvaj, N., & Kartal Toker, N. (2014). Effects of the Size of Particles on Rainfall-Induced Slope Instability in Granular Soils. *Geo-Congress 2014 Technical Papers*, (February), 4027–4036. https://doi.org/10.1061/9780784413272.391

Aubertin, M., Cifuentes, E., Apithy, S. A., Bussière, B., Molson, J., & Chapuis, R. P. (2009). Analyses of water diversion along inclined covers with capillary barrier effects. *Canadian Geotechnical Journal*, *46*(10), 1146–1164. https://doi.org/10.1139/T09-050

Aubertin, M., Cifuentes, E., Martin, V., Apithy, S., Bussière, B., Molson, J., … Maqsoud, A. (2006). *An Investigation of Factors that Influence the Water Diversion Capacity of Inclined Covers with Capillary Barrier Effects*. 613–624. https://doi.org/10.1061/40802(189)47

Aubertin, Michel, Bussière, B., Yanful, E. K., & De-Souza, L.-P. (Choo). (2001). Water Flow through Cover Soils Using Modeling and Experimental Methods. *Journal of Geotechnical and Geoenvironmental Engineering*, *127*(9), 810–812. https://doi.org/10.1061/(ASCE)1090-0241(2001)127:9(810)

Cho, S. E., & Lee, S. R. (2001). Instability of unsaturated soil slopes due to infiltration. *Computers and Geotechnics*. https://doi.org/10.1016/S0266-352X(00)00027-6

Collins, B. D., & Znidarcic, D. (2004). Stability analyses of rainfall induced landslides. *Journal of Geotechnical and Geoenvironmental Engineering*. https://doi.org/10.1061/(ASCE)1090-0241(2004)130:4(362)

Dhananjaya, K. K. D., & Kulathilaka, S. A. S. (2019). *Establishment of Soil Water Characteristic Curves for Sri Lankan Residual Soils*. University of Moratuwa.

Dharmasena, R. K. N., & Kulathilaka, S. A. S. (1998). Stabilization of Cut Slopes in Highways by Surface Drainage and Vegetation. *International Conference on Geotechnical Engineering*, 519–522. Colombo.

Dharmasena, U. K. N. P., Bandara, K. N., & Karunawardena, W. A. (2015). *Back Analysis and Rectification of a Failed Cut Slope in the Southern Expressway*.

543–546.

Disaster management centre. (2009). *Sri Lanka National Report on Disaster Risk, Poverty and Human Development Relationship*.

Fredlund, D. G., & Anqing Xing. (1994). Equations for the soil-water characteristic curve. *Canadian Geotechnical Journal*. https://doi.org/10.1139/t94-061

Fredlund, D. G., & Rahardjo, H. (1993). Soil Mechanics for Unsaturated Soils. In *Soil Mechanics for Unsaturated Soils*. https://doi.org/10.1002/9780470172759

Gee, G. W., Ward, A. L., Meyer, P. D., Stormont, J. C., & Morris, C. E. (1999). Method to Estimate Water Storage Capacity of Capillary Barriers. *Journal of Geotechnical and Geoenvironmental Engineering*, *125*(10), 918–920. https://doi.org/10.1061/(ASCE)1090-0241(1999)125:10(918)

Goode, D. J. (1986). *Selection of soils for wick effect covers.*

Harnas, F. R., Rahardjo, H., Leong, E. C., & Wang, J. Y. (2014). Experimental study on dual capillary barrier using recycled asphalt pavement materials. *Canadian Geotechnical Journal*, *51*(10), 1165–1177. https://doi.org/10.1139/cgj-2013-0432

Highland, L. M., & Bobrowsky, P. (2008). Introduction to Landslide Stabilization and Mitigation. In *The Landslide Handbook — A Guide to Understanding Landslides*.

Jotisankasa, A., Porlila, Wissanupong Soralump, S., & Mairiang, W. (2007). Development of a low-cost miniature tensiometer and its applications. *Proceeding of the 3rd Asian Conference on Unsaturated Soils.*, 480. Nanjinj, China: Unsat-Asia.

Kampf, M., & Montenegro, H. (1997). On the performance of capillary barriers as landfill cover. *Hydrology and Earth System Sciences*. https://doi.org/10.5194/hess-1-925-1997

Khire, M. V., Benson, C. H., & Bosscher, P. J. (1999). Field Data from a Capillary Barrier and Model Predictions with UNSAT-H. *Journal of Geotechnical and Geoenvironmental Engineering*, *125*(6), 518–527.

https://doi.org/10.1061/(ASCE)1090-0241(1999)125:6(518)

Khire, M. V., Benson, C. H., & Bosscher, P. J. (2000). Capillary Barriers: Design Variables and Water Balance. *Journal of Geotechnical and Geoenvironmental Engineering*, *126*(8), 695–708. https://doi.org/10.1061/(ASCE)1090-0241(2000)126:8(695)

Krisdani, H., Rahardjo, H., & Leong, E.-C. (2006). Experimental Study of 1-D Capillary Barrier Model Using Geosynthetic Material as the Coarse-Grained Layer. *Unsaturated Soils 2006*, 1683–1694. https://doi.org/10.1061/40802(189)141

Kulathilaka, S. A. S., & Kumara, L. M. (2011). Effectiveness of surface drainage in enhancing the stability of cut slopes during the periods of heavy rain. *Annual Transactions of IESL*, 127–137.

Lau, K. C., & Kenney, T. C. (1984). Horizontal drains to stabilize clay slopes. *Canadian Geotechnical Journal*. https://doi.org/10.1139/t84-027

Li, J. H., Du, L., Chen, R., & Zhang, L. M. (2013). Numerical investigation of the performance of covers with capillary barrier effects in South China. *Computers and Geotechnics*, *48*, 304–315. https://doi.org/10.1016/j.compgeo.2012.08.008

Mancarella, D., Doglioni, A., & Simeone, V. (2012). On capillary barrier effects and debris slide triggering in unsaturated layered covers. *Engineering Geology*, *147–148*, 14–27. https://doi.org/10.1016/j.enggeo.2012.07.003

Mancarella, D., & Simeone, V. (2012). Capillary barrier effects in unsaturated layered soils, with special reference to the pyroclastic veneer of the Pizzo d'Alvano, Campania, Italy. *Bulletin of Engineering Geology and the Environment*, *71*(4), 791–801. https://doi.org/10.1007/s10064-012-0419-6

Morris, C. E., & Stormont, J. C. (1999). Parametric Study of Unsaturated Drainage Layers in a Capillary Barrier. *Journal of Geotechnical and Geoenvironmental Engineering*, *125*(12), 1057–1065. https://doi.org/10.1061/(ASCE)1090-0241(1999)125:12(1057)

Muthuhetige, W. K., & Kulathilaka, S. A. S. (2020). Establishment of Soil Water Characteristic Curves for Sri Lankan Soils. *Srilankan Geotechnical Project Day*.

Ng, C. W. W., Liu, J., Chen, R., & Xu, J. (2015). Physical and numerical modeling of an inclined three-layer (silt/gravelly sand/clay) capillary barrier cover system under extreme rainfall. *Waste Management*, *38*(1), 210–221. https://doi.org/10.1016/j.wasman.2014.12.013

Nyhan, J. W., Hakonson, T. E., & Drennon, B. J. (1990). A Water Balance Study of Two Landfill Cover Designs for Semiarid Regions. *Journal of Environmental Quality*. https://doi.org/10.2134/jeq1990.00472425001900020014x

Ogunro, V. O., Podgorney, R., Inyang, H. I., Piet, S., & Ayoola, M. G. (2005). Drainage layer fouling as a consideration in capillary barrier design. *Practice Periodical of Hazardous, Toxic, and Radioactive Waste Management*, *9*(4), 273–280. https://doi.org/10.1061/(ASCE)1090-025X(2005)9:4(273)

Parent, S.-É., & Cabral, A. (2005). Material Selection for the Design of inclined Covers with Capillary Barrier Effect. *Waste Containment and Remediation*, *40789*(September), 1–5. https://doi.org/10.1061/40789(168)25

Pease, R., & Stormont, J. C. (1995). *Increasing the diversion length of capillary barriers*. (Doctoral dissertation, University of New Mexico)

Qian, T., Huo, L., & Zhao, D. (2010). Laboratory Investigation Into Factors Affecting Performance of Capillary Barrier System in Unsaturated Soil. *Water, Air, and Soil Pollution*, *206*(1–4), 295–306. https://doi.org/10.1007/s11270-009-0106-9

Rahardjo, H., Hritzuk, K. J., Leong, E. C., & Rezaur, R. B. (2003). Effectiveness of horizontal drains for slope stability. *Engineering Geology*. https://doi.org/10.1016/S0013-7952(02)00288-0

Rahardjo, H, Hua, C., Leong, E., & Santoso, V. (2010). Performance of an instrumented slope under a capillary barrier system. In *Unsaturated Soils* (pp. 1279–1284). https://doi.org/10.1201/b10526-200

Rahardjo, Harianto, Kim, Y., & Satyanaga, A. (2019). Role of unsaturated soil

mechanics in geotechnical engineering. *International Journal of Geo-Engineering*, *10*(1), 1–23. https://doi.org/10.1186/s40703-019-0104-8

Rahardjo, Harianto, & Tami, D. (2004). *Capillary Barrier for Slope Stabilisation*. (January).

Ross, B. (1990). The Diversion Capacity of Capillary Barriers. *Water Resources Research*, *26*(10), 2625–2629.

Sato, T., & Matsumaru, T. (2018). *Experimental and numerical study of capillary barrier diversion lengths on embankment slopes*.

Sawada, M., Mimura, M., & Yoshimura, M. (2017). Infiltration control using capillary barriers for conservation of historical tumulus mounds. *Japanese Geotechnical Society Special Publication*, *5*(2), 5–10. https://doi.org/10.3208/jgssp.v05.002

Somaratne, M. (2015). Challenges to overcome : An overview of recent landslides with special reference to Meeriabedda landslide. *NBRO Symposium 2015 - Innovations for Resilient Environment*.

Stormont, J. C. (1996a). The effectiveness of two capillary barriers on a 10% slope. *Geotechnical and Geological Engineering*, *14*(4), 243–267. https://doi.org/10.1007/BF00421943

Stormont, J. C. (1996b). The effectiveness of two capillary barriers on a 10% slope. *Geotechnical and Geological Engineering*, *14*(4), 243–267. https://doi.org/10.1007/BF00421943

Stormont, John C., & Anderson, C. E. (1999a). Capillary barrier effect from underlying coarser soil layer. *Journal of Geotechnical and Geoenvironmental Engineering*. https://doi.org/10.1061/(ASCE)1090-0241(1999)125:8(641)

Stormont, John C., & Anderson, C. E. (1999b). Capillary barrier effect in unsaturated soils. *Journal of Geotechnical and Geoenvironmental Engineering*, *125*(8), 641–648. https://doi.org/10.1061/(ASCE)1090-0241(1999)125:8(641)

Stormont, John C., & Morris, C. E. (1997). Unsaturated drainage layers for diversion of infiltrating water. *Journal of Irrigation and Drainage Engineering*.

https://doi.org/10.1061/(ASCE)0733-9437(1997)123:5(364)

Sujeevan, V., & Kulathilaka, S. A. S. (2011). Rainfall Infiltration Analysis in Unsaturated Residual Soil slopes. *Geotechnical Journal, Sri Lankan Geotechnical Society*, *6*, 9–19.

Suppiah, R., & Yoshino, M. M. (1984). *Rainfall Variations of Sri Lanka Part 1 : Spatial and Temporal Patterns*. *340*, 329–340.

Tami, D., Rahardjo, H., & Leong, E.-C. (2007). Characteristics of Scanning Curves of Two Soils. *Soils and Foundations*, *47*(1), 97–108. https://doi.org/10.3208/sandf.47.97

Tami, D., Rahardjo, H., Leong, E.-C., & Fredlund, D. G. (2004a). Design and laboratory verification of a physical model of sloping capillary barrier. *Canadian Geotechnical Journal*, *41*(5), 814–830. https://doi.org/10.1139/t04-036

Tami, D., Rahardjo, H., Leong, E. C., & Fredlund, D. G. (2004b). A physical model for sloping capillary barriers. *Geotechnical Testing Journal*.

Tidwell, V. C., Glass, R. J., Chocas, C., Barker, G., & Orear, L. (2003). Visualization experiment to investigate capillary barrier performance in the context of a Yucca Mountain emplacement drift. *Journal of Contaminant Hydrology*, *62–63*, 287–301. https://doi.org/10.1016/S0169-7722(02)00164-X

Tran, T. V., Trinh, M. T., Lee, G., Oh, S., & Nguyen, T. H. Van. (2015). Effect of Extreme Rainfall on Cut Slope Stability: Case Study in Yen Bai City, Viet Nam. *Journal of the Korean Geoenvironmental Society*. https://doi.org/10.14481/jkges.2015.16.4.23

Wang, F., Li, X., & Wu, Y. (2018). *A discussion on the design criteria of capillary barrier*. 1–6.

Ward, A. L., & Gee, G. W. (1997). Performance Evaluation of a Field-Scale Surface Barrier. *Journal of Environmental Quality*, *26*(3), 694–705. https://doi.org/10.2134/jeq1997.00472425002600030015x

Woyshner, M. R., & Yanful, E. K. (1995). Modelling and field measurements of water

percolation through an experimental soil cover on mine tailings. *Canadian Geotechnical Journal*, *32*(4), 601–609. https://doi.org/10.1139/t95-062

Yang, H., Rahardjo, H., Leong, E. C., & Fredlund, D. G. (2004). A study of infiltration on three sand capillary barriers. *Canadian Geotechnical Journal*, *41*(4), 629–643. https://doi.org/10.1139/T04-021

Yoshinori, K. (2015). *Landslides along National Roads in Central Highland in Sri Lanka : Review on Current Situation and Suggestion for Further Development of Landslide Mitigation along Highways in Sri Lanka*.

Zhang, W., Sun, C., & Qiu, Q. (2016). Characterizing of a capillary barrier evapotranspirative cover under high precipitation conditions. *Environmental Earth Sciences*, *75*(6). https://doi.org/10.1007/s12665-015-5214-9

APPENDICES

Appendix A – Calibration of moisture sensors

The moisture sensors used in the study gives the reading in the voltage values. These voltage readings from the sensors were depended on the soil type where the sensor was used to measure the moisture content. Voltage measurements from the sensors correspond to the volumetric water of the soil. Therefore, these sensors were calibrated for all the soils; river sand, M-sand(coarse) and residual soil before using them in continuous measurements. For calibrating the sensors soil samples were prepared with different moisture content values. Then these samples were filled in CBR mould and compacted well-using proctor hammers. After that moisture sensors were inserted into the sample and their voltage readings were recorded. Later by measuring the weight of the sample that was filled in the mould the bulk density of the sample was determined. Then gravimetric water content of samples was determined through the method of oven drying. From the gravimetric water content and bulk density of material their volumetric water content was derived using the following equation,

$$\text{Volumetric water content} = \text{gravimetric water content} \times \text{bulk density}$$

Table A.0.1: Experimental data from calibration of moisture sensors in M-sand

Sensor Number	Air Reading	Reading in soil	Trial No
MP 0218 - 43	4.02	3.19	01
		3.03	02
		2.9	03
MP 0218 - 44	4.01	3.19	01
		3.02	02
		2.9	03

Table A.1 above presents the sample experimental data from calibration of moisture sensors in M-sand coarse.

Fig. (A 1) below illustrates the calibration graphs obtained from the experiment for M-sand(coarse).

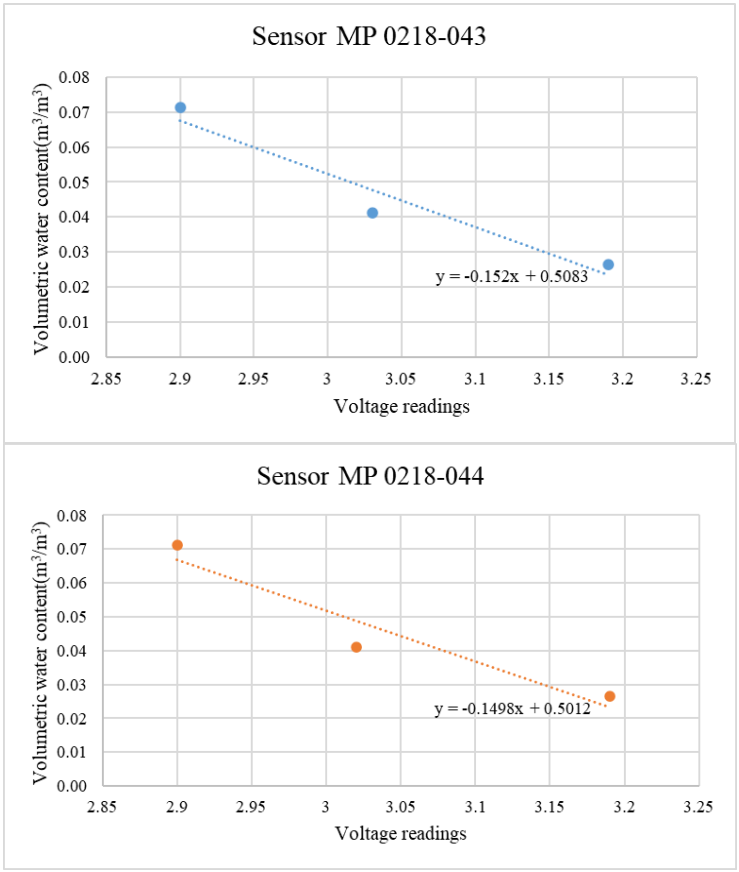

Figure A 1: Calibration graphs of two moisture sensors in M-sand (coarse)